Special Feature:
Dealing with Risk

Risk Assessment
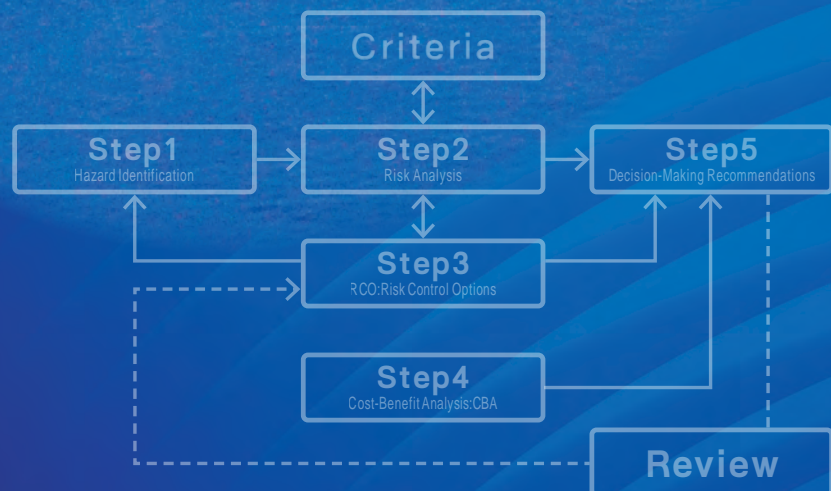
Criteria

Step1
Hazard Identification

Step2
Risk Analysis

Step5
Decision-Making Recommendations

Step3
RCO:Risk Control Options

Step4
Cost-Benefit Analysis:CBA

Review

ClassNK Technical Journal　No.6　2022（Ⅱ）

― CONTENTS ―

In recent years, discussion using risk has come to be widely used in the maritime field. As part of this trend, risk assessment was introduced in the offshore development field from the second half of the 1970s, and HSE activities, *etc*. are now making an important contribution to safety assessments. In the ship field as well, use of FSA, GBS and related approaches is continuing to expand in forums of discussion in the IMO. Therefore, this paper presents the basic concepts of safety and risk which are used in the maritime field, and explains the actual techniques of risk assessment and future expansion of its fields of application.

The social implementation of MASS is becoming a reality, and the time has come to consider a new framework that supports the social implementation of truly new technologies/solutions that transcend conventional frameworks. It is necessary to establish new ways of thinking such as functional safety and systems engineering, for the maritime industry. As one of these methods, this paper proposes the concept of vulnerability.

This paper introduces the fundamentals of risk-based design for structures, which has attracted attention recently, and its applications to rule development. First, structural reliability theory is explained, after which the characteristics of risk-based design are explained from the perspective of an optimum design problem. Next, the GBS-SLA (Goal Based Standards-Safety Level Approach) Interim Guideline which is a risk-based structural rule development guideline of the IMO, is introduced. Finally, as an example of application of risk-based design, a development method for fatigue strength criteria and its technical issues are described.

Technical Topics

Development of Local Scantling Formulae for Plate Members

Plate members are basic constituent elements of the ship hull structure, and local strength equations for out-of-plane (lateral) loading are extremely critical. This paper introduces the following content of a study which was conducted to review these equations in order to develop dimensional equations that are backed by theoretical equations and have a clearer correspondence with damage. First, the effect of in-plane stress on the fully-plastic moment and additional lateral loading was formulated as a basis for the dimensional equations, and after comparison with an elasto-plastic FEM analysis based on residual deflection criteria, dimensional equations using 2-point plastic hinge formation criteria were proposed. In addition, the influence of in-plane stress was interpolated between those of a longitudinally framed structure and a transversely framed structure, and a composite influence factor which considers this interpolation in combination with the aspect ratio correction factor was formulated.

World's First Zero Emission Battery-Propelled Tanker and Outlook for the Future

Reduction of emissions of greenhouse effect gases (GHG) as a measure against global warming is an urgent challenge. One solution for target achievement in ships is battery propulsion systems, which are increasingly used in automobiles. Kawasaki Heavy Industries delivered a large capacity battery propulsion system for coastal ships for the world's first zero emission battery-propelled tanker, the "Asahi," which was ordered by Asahi Tanker Co., Ltd. and completed at the end of March 2022. This paper introduces the background of development, the overview and features of the battery propulsion system, and the outlook for the future.

Introduction to "Guidelines for Additive Manufacturing (3D Printing)"

In recent years, the development of metallic products using additive manufacturing (AM) technologies, notably 3D printing, has spread rapidly, and in particular, AM technology is used in fields such as automobiles, aerospace, medicine and industrial machinery. Although there are still few examples of manufacturing using this technology in the shipbuilding field, full-scale introduction of AM technology is also expected in the shipbuilding field in the future, since the issues of cost reduction and productivity improvement are also the same in the shipbuilding. Against this backdrop, ClassNK issued guidelines which arrange the requirements for approval of metallic ship products, etc. manufactured using AM technology. This paper introduces the content of the Guidelines.

Estimation and Use of Wave Information for Ship Monitoring

Active development of real ship monitoring technologies is underway in the ship propulsion and structure field. Estimation and use of wave information is important in ship monitoring technologies, but use must be based on the respective strengths and limitations of this information. This paper first presents a brief explanation of the observation devices and analysis techniques which have generally been widely adopted and a bird's eye comparison of the features of the main types of wave information, and also discusses the applicability of each type of wave information to ship monitoring.

This article introduces recent topics discussed at the International Maritime Organization (IMO). In this issue, a summary of the decisions taken at the 78th Marine Environment Protection Committee (MEPC 78) and 105th Maritime Safety Committee (MSC 105) is provided.

Prefatory Note

Special Feature Articles on "Dealing with Risk"

Corporate Officer, Director of Research Institute, ClassNK

Yukihito FUJINAMI

On the publication of ClassNK Technical Journal No. 6, I would like to take this opportunity to welcome our readers.

Our technical newsletter, ClassNK Technical Journal, is published to contribute to technology in the maritime industry and related fields by publicizing the technical activities and research achievements of the Society. The previous Special Feature in ClassNK Technical Journal No. 5 focused on zero emission ships, and reported on related trends in technology and the results of research and development.

In recent years, quick and comprehensive identification of risks and study of a rational response has been demanded not only in the offshore development field, but also in the ship field, covering each of the phases of development and design, construction and operation of ships, beginning with various types of new concept ships such as alternative fuel ships and autonomous ships.

This ClassNK Technical Journal No. 6 includes a Special Feature entitled "Dealing with Risk," which introduces the concepts of risk assessment and risk-based design in the maritime field and the necessity of a new framework to support social implementation of autonomous ships. This issue also includes a diverse range of articles and papers, presenting the results of various research and development and trends in the IMO.

Based on the needs of society and industry, ClassNK will continue to make diligent efforts in research and development which contributes to securing the safety of life and property at sea, protecting the marine environment and creating innovations that lead society, and will endeavor to contribute to the further development of the maritime industry.

In conclusion, I would like to request the continuing understanding and support of all those concerned.

Risk in the Maritime Sector

— Dealing Skillfully with Risk —

Kenkichi TAMURA[*]

1. INTRODUCTION

The word "risk" is now used frequently even in everyday life, as seen in terms such as "risk hedge" and "country risk." However, while "risk" is generally considered to mean "the very picture of danger" in Japan, the understanding is quite different in Europe and the United States, where "risk" is only a "possibility," that is, "the possibility that an adverse event may occur."

Although various explanations of the origin of the word "risk" have been proposed, including the Italian *risicare* (to attempt something with courage) or *risico* (disaster) and the Spanish *risco* (a steep, rocky reef), its etymology remains unclear. Nevertheless, it is certain that the development of the concept of "risk" was greatly influenced by the maritime fields of navigation and foreign trade, among others. For example, there is a widely known story that around the end of the 17th century Lloyd's Coffee House, which was managed by Edward Lloyd in London, England, created a newspaper by gathering information from sailor and merchants, and organized a syndicate to disperse the risk based on it, thus laying the foundation for the marine accident insurance system.

In this paper, the author introduces the concept and practical techniques related to recent risk assessment, particularly to risk assessment in the maritime sector, and would also like to discuss future expansion in the commercial field.

Here, it may be noted that both "risk assessment" and "risk evaluation" are frequently translated as "risk assessment" in Japanese. However, the two terms are slightly different. While "evaluation" simply means the act of evaluating, "assessment" also adds "consideration based on the results of that evaluation" (i.e., the overall process of risk analysis based on risk evaluation), and thus extends to the act of "judging." Because "judgment" is also included in the meaning in this paper, "risk assessment" will be used here to avoid confusing the two terms.

2. SAFETY

2.1 What Is Safety?

The slogan "Safety First" is often seen in cities and towns. This motto had its origin in 1901, when Elbert Henry Gary, who was the President of US Steel, the world's leading steel company at the time, was pained by the company's failure to reduce industrial accidents and revised the general management policy in the industry, "Production First, Quality Second, Safety Third," to "Safety First, Quality Second, Production Third." Under this management policy, US Steel not only reduced accidents, but also achieved excellent quality and high productivity in spite of the labor shortage during the wartime, and afterward, the slogan "Safety First" permeated the entire country.

Although realizing "Safety First" is a challenge for humankind, the meaning of "safety" is itself vague and is difficult to define clearly. Conversely, "danger," which is the opposite concept to "safety," is clearly visible, for example in diseases and accidents involving injury, and its handling is also practical. This suggests that it is appropriate to define "safety" from the viewpoint of "danger."

According to ISO/IEC Guide [1], "safety" is defined as "freedom from risk which is not tolerable. A note states that "For the purposes of this Guide, the terms "acceptable risk" and "tolerable risk" are considered to be synonymous. Similarly, the JIS standard [2] states to the effect that safety is "a condition in which the danger of harming persons or damage is held to a tolerable level." In other words, "safety" is defined in terms of "risk" and "danger." At the same time, even assuming that a condition is "safe," some degree of risk remains. Therefore, "safety" means a condition in which this element of risk is held to a low level which can be accepted or tolerated. The idea of "absolute safety" (zero risk) is abandoned from the outset, and there is a common recognition of this worldwide.

[*] Member, Japan Transport Safety Board, Ministry of Land, Infrastructure, Transport and Tourism (MLIT)

2.2　Security and Safety

As can be seen in the slogan "Contributing to the security and safety of the nation's people," "security" and "safety" have frequently been used as a pair in recent years. However, what is the difference between security and safety? While the Japanese word *anzen* (安全) is translated as "safety" in English, the Japanese word for security, *anshin* (安心), is more difficult to translate. If one is forced to choose, "peace of mind" may be possible, but the meaning of this expression is subjective. When the issue of relocating Tokyo's famous fish market to Toyosu became controversial, Tokyo's Governor Koike declared that "Toyosu is safe, but it doesn't inspire peace of mind." This sense of "knowing objectively that a situation is safe, but still feeling uneasy" might be a representative example of the thinking of the Japanese people.

Again, the term *fuuhyou higai* (風評被害), what might be called "reputational damage," is used when unfounded rumors or falsehoods cause some time of adverse effect, particularly economic damage, by affecting the reputation of the person or region concerned. This can also be thought to arise from the same "safe, but not secure" feeling. Why can't a person feel secure, even though they say a situation is safe? Since one cause of this is biased or inadequate knowledge on the user's side, or disregarding knowledge due to indifference, an attitude of self-education is needed. However, this feeling of security is possible only when the user can trust an organization or person that has realized and guarantees safety. Active messaging and mutual communication from such organizations and persons to users are also indispensable for building a feeling of security.

2.3　Safety Targets

Under a condition where absolute safety does not exist, the following problem arises: "How far must risk be reduced before the condition can be called safe?" While the terms "acceptable" and "tolerable" are used in definitions of safety, the ISO/IEC Guide [1] defines "tolerable risk" as "risk that is accepted in a given context based on the current values of society." This suggests that there are no clearcut criteria for determining how far risk must be reduced in order to be safe, and instead "safety" is decided based on the balance of the magnitude of risk, convenience, costs and other factors. The following are examples of typical judgment criteria [3].

- Risk-utility criterion

Concept of judging acceptability by comparing the utility, merits and convenience of using a product and the risks associated with using that product.

- Cost-benefit criterion

Concept of judging how far risk should be reduced by comparing the required cost of implementing risk reduction measures against the benefits and utility obtained by implementation.

- Consumer expectation criterion

Criterion based on the safety that ordinary consumers rationally expect; a concept in which the minimum level of risk that must be maintained is set based on common sense.

- Deviation-from-standard criterion

In cases where standards or legal requirements exist, this is the concept that the safety level is acceptable provided those requirements are satisfied.

2.4　ALARP

In many cases, judgments of actual safety targets are made based on the principle called ALARP (As Low as Reasonably Practicable). ALARP is the concept that risk must be reduced as far as is reasonably possible. In this case, risk is reduced as far as possible in accordance with criteria such as the above-mentioned risk-utility or cost-benefit criterion. In actuality, however, risk above a certain level cannot be tolerated ("intolerable"), while risk below a certain level is broadly tolerable ("negligible"), and the ALARP region is the range that is reasonable possible between those two levels. Risk can be limited to this ALARP region only in case it can be shown that the costs required to reduce that risk would be extremely large in comparison with the benefits obtained. Fig. 1 shows a conceptual diagram of the ALARP region, which is called a carrot diagram owing to its carrot-like shape. The handling of the safety targets when using the ALARP principle are quite different depending on the object field, for example, in the nuclear power industry, chemical engineering, transportation (automobiles, aircraft, railways, ships), computers and telecommunications. The applicable safety targets for the various fields are also currently being explored, including in the Science Council of Japan.
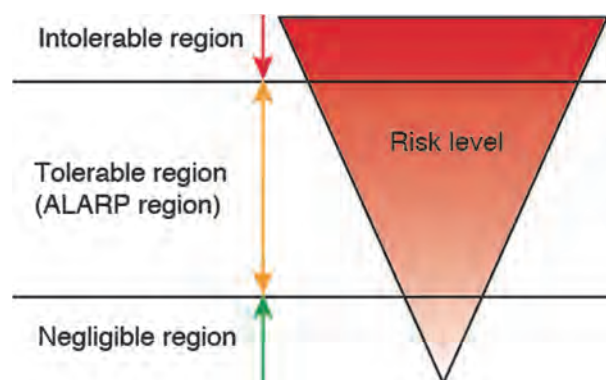
Fig. 1　Concept of ALARP (carrot diagram)

3.　RISK

3.1　Various Types of Risk

There are various types of risk. For example, "environmental risk" indicates the possibility that chemical substances, etc. may have adverse impacts on human health or the habitats of living organisms by way of the environment. "Country risk" means the degree of risk of loss of profit when engaged in overseas investment or foreign trade due to changes in the government, economy or social environment of the counterpart country, unrelated to the commercial risk associated with partners in individual projects. The risk caused by the Russian invasion of Ukraine is a typical example of this. Among these various types of risk, the following explains risk in economics and risk in safety engineering, where the concepts are comparatively well-established.

3.2　Risk in Economics

In this field, risk is generally considered to be "uncertainty regarding the variability of certain events." In other words, risk = uncertainty. Therefore, this type of risk does not include the importance of results.

According to this definition, since the situation that a person is walking along the edge of a sheer precipice is unknown whether he will fall or remain safe, uncertainty, that is, risk is high. However, once the person steps over the edge of the cliff, death is certain, and risk is no longer a question after the person takes that step.

3.3　Risk in Safety Engineering

In safety engineering risk [1] is defined as the degree of uncertainty of an undesirable event for human life or economic activity and the magnitude of the effect of such an event. In other words, risk can be considered as the combination of the frequency of occurrence (frequency) and the seriousness (consequence) of the result. In this case, either the frequency or the consequence of the event must be reduced in order to reduce risk.

For example, considered in the simplest terms, the value obtained by multiplying the consequence of the result and the frequency of its occurrence can be defined as "risk," as shown in Expression (1), and in fact, this equation is widely used.

$$\text{Risk} = (\text{Consequence}) \times (\text{Frequency}) \qquad (1)$$

However, if this expression is used, the case where the consequence is high but the frequency is low, and the case where the consequence is low but the frequency is high, may result in the same value of risk. As can be understood from airplane accidents and automobile accidents, cases where the frequency is low but the consequence is high attract overwhelmingly high attention. In that sense, there is still much room for consideration in deciding what combination of consequence and frequency should be used to determine the value of risk.

3.4　Terminology Related to Accident Scenarios [4]

In safety engineering, the terminology shown below is used when handling accident scenarios.

"Hazard" is a word that is heard frequently in recent years, for example, in the term "hazard map," but it expresses a threat to human life, etc. Hazard refers to so-called hazardous situations due to circumstances or conditions that may cause an accident, so-called danger circumstances: A road frozen with snow, a house located near a river and a cup of coffee beside a notebook PC are typical examples. Risk and hazard are also sometimes used interchangeably, but when seen from the viewpoint of risk

assessment, they are different terms. That is, "hazard" expresses the dangerous or harmful nature of natural disasters, power outages, deterioration of structures and the like, while "risk" is the degree of possibility (probability) that a hazard may cause adverse effects. In other words, if there is no hazard, risk does not exist.

"Peril" is a direct cause of damage or loss. It indicates all the causes of hazard, and refers to accidents that cause damage or loss, such as fires, explosions, traffic accidents, etc., or the accidents that cause them. Examples include fires, lighting, typhoons, collision, floods, etc.

"Consequence," as mentioned above, expresses the degree of seriousness of an accident. In many cases, consequence is defined in terms of human death and injury (persons) or the cost of damage (yen or dollars).

In the accident scenario "three persons died when an oil platform was destroyed by a hurricane," the hazard is the hurricane, the peril is the destruction of the oil platform, and the consequence is the three deaths.

3.5　Image of Occurrence Frequency

Occurrence frequency is a probability and is a nondimensional quantity having a value in the range of [0, 1]. In obtaining the probability of occurrence, first, it is necessary to specify the referenced period, for example, per 1 hour, per 1 year, per 1 voyage, etc. When the object is ships, reference periods such as per ship-year, per working-hour, etc. are used in some cases.

Because frequency of occurrence is a probability, it normally has a small value but is not zero. Accordingly, the discussion will be out of touch with reality if we do not understand the meaning of that value and discuss it using concrete images. An annual probability of 10^{-2} means a probability of occurrence of once in a lifetime, while a probability of 10^{-10} means 1 time since the birth of the universe. For example, there are data showing that the probability of being struck by lighting is about 10^{-6}, but the probability of winning the lottery in Japan is 10^{-7}. While these are not probabilities that should cause concern, they are not probabilities that can be totally ignored.

4.　RISK ASSESSMENT

4.1　What Is Risk Assessment?

The ISO standard indicates that risk assessment is a total process which includes risk identification, risk analysis and risk evaluation.

Risk identification (or hazard identification) is the process of discovering, recognizing and describing risk, while risk analysis is the process of understanding the special characteristics of that risk and determining the risk level.

Risk evaluation is the process of comparing the results of the risk analysis with risk criteria in order to determine the acceptability (or tolerability) of the risk (and its magnitude).

Risk assessment is essentially a subprocess within the risk management process. Normally, after a risk assessment, the magnitude of the tolerable risk (tolerable value) is compared with the predicted value of the risk (predicted value), and when the predicted value exceeds the tolerable value, a decision-making action is carried out to decide whether to take risk reduction measures or risk avoidance measures, and a process that realizes a safer condition is implemented.

4.2　Reality of Risk Assessment

4.2.1　Overview of FSA [5]

Here, FSA (Formal Safety Assessment), which is actually used widely as a risk assessment technique in the maritime field, will be presented as an example. As shown in Fig. 2, the FSA procedure is divided into 5 steps (Step 1 to Step 5). The work in each step will be explained.
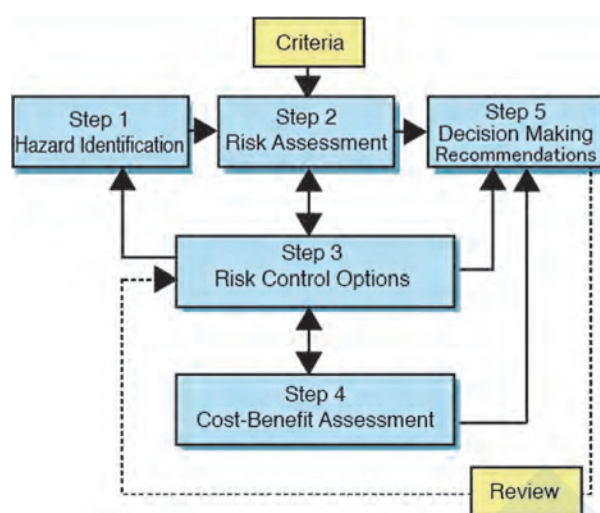
Fig. 2　Procedure of FSA

4.2.2　Step 1: Identification of Hazard

In Step 1, first, the various types of hazards that lead to accidents are identified by utilizing a combination of HAZID meetings and analysis methods.

A HAZID meeting is made up of multiple experts from different fields and held to quantify the consequence and frequency of accidents through meetings in line with a schedule. Analysis methods are used to assign priorities to all accident scenarios by risk level using available data.

In Step 1, it is possible to obtain 3 types of outputs, namely, the hazard list, related scenarios ranked by risk level, and the causes of the accidents and the description of their effects.

4.2.3　Step 2: Risk Analysis

In Step 2, a detailed risk analysis of the scenarios obtained in Step 1 is carried out, and the total risk of the target is obtained as the sum total of the risk of the individual accident scenario based on the accident probability, the probability that the disaster will spread after the accident (secondary disaster), and the seriousness of the accident and secondary disaster.

The risk of this case is an index of safety. Risk is defined as the product of the frequency and consequence of an accident, as shown above in Expression (1), and the assumed types of damage are loss of human life (fatalities), environmental impacts and loss of property. Risk evaluation indexes include individual risk and social risk. As examples, individual risk is an index that shows the frequency of death or injury of an individual while using some means of transportation, and social risk is an index showing the frequency of death or injury of a group using transportation during a target period being considered. The social risk of the group is obtained by multiplying the risk of the individuals who belong to that group by the size of the group. One index of social risk is PLL (Potential Loss of Lives). In the case of ships, PPL is the number of fatalities per 1 ship in 1 year (1 ship-year). Even though the PPL is the same, accidents become increasingly intolerable as the number of fatalities in one accident increases. As an index which reflects this fact, analyses are conducted using an FN (Frequency-Number of fatalities). This is a diagram that graphs the number of fatalities against the frequency of occurrence of accidents that result in a certain number of fatalities or more.

In FSA, the upper and lower limits of the ALARP region are set as risk tolerance criteria. Although the lower limit of the ALARP region for individual risk is 10^{-6}, the upper limit has been set at 10^{-3} for crew members and at 10^{-4} for passengers and the general public, that is, one order of magnitude stricter than for crews. It should be noted that these risk tolerance criteria are provisional values and a review is being studied, as there are also many opposing views.

4.2.4　Step 3: Drafting of Risk Control Options

In Step 3, Risk Control Options (RCO) are examined, and the reduction of risk in case they are introduced is estimated. Here, RCO are defined as safety measures for suppressing the very picture of high-risk hazards in cases where the risk is in the ALARP region, or the occurrence of accident scenarios. In the FSA approach, the individual measures are called RCMs (Risk Control Measures), and the RCMs are collectively called RCO. RCO comprise preventive measures for reducing the frequency of occurrence of accidents and mitigation measures for reducing the seriousness of the result.

4.2.5　Step 4: Risk Evaluation

In Step 4, the cost of achieving the various types of RCO drafted in Step 3 is evaluated, a Cost Benefit Analysis (CBA) is carried out, and the RCO are ranked in order of priority. In the FSA, two indexes are used for this purpose, Gross Cost of Averting a Fatality (GCAF) and Net Cost of Averting a Fatality (NCAF), as shown in Expression (2).

$$GCAF = \Delta C \, / \, \Delta R$$
$$NCAF = (\Delta C - \Delta B) \, / \, \Delta R \qquad (2)$$

ΔC : Additional cost incurred by introducing RCO (US$)
Includes the cost of RCO, training costs, lost profit, etc.
ΔR : Reduction of risk by introducing RCO
ΔB : Economic benefit of introducing RCO

GCAP means the costs considered necessary to reduce risk by one unit, while NCAF means the net cost in case an economic benefit is obtained by introducing the RCO and includes the monetary value of the damage which is prevented by introduction of the RCO as an economic benefit.

If the value of GCAF or NCAF is smaller than the threshold of the evaluation criterion, the RCO is effective from the viewpoint of costs and benefits (CBA), and introduction of that RCO is carried out. As the threshold of the current Guidelines for Formal Safety Assessment (FSA), US$3 million is used in case of death or disability based on the current condition of GCAF in the OECD countries. However, there are currently moves to review this criterion, as there are many views that this number should be higher.

4.2.6　Step 5: Decision-Making Action

In Step 5, the results of Step 4 are judged, and the RCO which should be introduced is proposed.

5.　RISKS IN THE OCEAN DEVELOPMENT FIELD

5.1　Safety Management System for Ocean Development

For ships, there is a unified international safety standard called the SOLAS Convention (Convention for the Safety of Life at Sea). However, the safety management system and regulations for offshore structures used in oil and gas development are established by the producing countries themselves. Well-known safety supervision organizations include the NPD (Norwegian Petroleum Directorate), the HSE (Health and Safety Executive) of the United Kingdom, and the BSEE (Bureau of Safety and Environmental Enforcement) and BOEM (Bureau of Ocean Energy Management) in the United States.

Table 1　History of introduction of risk assessment in the maritime field

Year	Main events of period	Outline
1977	Ekofisk Oil Field blow-out accident in Norwegian sector of North Sea oil field	A blow-out discharged about 150,000 barrels of oil in 1 week. Near-uncontrollable condition, causing a large-scale environmental disaster.
Second half of 1970s	Start of project to apply Quantified Risk Assessment to Offshore Industry.	Research level. Introduction of the approach used in the nuclear power industry.
1980	Alexander L Kielland offshore oil drilling rig accident	Total loss and sinking of an oil rig due to the absence of structural redundancy after fatigue failure of 1 brace.
1981	NPD regulations	Mandatory application of QRA in the conceptual design stage for all newly constructed structures. Verification of Accidental damage Limit State (ALS) or Progressive collapse Limit State (PLS).
1984	NPD regulations	Introduction of quantitative evaluation criteria of ALS.

1988	Explosion and fire accident at Piper Alpha oil rig in UK sector of North Sea oil field	Poor contact at time of shift change. Permission was given for maintenance and other work on a pressure safety valve. Organizational issues of responsibility and authority.
1990	Safety Case of UK Health and Safety Executive (HSE)	Change from prescriptive regulation to goal-setting regulation. Applied to specified facilities and systems.
1997	Guidelines on the Application of Formal Safety Assessment (FSA) to the IMO rule making process	Safety assessment procedure for rule making for ships in the IMO. Applicable to generalized ships.

The history of the introduction of risk assessment in the maritime sector is shown in Table 1. Risk assessment was introduced in the maritime sector from the second half of the 1970s, which as almost the same period as introduction in the nuclear power sector. The FPSO Rule responding to the subsequent Safety Case has already become a *de facto* standard in the United Kingdom, Australia and some other countries. In the ship sector, FSA was adopted in procedures for establishing regulations in the IMO in the second half of the 1990s, and the number of proposals of standards using FSA has continued to increase in recent years.

5.2 Why Is the Concept of Risk Necessary in Offshore Structures?

Why was risk assessment introduced in the field of ocean development from an early date among all industries? The first reason lies in the enormous amount of capital required in ocean development of offshore oil and gas fields. The probability of discovering an oil field by exploratory drilling has increased remarkably from earlier times thanks to technological innovations such as geophysical exploration, but even so, is still less than 20%. Among the offshore oil fields that are discovered, it is said that the number of discoverable fields with a scale of 1 million bbl or more, which is considered to be required for commercial profitability, is about 2 in 100 trials. Therefore, in spite of differences in the cost of developing offshore oil fields differs depending on the location and scale of exploration, a total investment on the order of several tens of millions of US dollars (several billion yen) is necessary at minimum, and a risk assessment is essential in order to attract investors.

The second reason is the fact that rigs are frequently destroyed as a result of the severe natural environment in which they are placed, which includes hurricane attacks, etc. even after reaching the operational condition. Thus, an estimate of the potential loss of life and damage to equipment is also essential for production of oil or natural gas from the sea bottom.

As the third reason, many major accidents attributable to human error have occurred in the past in the development of offshore oil and gas fields, the damage to human life and the environment when an accident occurred was enormous in some cases. For this reason, the importance of rational safety management based on risk assessment was widely recognized, and QRA (Qualified Risk Assessment), which had been researched in the nuclear power sector, was also applied to offshore structures in a project that began from a comparatively early date, in the 1970s. Since the Piper Alpha accident had particularly large influence, the following will briefly introduce the outline of that accident and the subsequent investigation of the cause.

5.3 Piper Alpha Accident

On July 6, 1988, a large gas leak led to a fire, explosion and the collapse of the Piper Alpha, an English fixed-type oil and gas production platform in the North Sea oil field. Of the crew of 229, 167 died, and 2 members of the rescue team also died.

An accident investigation committee chaired by the Hon. Lord William Cullen was organized to investigate the cause of the accident and issued a report on the accident called the Cullen Report [6] in 1990.

The report consisted of two parts. As the result of the inquiry and elucidation of the root cause of the accident, the first part found that four accidental factors occurred simultaneously in an overlapping manner, leading to a major accident; these were (1) poor operation, (2) unclear authority and responsibility, (3) poor design changes and (4) disregard for training for emergency situations. The second part presented 106 recommendations as countermeasures for the future, which can be summarized in two key points, (1) requirement of a voluntary safety management system by the operator and (2) objective safety assessment.

The Piper Alpha accident showed the world that "proactive investment in safety that is reasonably practicable is the correct management policy," and the Cullen Report had a decisive influence on the subsequent form and logic of activities of the HSE.

5.4 Swiss Cheese Model

The "Swiss cheese model" is a model of the process by which human error leads to accidents and other troubles which was proposed by the English psychologist James Reason. In this model, a number of "barriers" (elements that prevent error) are provided for events that are assumed to be accidents, and accidents are normally prevented by overlaying many of these barriers.

However, each of the barriers has "holes" in the form of weak parts of individual layer and chain-reaction errors, as illustrated in Fig. 3, and an accident occurs if these holes unfortunately overlap in a straight line so that an error can pass successively through them. Reason's proposed model likens these holes in an organization's layers of defense to sliced Swiss cheese. Because four separate failures overlapped at one time in the Piper Alpha accident, this accident is considered to be a typical example of the Swiss cheese model.
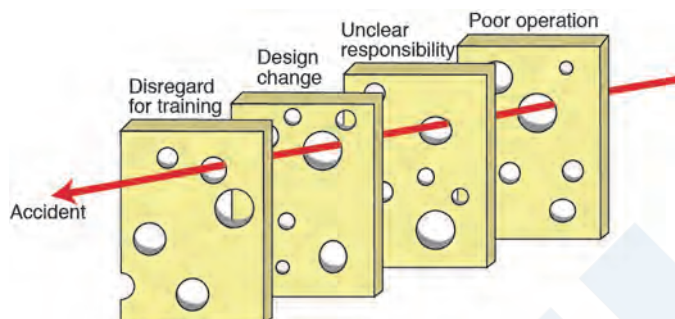

Fig. 3 Concept of the Swiss cheese model

6. LABOR SAFETY AND RISK

6.1 Labor Safety Law in the UK [7]

In England, which was the birthplace of the Industrial Revolution, the Factory Act was established in 1802 as the world's earliest law for worker protection, but with changing times, it became difficult for regulations to keep pace with the progress of industrial technologies. Therefore, a committee chaired by Lord Robens carried out repeated deliberations on safety and health issues (mainly in the administrative aspect) and released the Robens Report [8] in 1972. Although the Robens Report was an extremely large work consisting of 19 chapters, several of its assertions will be introduced here.

(1) Questions were raised regarding improvement of safety and health by legal and supervisory means. It can be said that there are too many laws for improvement of safety and health, which is counterproductive for achieving the essential goals. New laws must be created successively in line with the progress of society, and laws that have become outdated must be revised.

(2) The subdivision of labor safety and health administration is excessive (at the time, safety and health administration in the UK was divided into 5 related ministries and agencies and 7 supervisory agencies). Responsibility is unclear, and quick measures are not taken.

(3) Based on an awareness of these issues, the Report advocated a shift from a legal and supervisory-centered approach to a voluntary response and unification of administrative authorities.

Based on the Robens Report, in 1974 the UK enacted the new Health and Safety at Work Act (1974 HSW Act) and established the Health and Safety Executive (HSE), which promoted modernization of laws related to labor health and safety over several decades thereafter.

6.2 Basic Concept of the Safety Case Law

In response to the 106 recommendations of the Cullen Report of 1990, the HSE requires operators engaged in the production of oil and gas to prepare and submit a document called a Safety Case. Based on this, the Safety Case Act was enacted, and its practice is linked to HSE (Health, Safety and Environment) activities. Due to the increasing complexity of production technologies, it would be impossible to cover every item which should be done only by laws and ordinances. Therefore, autonomous thinking-type management is required so that each company can discover and solve important problems in the company by itself.

6.3 Safety Case Law

The Safety Case Law refers to Offshore Installations Regulations, which aim to reduce the risk of serious accidents and disasters involving offshore structures operated in British territorial waters and the continental shelf, and requires "objective safety assessment" and an "autonomous safety management system." Documentary reviews are conducted by the HSE, and certification must be renewed every 3 years.

The Safety Case Law is not a conventional law that requires compliance with regulations, but rather, is a goal-setting type

law under which companies are allowed to set their own goals and then demonstrate that they have satisfied them. Its basis is the ALARP concept, that is, reducing risk as low as is reasonably practicable, considering cost-effectiveness.

A "Safety Case" is a document in which each company itself argues the safety of its system, using test results and verification results as evidence, in order to assure or convince those responsible for system certification, users and others of its safety.

The description of an actual Safety Case consists broadly of the following three stages:

(1) FD (Facility Description), meaning a description of the system

(2) FSA (Formal Safety Assessment)

(3) SMS (Safety Management System)

Safety Cases are necessary through the entire Life Cycle of design, operation and disposal, and a Safety Case consisting of the respective stages is required.

6.4　Expanding HSE Activities

The voluntary organization of the oil majors called OCIMF (Oil Companies International Marine Forum) accepted the Safety Case Law fully and cooperatively, and since that time has practiced HSE activities for offshore structures throughout the world and popularized the concept.

Based on the enactment of the Safety Case Law, the E&P Forum (Oil industries Exploration & Production Forum) published Guidelines for the Development and Application of Health, Safety and Environmental Management System (E&P Forum). The main points of these Guidelines are as follows: A PCDA cycle based on risk assessment is followed. All risk reduction measures that are both reasonable and practicable are adopted. Those concerned cooperate in the establishment, practice and dissemination of HSE activities in the offshore field to provide indirect support for the activities of the Health and Safety Executive (HSE).

In addition, the oil majors require practice of HSE activities not only for offshore structures, but also for the navigation and construction of related merchant ships, i.e., LNG carriers and tankers.

Based on this kind of comprehensive backing by the oil majors, the Safety Case Law and HSE activities as its practice have grown remarkably from simply a local system within the UK to activities that are practiced worldwide as a *de facto* standard.

7.　RISK IN THE SHIP SECTOR

7.1　FSA (Formal Safety Assessment)

Where ships are concerned, the first version of the unified global standard called the SOLAS Convention (The International Convention for the Safety of Life at Sea) was concluded in response to the sinking of the Titanic in 1912, and since that time, the standard has been revised more than 30 times up to the present. Accordingly, the basic initiatives for safety management of ships that sail on international routes are discussed in the International Maritime Organization (IMO) and reflected in the rules of ship classification societies and various types of standards.

However, since discussions of revisions of rules and regulations in the IMO are frequently carried out in response to a major accident, revisions tend to be unnecessarily excessive due to conditions immediately after the accident. Moreover, because possibly political proposals intended to advantage one's own country were also rampant, FSA (Formal Safety Assessment) based on risk assessment has been introduced as a more rational method for establishing rules.

FSA was proposed by the UK at IMO/MSC62 (62nd meeting of the Maritime Safety Committee) in 1993, and the provisional Guideline was revised and the final FSA Guideline was approved in MSC74 in 2001 based on repeated discussions and test application thereafter. FSA is a comprehensive, rational safety assessment method which is structured and has objectivity and traceability. Its aim is to reduce special proposals and enforcement and drastically limit political discussion so as to create a more rational process for establishing rules in the IMO. While this does not mean that application of FSA to all proposals is mandatory, revision of many standards to apply FSA has been proposed and discussed recently in the IMO. Although FSA has difficulties in the complexity of the procedure and verification, the number of proposals using FSA is increasing year by year.

7.2　GBS (Goal-Based Standards)

The Nakhodka accident in 1997 caused an oil spill of about 6,200 tons of heavy oil in the Japan Sea, resulting in serious damage in coastal areas. This was followed by a series of other major accidents involving aging tankers, including a spill of about 10,000 tons of heavy oil off the coast of France in the Erika accident in 1999 and a spill of about 77,000 tons of cargo oil off the Spanish coast in the Prestige accident of 2002.

These accidents led directly to measures such as the promotion of a phase-out of single hull tankers (by 2010), a ban on the transportation of heavy fuel oil by single hull tankers, and setting of Particularly Sensitive Sea Areas (PSSA). Indirectly, however, they also strengthened the claims of the European Council, that is, the European countries which suffered damage, and shook confidence in the IMO and IACS (International Association of Classification Societies), which had established the rules up to that time. In order to restore the confidence and leadership position of these organizations, the IMO and IACS shifted the focus from responding after an accident to avoiding risk in advance. The IMO introduced GBS (Goal-Based Standards) to clearly specify the purpose, safety levels and functional requirements of rules and regulations, while the IACS introduced CSR (Common Structural Rules) as a unified set of rules for ship construction which is rational and transparent.
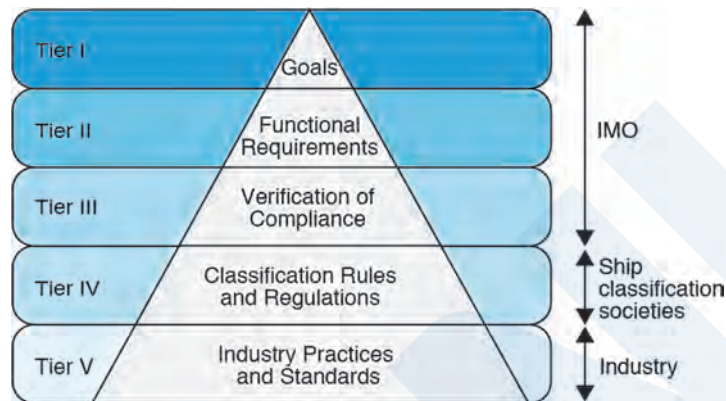

Fig. 4　Composition of GBS

The GBS system is different type of safety assessment from the FSA, in that Tier I to Tier V take the form of a pyramid, as shown in Fig. 4, the tolerable risk levels are set as goals, and rules are established based on the functional requirements for the respective safety levels in order from the top to the bottom of the pyramid.

8.　DEVELOPMENT OF RISK ASSESSMENT IN THE MARITIME SECTOR

8.1　Environmental FSA

In comparison with safety, it has been considered difficult to introduce environmental risk assessment because the parties responsible for damage and the monetary amount of that damage are not as clear. However, based on the safety-related results achieved by FSA, use of the concepts of FSA when introducing new criteria for protection of the marine environment and incorporation of EREC (Environmental Risk Evaluation Criteria) in the FSA Guidelines were studied. The joint research project SAFEDOR (Design, Operation and Regulation for Safety) in the EU introduced an item for oil spills called CATS (Cost of Averting a Tonne of Oil Spilt), that is, "the monetary amount to be contributed as a risk control option (RCO) that is implemented to avoid 1 ton of spilled oil," and proposed the assessment criterion shown in Expression (3)

$$\Delta C / \Delta R = CATS < CATS_{thr} \qquad (3)$$

ΔC : additional cost of introduction in RCO (US$)

ΔR : oil pollution risk reduction effect of RCO

$CATS_{thr}$: threshold for judging that an arbitrary RCO is cost-effective

Initially, a fixed amount of US$60,000/ton was proposed in SAFEDOR as the threshold $CATS_{thr}$. However, in response to this, Japan and others carried out a regression analysis for the amount of oil pollution (W) and the cost of damage caused by oil pollution (C) based on oil pollution data for the years 1970 to 2005 of the International Oil Pollution Compensation Funds (IOPCF). The results showed that C/W is not a constant value, but rather, is a function of W, and as W increases, C/W becomes smaller. Based on this regression analysis, a functional-type $CATS_{thr}$ was proposed, and this was adopted by the IMO. Although moves to introduce FSA in marine environmental protection are currently limited to oil spills, precisely because the effect will

be great, future moves will attract considerable attention.

8.2 RBM (Risk Based Maintenance)

RBM is the concept of evaluating the risks of equipment aging, abnormalities and failures and preparing maintenance and inspection plans based on the evaluation results. It is a method for making rational judgments about maintenance by evaluating risk by calculating from the "magnitude of effect when an equipment failure occurs" and the "ease of occurrence of failure." In the United States, it has been introduced in infrastructure maintenance and other fields in recent years, as it had become impossible to respond to all maintenance needs due to the increasing number of facilities that require maintenance. The API (American Petroleum Institute) and ASME (American Society of Mechanical Engineers) are promoting wider application of RBM, and use has also begun at petroleum plants affiliated with the oil majors. In Japan as well, the use of this concept in maintenance, etc. of offshore (floating) oil storage bases is considered to be significant, but plans for actual introduction still have not been established.

9. CONCLUSION

This paper has examined risk assessment as a technique for clarifying risk and achieving safety. However, the primary factor which threatens safety is the human factor. Human beings are endowed with characteristics that cause error. Although the concepts of "fool-proof," "fail-safe," "advance prevention" and "defense-in-depth" have been researched as methods for preventing accidents caused by the human error, one solution is considered to be cultivating a culture of safety. A "culture of safety" is a condition in which every person in an organization, from top management to each individual at the actual work site, has an awareness that safety is the highest priority and makes efforts to secure safety as an organization, but this is also difficult to quantify. Thus, utilizing risk assessment in prevention of accidents caused by the human factor is an important challenge for the future.

REFERENCES

1) ISO/IEC Guide 51, 2014 Ed.
2) JIS Z 8115, Glossary of terms used in dependability (in Japanese)
3) Masao Mukaidono, Philosophy of Safety, Trends in the Sciences (in Japanese) (2009)
4) The Society for Risk Analysis Japan, Eds., The Encyclopedia of Risk Research, Maruzen Publishing Co., Ltd. (in Japanese) (2019)
5) Consolidated text of the Guidelines for Formal Safety Assessment (FSA) for use in the IMO rule-making process (MSC/Circ. 1023-MEPC/Circ.392), MSC 83/INF.2 (2007).
6) Lord Cullen, The Public Inquiry into the Piper Alpha Disaster (1990).
7) ClassNK, Guidelines for Introduction of HSE Management System (in Japanese) (2015)
8) Lord Robens, Safety and Health at Work (1972).

Necessity of New Framework to Support Social Implementation of Maritime Autonomous Surface Ships
— Construction of a vulnerability database and consideration of its use in risk assessment —

Tomoaki YAMADA[*], Noriyuki KAJITA[**]

1. INTRODUCTION

The development of MASS (Maritime Autonomous Surface Ship) is progressing worldwide. For example, in the fully autonomous ship program "MEGURI 2040 [1]" of the Nippon Foundation, five consortiums are conducting demonstration tests on actual commercial routes by a tourist ship, coastal container ships, large coastal ferries, etc. Berth-to-berth automated navigation was also carried out with shadowing by the crew, and the vessels were successful in automatically avoiding other ships and fishing ships engaged in commercial activities.

Active discussions on the development of international regulations for MASS are also underway in the International Maritime Organization (IMO). At IMO MSC105, a roadmap for developing a goal-based MASS Code was endorsed, in which non-mandatory MASS guidelines will be developed in 2024 and a mandatory goal-based MASS Code will be developed targeting enforcement in 2028.

When using autonomous navigation technologies for purposes (e.g. labor saving and unmanned operation) that exceed the support tools of existing ships, it is important to conduct appropriate safety evaluations for autonomous navigation systems, and risk assessment is attracting attention as a method for this purpose. The interim guidelines issued by IMO [2] and guidelines issued by some flag states [3-5] specify the implementation of risk assessment. Guidelines for MASS have already been issued by multiple classification societies [6-9], and risk assessment is also emphasized in all of them. For example, in the ClassNK guidelines [6], it is necessary to carry out risk assessments depending on the development phase of the autonomous ship system.

When performing a MASS risk assessment, the key points are how to exhaustively extract the risks of unproven new technologies and how to accurately estimate those risks. Although there is no alternative to accumulating experience and knowledge through demonstration tests, etc., new technologies will inevitably have aspects that cannot be understood until they are used. When considering the social implementation of MASS, it is necessary to allow some degree of imperfection and consider how it should be operated. While implementation of MASS is premised on thorough pre-verification, it is also necessary to create a process for updating MASS safety-related knowledge and improving safety evaluations after implementation.

Although the principle is to create robust rules [10], it is important that those responsible for rule development and safety evaluations, such as classification societies, take the perspective that incompleteness (i.e., vulnerability [11]) will remain in the rules and standards created for new technologies with no track record, and adopt a stance of flexibly reviewing those rules in the product life cycle. To this end, it is necessary to construct a framework for timely reporting of information (particularly failure cases) that is discovered after actual use to the rule development and safety evaluation side. Moreover, if public institutions can create a database of such information and appropriately disclose it not only to technology developers but also to the rule development and safety evaluation side, further improvement in the safety of MASS by building a PDCA cycle can be expected.

2. CONCEPT OF VULNERABILITY

2.1 What Is Vulnerability?

The word "vulnerability" is often heard in everyday life, for example, in connection with information security involving personal computers. It is well known that vulnerability is difficult to completely counteract, and the current situation is that new vulnerabilities are being discovered one after another. Even if a vulnerability is blocked once, there is a possibility that a new

[*] Research Institute, ClassNK
[**] Digital Transformation Center, ClassNK

vulnerability will be discovered again, so it is always necessary to collect new information on OS and software and update them as quickly as possible. These are the characteristics of vulnerability that the authors would like to focus on in this paper.

Vulnerability is a concept adopted by the National Institute of Standards and Technology (NIST) in the United States, which publishes many security-related documents. For example, the Framework for Critical Infrastructure Cybersecurity Version 1.1 (April 2018) [12] describes not only the consideration of vulnerability when judging risk, but also the disclosure cycle of vulnerability information. The SP-800 series [13] also requires reuse of vulnerability information. It is interesting to note that vulnerability information is made available from a variety of public and private sources, including the National Vulnerability Database (NVD). In other words, since NIST assumes that information security is fragile and vulnerabilities will always be breached, the scope of security includes the response to cases where a vulnerability has been breached.

2.2　Safety and Vulnerability

ISO/IEC GUIDE 51: 2014 defines safety as "no unacceptable risk". Safety includes intrinsic safety and functional safety. As systems become more complex, the concept of functional safety, which ensures an acceptable level of safety by installing functional devices (functions to ensure safety: safety functions), has been adopted in various industries. In MASS as well, safety is ensured by making full use of safety functions based on the concept of functional safety [14].

If vulnerability remains in this safety function, it poses a great risk, so it is necessary to quickly and accurately collect information on the vulnerability of this safety function.

3.　EXAMPLES OF APPLICATION IN OTHER INDUSTRIES

3.1　Autonomous Vehicles Case in California, USA

In the United States, state governments have jurisdiction over road administration within their states, and state authorities are also in charge of licensing public road tests for autonomous driving. As part of the promotion of the introduction of autonomous driving, California revised the regulations regarding testing of autonomous vehicles (Article 3.7 – Testing of Autonomous Vehicle) on April 2, 2018 (the latest version took effect on April 13, 2022 [15]). The following are mandatory for developers of self-driving cars [16].

a) Prove that the developer of an autonomous vehicles has tested the controllability of the vehicle in an environment close to the real environment.

b) Prove that the vehicle can detect and respond to road conditions in accordance with state and local government vehicle operation regulations.

c) After notifying the local government of the autonomous vehicle test plan, monitor the test status via a two-way communication link.

d) Report to the state in the event of an accident or in cases where it is necessary to cancel the automatic driving mode.

In this paper, we would like to focus on d) above. From the public road test stage, there is an obligation to report within 10 days in the event of a collision accident (see § 227.48 [15]) and submit an annual report on cases where the automatic driving mode had to be canceled to the State of California even if no accident occurred. (see § 227.50 [16]). In addition, any identified defects that may pose an unreasonable risk to safety are subject to reporting requirements (see 3.8. Development of Autonomous Vehicle § 228.12 [17]). In this way, the fact that a framework for collecting data is incorporated from the stage of granting approval to conduct tests should be an extremely useful reference.

In California, trial operation of an autonomous driving delivery service and commercialization of robo-taxis have begun, and advanced efforts are being made in the field of autonomous driving vehicles. Since these efforts are supported by the aforementioned regulations, this may show the importance of timely sharing of vulnerability data with the rule development/safety evaluation side, which tends to be difficult to submit to those responsible for rule development/safety evaluation.

3.2　Examples from the Commercial Aviation Industry

The commercial aircraft industry, which achieved rapid development after World War II, has a history of improving safety by revising rules based on "accidents".

As with the maritime industry, the International Civil Aviation Organization (ICAO), a subordinate organization of the United Nations, establishes international standards for the civil aviation industry, and member countries have introduced frameworks

which obligate them to develop domestic laws that comply with these rules. However, there are no third-party organizations similar to the classification societies in the maritime industry.

This rule was enacted as an annex to the Convention on International Civil Aviation (commonly known as the Chicago Convention) adopted in 1944, and it is a important feature that fields related to aircraft design, manufacturing, operation, etc. are inclusively covered under one Convention Annex.

Annex 13 [17] defines "Aircraft Accident and Incident Investigation". Its Chapter 3 GENERAL OBJECTIVE OF THE INVESTIGATION states that "3.1 The sole objective of the investigation of accident or incident shall be the prevention of accidents and incidents. It is not the purpose of this activity to apportion blame or liability".

It can be said that this expresses the idea that it is necessary to recognize that the enacted regulations are not perfect, and to learn from actual accidents and incidents in order to prevent future accidents and incidents which have the same cause, since accidents and incidents are unavoidable events in aircraft.

In fact, in the United States, a law has been enacted that does not impose criminal penalties except in cases of intentional or malicious negligence in order to enable accurate interviews for investigations of aircraft accidents.

Based on this spirit, in the commercial aircraft industry, a framework has been introduced for each industry stakeholder (including the government authorities of each country) to report, disclose, analyze, and formulate countermeasures not only for accidents and incidents but also for various failure cases, and a framework for improving aviation safety on a daily basis has been put in place.

The important parts of this safety activity can be summarized in the following two points.

(1) Taking countermeasures will lead to improvements in safety, as accidents and incidents will inevitably occur.

(2) Collecting and disclosing various vulnerability information representing accidents and incidents in order to take countermeasures.

This is an example showing that vulnerability, which is the theme of this paper, is very effective in improving safety. Fig. 1 shows an overview of the PDCA cycle based on vulnerability in the commercial aircraft industry.
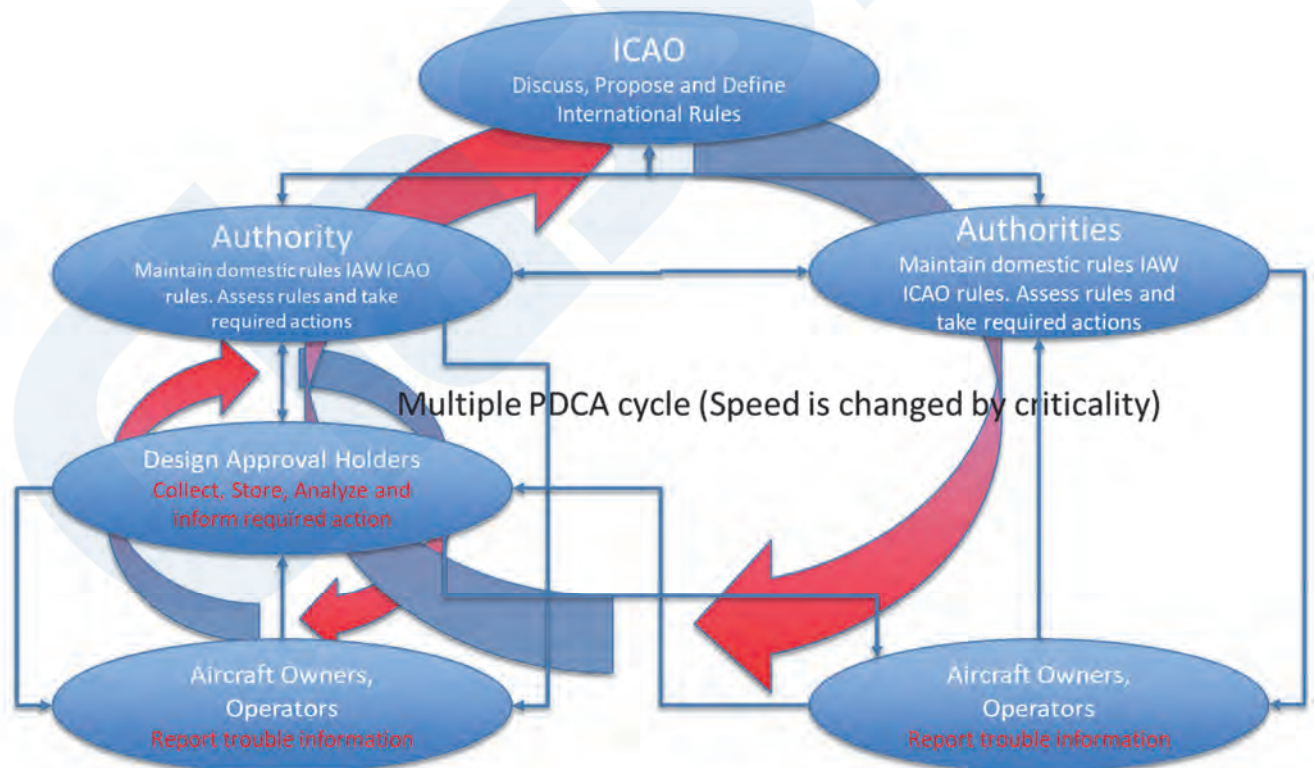
Fig. 1 Overview of the PDCA cycle based on vulnerability in the commercial aircraft industry

4. APPLICATION TO AUTONOMOUS SHIPS

4.1 Building a Vulnerability Database

As mentioned above, accepting a certain degree of imperfection and thinking about the optimum form of operation under this condition is a necessary way of thinking when confronted with new technologies. It is also necessary to create a framework for social acceptance of those technologies. The framework of collecting cases related to vulnerability, creating a database, and using it to improve the accuracy of safety evaluations has already been adopted in other industries, and we believe that it will also an effective approach for MASS.

In constructing a vulnerability database for MASS-related technologies, it is necessary to organize the classification and collection methods, but vulnerability has the property of decreasing as technology maturity increases. Therefore, we would like to propose that vulnerability levels be divided into two axes, that is, the status of the technology and the area of application [18], and that the reporting frequency be set according to the level. Tables 1 and 2 are shown only as examples. While setting the levels and reporting frequency according to the level of technical maturity at the time of social implementation, it is also necessary to consider conducting periodic reviews corresponding to improvements in the level of technology maturity.

Table 1　Example of vulnerability classification

		Technology Status		
		Proven	Limited field history	New or unproven
Application Area		SOLAS mandatory	On-shore ISO/IEC	Others
Known	On-market products	1	2	3
Unknown	On-market products	2	3	4
New	Development / Update	3	4	5

Table 2　Example of vulnerability reporting frequency

	Level of vulnerability				
	1	2	3	4	5
Defects that caused an accident	Immediately	Immediately	Immediately	Immediately	Immediately
Defects that caused disengagement of autonomous mode	Semi-annually	Quarterly	Quarterly	Quarterly	Monthly
Other defects found during operation	Annually	Semi-annually	Quarterly	Monthly	Monthly

4.2 Utilization in Risk Assessment

Risk assessment is also being carried out in the MASS demonstration project, and the safety of MASS is evaluated by analyzing the risks inherent in the new technology itself and the risks when the technology is installed on ships while verifying the differences with the existing technology. However, in the trial verification stage, it is very difficult to extract all the hazards of new technologies that have no track record and accurately estimate the risks that they may cause. Therefore, at present, evaluations are made in conjunction with the size of the safety margin set in the demonstration experiment.

On the other hand, for social implementation, it is necessary to optimize this safety margin. In this regard, we believe that incorporating the concept of vulnerability is one option. For example, use of a vulnerability database will ensure that risk assessments can always be performed based on the latest information. This will not only prevent the omission of verification of important risks, but also contribute to preventing excessive safety measures (rationalization of safety margins).

4.3 Build and Thoroughly Implement the PDCA Cycle

In the development phase, information and experiences such as failure cases and near-miss incidents should be shared with the rule development and safety evaluation side from the stage of demonstration experiments in order to prevent omission of verification when certifying the technology.

In the operation phase, considering that new technologies with little track record can be understood only after they are used, feedback from seafarers, who are the users, should be appropriately distributed to those responsible for technology development, rule development and safety evaluation. This will lead to improvements in technology, regulation and evaluation. Building a vulnerability database and appropriately using the PDCA cycle will lead to improvements in the safety of operation of MASS.

First, the vulnerability database is expanded, and the PDCA cycle is constructed based on vulnerability from the standpoints of technology development, rule development and safety evaluation. Then, this PDCA cycle must continue to be used effectively. We believe that such a framework is necessary for MASS, in which hardware failures, software defects, operation and management problems and other factors are interrelated in a complex manner.

5. CONCLUSION

As social implementation of MASS is now becoming a reality, the time has come to consider a new framework which supports the social implementation of truly new technologies and solutions that transcend the conventional framework, that is, a framework which can complement imperfect regulations and institutions. It is also necessary to incorporate concepts such as functional safety and systems engineering, which are new concepts for the maritime industry. As one of these methods, this paper proposed the concept of vulnerability.

To ensure that these new concepts take firm root, it is necessary to formulate the optimum approach and define the division roles within the industry. For this, a forum should be built, for careful discussion within the industry to determine who will assume the leadership position, what type of framework is needed to impose reporting obligations, and where the vulnerability database. In this regard, since classification societies have a neutral position, they should have a large role to play. We would like to work to stimulate discussions in the industry.

ACKNOWLEDGMENT

REFERENCES

1) The Nippon Foundation: "The Nippon Foundation MEGURI2040 Fully Autonomous Ship Program",
https://www.nippon-foundation.or.jp/en/what/projects/meguri2040
2) IMO MSC.1/Circ.1604 (2019), INTERIM GUIDELINES FOR MASS TRIALS
3) Maritime Bureau, Ministry of Land, Infrastructure, Transport and Tourism: Guidelines for Safety Design of MASS
(*Jidouunkousen no anzen sekkei gaidorain*) (2020) (Japanese)
4) VTMIS, EU OPERATIONAL GUIDELINES FOR SAFE, SECURE AND SUSTAINABLE TRIALS OF MARITIME
AUTONOMOUS SURFACE SHIPS (MASS)
5) Norwegian Maritime Authority, RSV 12-2020: Guidance in connection with the construction or installation of automated
functionality aimed at performing unmanned or partially unmanned operations
6) ClassNK: Guidelines for Automated/Autonomous Operation on Ships (Ver. 1.0) (2020)
7) DNVGL: Autonomous and remotely operated ships, DNVGL-CG-0264 (2018)
8) Bureau Veritas: Guidelines for Autonomous Shipping, Guidance Note NI 641 DT R01 E (2019)
9) ABS: ABS advisory on autonomous functionality (2020)
10) IMO Resolution A.1103(29): PRINCIPLES TO BE CONSIDERED WHEN DRAFTING IMO INSTRUMENTS
11) ISO 31073:2022, Risk management - Vocabulary
12) National Institute of Standards and Technology: Frame work for Critical Infrastructure Cybersecurity Version 1.1, April
16, 2018
https://www.ipa.go.jp/files/000071204.pdf
13) National Institute of Standards and Technology: Computer Security Resource Centre

https://csrc.nist.gov/publications/sp

14) Yamada T: Safety Evaluation for Technologies related to Autonomous Ships, ClassNK Technical Journal No. 3, 2021(I)

15) California Department of Motor Vehicles (DMV): Article 3.7. Testing of Autonomous Vehicles
   https://www.dmv.ca.gov/portal/file/adopted-regulatory-text-pdf/

16) California Department of Motor Vehicles (DMV): Article 3.8. Deployment of Autonomous Vehicles
   https://www.dmv.ca.gov/portal/file/adopted-regulatory-text-pdf/

17) International Civil Aviation Organization: Annex 13 to the Convention on International Civil Aviation, "Aircraft Accident and Incident Investigation"

18) IMO MSC.1/Circ.1455 "GUIDELINES FOR THE APPROVAL OF ALTERNATIVES AND EQUIVALENTS AS PROVIDED FOR IN VARIOUS IMO INSTRUMENTS", Annex, page 9, Table 1: Categorization of new technology

Fundamentals and Applications for Risk-Based Design

Makoto ITO[*]

1. INTRODUCTION

The designs of engineering systems such as ships and aircraft should consider safety as the highest priority. On the other hand, since designs which do not consider economy are unrealistic, how to design attractive and competitive engineering systems while also ensuring safety is important. To achieve this, it is desirable to establish rules with a high degree of freedom, which are capable of incorporating new technologies and concepts, especially in the design of new concept ships.

Risk-based design [1] is an effective concept for ensuring safety in design with high degree of freedom. Risk-based design is based on reliability-based design and uses "risk" as an indicator for setting the criteria of functions such as the upper limit of the probability of failure in structural design. Use of "risk" as an indicator results heightens the universality and transparency of evaluation criteria. Moreover, this approach is also expected to enable countermeasures against unknown phenomena.

In this paper, the structural reliability theory is introduced as the basis for understanding risk-based design, and the difference between reliability-based design and risk-based design is described by using a design optimization problem. In addition, applications of risk-based design are considered. The GBS-SLA (Goal Based Standards-Safety Level Approach) interim guidelines [2] are introduced as an IMO guideline for risk-based structural rules development, after which a method for applying acceptance criteria for fatigue and the technical issues for risk-based structural rules development are explained.

2. STRUCTURAL RELIABILITY THEORY

2.1 General

According to the Japanese Industrial Standards (JIS) [4], reliability is defined as the ability of an item to function as required without fault under the given conditions during the given period. The aim of reliability engineering is to quantify reliability to enable use in system design and maintenance. Concretely, reliability is quantified as the probability that an item will not fail or malfunction.

Structural reliability is reliability for the strength function of structures. In structures, since a fault in the strength function is considered as failure, structural reliability is the property where the state of the structure is not failure. In structural reliability theory, the probability that the structure will fail (probability of failure) is used. According to this definition, the relationship of the probability of failure P_f and reliability R is shown in Eq. (1).

$$P_f = 1 - R \tag{1}$$

If the severity of a failure mode is given by C_D, the quantified risk is formulated as follows:

$$(\text{Risk}) = C_D \times P_f \tag{2}$$

The following sections introduce a calculation method for the probability of failure for cases expressed by a stress-strength model and limit state function, respectively, based on references [5)-7)] of the structural reliability theory.

2.2 Evaluation of Probability of Failure based on Stress-Strength Model

In the structural reliability theory, stress x_s and strength x_r are considered to have uncertainty. Here, we assume that these properties are modeled as independent random variables. In this case, the probability of failure is formulated as follows:

---

[*] Research Institute, ClassNK

$$P_f = P[x_r \leq x_s] \tag{3}$$

Now let us consider the evaluation method for the probability of failure in case the stress takes a certain realization (observed value) s. The failure condition occurs when strength x_r is smaller than the realized value of stress s. This is formulated as follows:

$$P_f = \int_0^s f_R(x_r)dx_r = F_R(s) \tag{4}$$

where $f_R(\cdot)$ and $F_R(\cdot)$ are respectively represented as the probability density function and the cumulative distribution function of strength. The probability that the realization of stress is equal to s is formulated as $f_S(s)ds$, where $f_S(\cdot)$ is the probability density function of stress. Therefore, the probability of failure where stress and strength are random variables can be introduced by the integral of Eq. (4) with respect to the realization as follows:

$$P_f = \int_0^\infty F_R(x_s)f_S(x_s)dx_s \tag{5}$$

Next, as a typical example, the case where stress and strength follow independent normal distributions is considered.

$$x_s \sim N(\mu_s, \sigma_s^2) \tag{6A}$$
$$x_r \sim N(\mu_r, \sigma_r^2) \tag{6B}$$

The safety margin x_m, which is the difference between stress and strength, also follows a normal distribution as in Eq. (7).

$$x_m \sim N(\mu_m, \sigma_m^2) \tag{7A}$$
$$\mu_m = \mu_r - \mu_s \tag{7B}$$
$$\sigma_m^2 = \sigma_r^2 + \sigma_s^2 \tag{7C}$$

The failure condition means the safety margin is negative. Therefore, the probability of failure is evaluated as follows:

$$P_f = P[x_m \leq 0] = P\left[\frac{x_m - \mu_m}{\sigma_m} \leq -\frac{\mu_m}{\sigma_m}\right] = \Phi\left(-\frac{\mu_m}{\sigma_m}\right) = \Phi(-\beta) \tag{8}$$

where $\Phi(\cdot)$ is the standard normal cumulative function and β is a reliability index corresponding to the probability of failure. Using Eqs. (6) and (8), the probability of failure is formulated as shown in Eq. (9). As reference, Table 1 shows the relationship of the reliability index and the probability of failure.

$$P_f = \Phi\left(-\frac{\mu_r - \mu_s}{\sqrt{\sigma_r^2 + \sigma_s^2}}\right) \tag{9}$$

Table 1　Reliability index and probability of failure

Reliability index	Probability of failure
1.0	0.159
2.0	2.27×10^{-2}
3.0	1.35×10^{-3}
4.0	3.17×10^{-5}

2.3 Limit State Function Method

In calculating the probability of failure for general structures, the failure condition is often represented by multiple parameters such as the dimensions, material properties and use environment. In this case, the limit state function is frequently utilized to represent the failure conditions mathematically. The limit state function is shown in Eq. (10) using a random vector $x = (x_1, \cdots, x_{n_r})^T$ and deterministic vector $z = (z_1, \cdots, z_{n_d})^T$.

$$g(x, z) \begin{cases} > 0 & \text{safe} \\ = 0 & \text{limit state} \\ < 0 & \text{failure} \end{cases} \tag{10}$$

Using Eq. (10), the probability of failure is formulated as follows:

$$P_f = \int_{g(x,z) \leq 0} f_X(x) dx \tag{11}$$

Since an analytical solution of Eq. (11) is generally difficult, several approximation methods have been studied. This paper explains three approaches: The Monte Carlo method (MC), the First Order Reliability Method (FORM) and the Second Order Reliability Method (SORM). MC is a numerical simulation method, whereas FORM and SORM are approaches which approximate limit state functions. In the following discussion, the deterministic vector z is omitted from the equations.

2.3.1 Monte Carlo Method (MC)

MC reproduces pseudo-stochastic phenomena by generating random numbers followed by their probabilistic distributions to evaluate the probability of failure approximately. Since the probability of failure for structural reliability is generally very small, a very large number of random numbers is required in order to obtain probability with sufficient accuracy.

Here, the index function is defined depending on the value of the limit state function as follows:

$$I(x) = \begin{cases} 1, & g(x) \leq 0 \\ 0, & g(x) > 0 \end{cases} \tag{12}$$

The expected value of $I(x)$ is evaluated following its definition as shown in Eq. (13).

$$\mathrm{E}[I(x)] = \int I(x) f_X(x) dx = \int_{g(x)>0} 0 \cdot f_X(x) dx + \int_{g(x)\leq 0} 1 \cdot f_X(x) dx = \int_{g(x)\leq 0} f_X(x) dx = P_f \tag{13}$$

Eq. (13) means that the expected value of $I(x)$ is equal to the probability of failure. The expected value of $I(x)$ is the ratio of the number of random numbers (samples) that satisfy the failure condition to the number of generated samples. Assuming the numbers of generated samples and samples that satisfy the failure condition are respectively represented as N and N_f, the approximated value of the probability of failure $\widehat{P}_f$ can be calculated as follows:

$$\widehat{P}_f = \frac{N_f}{N} \tag{14}$$

Since it is obvious that approximate accuracy improves as N is increased, the size of N is determined by an approximation accuracy criterion (threshold). One well-known method uses the coefficient of variety of the probability of failure [7].

2.3.2 First Order Reliability Method (FORM)

FORM linearizes limit state functions (generally non-linear) using the Taylor series and evaluates the probability of failure by using the linearity of the expected value. Since the Taylor series depends on the point of expansion, the choice of this point

is important. In the FORM approach, the consistency of the reliability index is assured by choosing the point of expansion on the limit state function.

For simplicity, the random vector $\boldsymbol{x}$ is assumed to follow an independent normal distribution in the following explanation. If this assumption does not hold, the random vector $\boldsymbol{x}$ is approximated as an independent normal distribution by the Rosenblatt transformation [4], and the following discussion is the same.

The standard normal vector using the expected value and the standard deviation of $\boldsymbol{x}$ is represented as $\boldsymbol{u} = \left(u_1, \cdots, u_{n_r}\right)^T$ in Eq. (15), and linear mapping of the limit state function is represented as $G(\cdot)$.

$$u_i = \frac{x_i - \mu_i}{\sigma_i} \quad (i = 1, \cdots, n_r) \tag{15}$$

Here, a point $\boldsymbol{u}^*$, which is on the limit state and is nearest to the origin, is considered. This point is called the Most Probable Point (MPP). The following optimization problem must be solved to obtain MPP.

$$\text{Min.:} \quad \boldsymbol{u}^T \cdot \boldsymbol{u} \tag{16A}$$
$$\text{s.t.:} \quad G(\boldsymbol{u}) = 0 \tag{16B}$$

The Lagrange multipliers method [8] is adopted for the optimization problem in Eq. (16). Using the Lagrange multiplier λ, the necessary condition is as follows:

$$\nabla(\boldsymbol{u}^T \cdot \boldsymbol{u}) + \lambda \nabla G(\boldsymbol{u}) = 0$$
$$\therefore \boldsymbol{u} = -\frac{\lambda}{2} \nabla G(\boldsymbol{u}) \tag{17}$$

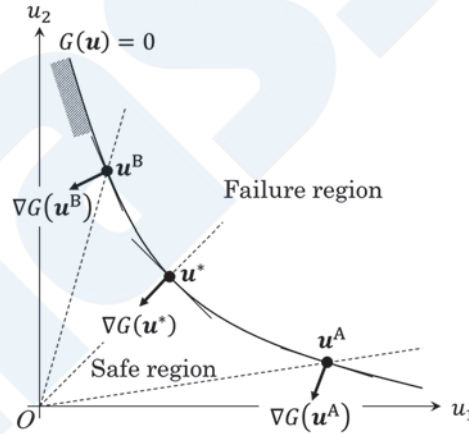Eq. (17) means that the position vector of MPP is directly opposite the gradient vector at MPP (Fig. 1).

Fig. 1　Relationship between position vectors and gradient vectors

Next, the limit state function is linearized by using the Taylor series about MPP, as follows:

$$G(\boldsymbol{u}) \approx G_l(\boldsymbol{u}) = \nabla^T G(\boldsymbol{u}) \cdot (\boldsymbol{u} - \boldsymbol{u}^*) \tag{18}$$

Since the linearized limit state function $G_l(\boldsymbol{u})$ is the sum of independent random variables, the expected value and its variance are obtained as follows:

$$\text{E}[G_l(\boldsymbol{u})] = -\nabla^T G(\boldsymbol{u}) \cdot \boldsymbol{u}^* \tag{19A}$$
$$\text{Var}[G_l(\boldsymbol{u})] = |\nabla G(\boldsymbol{u})|^2 \tag{19B}$$

According to Eq. (8), the probability of failure is obtained as follows:

$$P_f \approx P[G_l(\boldsymbol{u}) \leq 0] = \Phi\left(-\frac{\mathrm{E}[G_l(\boldsymbol{u})]}{\sqrt{\mathrm{Var}[G_l(\boldsymbol{u})]}}\right) = \Phi\left(\frac{\nabla^T G(\boldsymbol{u})}{|\nabla G(\boldsymbol{u})|} \cdot \boldsymbol{u}^*\right) = \Phi(-\beta)$$

$$\therefore \beta = -\frac{\nabla^T G(\boldsymbol{u})}{|\nabla G(\boldsymbol{u})|} \cdot \boldsymbol{u}^* \tag{20}$$

Since the position vector of MPP is opposite the gradient vector at MPP according to Eq. (17), the reliability index is formulated as follows:

$$\beta = -\frac{\nabla^T G(\boldsymbol{u})}{|\nabla G(\boldsymbol{u})|} \cdot \boldsymbol{u}^* = \left(-\frac{\nabla^T G(\boldsymbol{u})}{|\nabla G(\boldsymbol{u})|} \cdot \frac{\boldsymbol{u}^*}{|\boldsymbol{u}^*|}\right) \cdot |\boldsymbol{u}^*| = |\boldsymbol{u}^*| \tag{21}$$

Eq. (21) means that the reliability index is equal to the distance between the origin and MPP. Consequently, the reliability index in FORM can be obtained as the distance by solving the optimization problem in Eq. (16). To solve the optimization problem in Eq. (16), an iteration method such as the Rackwitz-Fiessler method are required [5][7].

Finally, the principle of FORM is illustrated in Fig. 2. As shown this figure, in FORM, the probability of failure is evaluated by using a one-dimensional standard normal density function having an axis along the gradient vector of limit state function. As shown in the figure, changes in the failure region due to the non-linearity of the limit state function cause approximate error in the probability of failure. However, because the effect on the probability of failure decreases as the distance becomes larger, the degree of this approximate error is regarded as negligible. On the other hand, when the accuracy requirement is higher (error of probability of failure is minimized further), it is preferrable to use an evaluation method that considers the curvature of the limit state function such as the Second Order Reliability Method (SORM), which is introduced in Section 2.3.3.
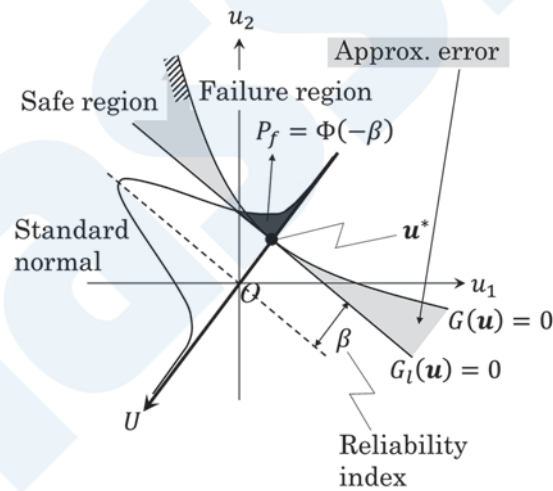

Fig. 2　Principle of FORM

2.3.3　Second Order Reliability Method (SORM)

SORM approximates the limit state function in a second-order Taylor series. Although several methods have been proposed, and the author's work [9] will be briefly introduced in this paper.

Under the assumption that the random vector $\boldsymbol{x}$ follows an independent normal distribution, the limit state function is approximated by a second-order Taylor series about MPP.

$$g(\boldsymbol{x}) \approx g_s(\boldsymbol{x}) = \boldsymbol{x}^T \boldsymbol{A} \boldsymbol{x} + \boldsymbol{b}^T \boldsymbol{x} + c \tag{22}$$

The limit state function $G_s(\boldsymbol{u})$ mapped by standard normalization of Eq. (22) is formulated as follows:

$$G_s(\boldsymbol{u}) = \boldsymbol{u}^T \boldsymbol{A}' \boldsymbol{u} + {\boldsymbol{b}'}^T \boldsymbol{u} + c' \tag{23}$$

According to the author's work [9], the probability of failure can be evaluated by dividing the cases depending on whether the sign of the eigenvalue of $\boldsymbol{A}'$ is positive or negative. Details will be omitted here due to their complexity, but the approximate accuracy evaluated by this method is higher than that evaluated by FORM.

2.4 Categories of Uncertainty

In evaluation of the probability of failure, the structural reliability theory supposes that the uncertainty of factors such as stress or strength is represented as a reasonable model. However, uncertainty can be divided into various categories. In structural reliability theory, the following categorization is generally considered [10].

✓ Aleatory uncertainty: Essential uncertainty such as physical phenomena, e.g., wave height and material property. Aleatory uncertainty cannot be reduced by collecting knowledge and information.

✓ Epistemic uncertainty: Uncertainty due to a lack of information. Epistemic uncertainty can be decreased by technical improvements, e.g., model uncertainty including formulae in rules.

Whereas the uncertainty inherent in a certain type of performance is aleatory uncertainty, epistemic uncertainty is related to the degree to confidence or reliability of the information. While a grasp of aleatory uncertainty allows a statistical understanding of the target phenomenon, an understanding of epistemic uncertainty makes it possible to understand the validity of the statistical model and the sources of uncertainty that should be reduced. An engineering application of the structural reliability theory to structural problems only becomes possible when these uncertainties are quantified. The basic techniques for quantifying uncertainty (i.e., uncertainty quantification) have been organized mathematically in the literature [11].

3. DIFFERENCE OF RELIABILITY DESIGN AND RISK-BASED DESIGN CONSIDERING DESIGN OPTIMIZATION PROBLEM

3.1 Reliability-Based Design Optimization

This section considers reliability-based design and its application to design optimization problems. This approach is called Reliability-Based Design Optimization (RBDO). RBDO searches for the design solution where the desired performance is minimized (or maximized) subject to the constraints of the probability of failure. When the design vector and random vector are represented as $\boldsymbol{d} = (d_1, d_2, \cdots, d_n)^T$ and $\boldsymbol{x} = \left(x_1, x_2, \cdots, x_{n_r}\right)^T$, respectively, a RBDO problem can be formulated as follows:

$$\text{Min.}: f(\boldsymbol{d}) \tag{24A}$$

$$\text{s.t.}: P\big[g_j(\boldsymbol{d}, \boldsymbol{x}) \leq 0\big] \leq \Phi\big(-\beta_j^{\text{Tar}}\big) \ (j = 1, \cdots, m) \tag{24B}$$

where $f(\cdot)$, m, β_j^{Tar} are an objective function (performance to be minimized, e.g., weight), the number of limit state functions and the target reliability index of the jth limit state function, respectively. The target reliability index provides the upper limit of the probability of failure (a lower limit of reliability or target reliability) for each failure mode and is generally set by the designer.

3.2 Risk-Based Design Optimization

This section considers the application of risk-based design to design optimization problems, which is called risk-based design optimization. The optimal solution is obtained by considering risk, where risk is regarded as objective constraint functions. In this paper, the quantified risk in Eq. (2) is regarded as the expected value of the cost of failure, and an optimization problem to minimize the sum of the expected value of the cost of failure and costs from the other sources C_0 (called initial cost) is considered. This problem can be formulated as follows:

$$\text{Min.}: f(\boldsymbol{d}) = C_0(\boldsymbol{d}) + \sum_{j=1}^{m} C_{Dj}(\boldsymbol{d}, \boldsymbol{x}) \cdot P_{fj} \tag{25A}$$

$$\text{where}: P_{fj} = P\big[g_j(\boldsymbol{d}, \boldsymbol{x}) \leq 0\big] \ j = 1, \cdots, m \tag{25B}$$

For simplicity, here, severity C_D is considered to be independent of the design variables, and a single failure mode is considered for simplicity. Under these assumptions, the objective function in Eq. (25) can be reformulated as follows:

$$f'(\boldsymbol{d}) = \alpha \cdot C_0(\boldsymbol{d}) + (1 - \alpha) \cdot P_f \tag{26A}$$

$$\text{where:}\, \alpha = \frac{1}{C_D + 1} \tag{26B}$$

Eq. (26A) is the linear weighted sum of the initial cost and the probability of failure using the weighting factor α. This means that a multi-objective design optimization problem to minimize the initial cost and the probability of failure is solved simultaneously. Eq. (25) can be reformulated as follows:

$$\text{Min.:}\, C_0(\boldsymbol{d}) \tag{27A}$$

$$\text{Min.:}\, P_f(\boldsymbol{d}, \boldsymbol{x}) \tag{27B}$$

Optimal solutions of the multi-objective design optimization problem in Eq. (27) are provided as a Pareto front, which is a set of undominated solutions called Pareto solutions. Fig. 3 shows an illustration of Pareto solutions in an objective function space. As shown in this figure, a Pareto solution can be chosen in accordance with the value of the weighting factor α. That is, since the weighting factor α is determined by severity according to Eq. (26B), a Pareto solution can be chosen according to severity.
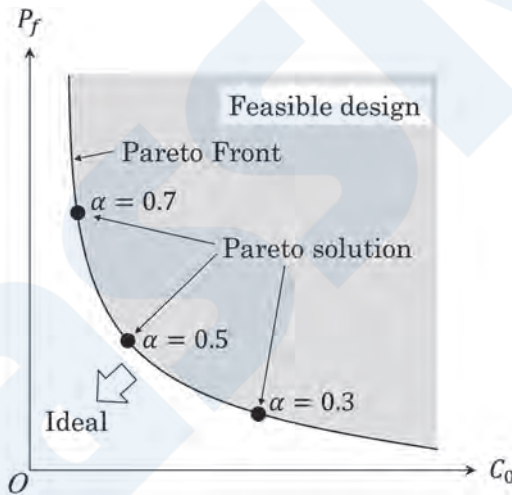

Fig. 3   Pareto solutions of risk-based design optimization

Finally, the interpretation of the Pareto solution in risk-based design will be considered. As an example, Fig. 4 shows the feasible region when the failure probability of the Pareto solution at $\alpha = 0.7$ is set as the upper limit. As shown in this figure, the design that minimizes the initial cost C_0 in the feasible region is the Pareto solution at $\alpha = 0.7$. Thus, the Pareto solution can be interpreted as the result of searching for the solution that minimizes C_0 subject to the limit of the probability of failure. Although this point is essentially the same as in the RBDO in the previous section, the difference between the two is whether the target reliability index is determined by the designer, as in RBDO, or by severity, as in the risk-based design optimization. In other words, the characteristic feature of the risk-based design optimization is that the threshold is determined based on values that are objective and reasonable, namely, severity.
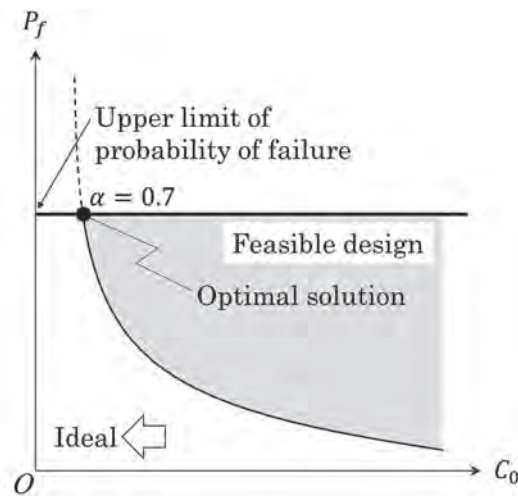
Fig. 4 Interpretation of Pareto solution

4. APPLICATIONS OF RISK-BASED DESIGN

4.1 GBS-SLA Interim Guideline

In the past, the structural rules for the construction of ships engaged in international voyages were substantially managed by classification societies. However, bulk carrier and oil tanker accidents occurred frequently from the 1980s, which heightened the momentum toward greater involvement of IMO in establishing structural rules for ships. Against this background, IMO MSC77 (Maritime Safety Committee) held in 2003 agreed to establish the GBS, a top-down rule system. Based on this agreement, the IMO began the development of rules, and the IACS also started the development of CSR (Common Structural Rule) in response to the agreement. The CSR conforming to the GBS is generally regarded as an extremely prescriptive rule with a low degree of freedom. Due to these characteristics of the CSR, a different approach has been required to deal with new designs for ships such as new concept ships. Therefore, the need to develop GBS-SLA based on SLA, which sets quantitative safety levels, has been emphasized, and it was agreed that risk should be used as a quantitative index of safety. In addition, the Guidelines for Formal Safety Assessment (FSA) [3],which was issued prior to the discussions on the GBS, was also a focus of attention due to its affinity with SLA. As a result, GBS-SLA was developed referring to many of the approaches in FSA. Table 2 shows the history of moves related to the GBS-SLA.

The GBS-SLA is composed of the following five tiers.

I. Goals
II. Functional requirements
III. Verification of conformity
IV. Rules and regulations for ships
V. Industry practices and standards

Among the five tiers, Tiers I and II are included in IMO conventions and Tier IV, which is the detailed technical rules, is included in IMO Codes and the classification society rules. This paper will introduce Tiers I and II.

Goals (Tier I) are high-level objectives which are to be met and should reflect required safety levels. The safety level means the maximum measure of exposure to risk, and should be a level that is acceptable to society. According to the Interim Guideline, the required safety level can be specified explicitly by a quantitative safety level or implicitly by a process to be used for achieving the highest practicable safety level. Goals are established by the Maritime Safety Committee.

Functional requirements (Tier II) provide the criteria to be satisfied in order to meet the goals and are established by IMO in the responsible Committees. Functional requirements should comply with the following conditions:

1. Cover all areas necessary to meet the goal.
2. Address all relevant hazards. Methods for hazard identification as well as their ranking are described in the FSA Guidelines.
3. Provide criteria for verification of the compliance of Tier IV rules.
4. Be independent of specific technologies to allow for further technological development.

5. Clearly describe the functions that should be achieved.

GBS-SLA requires procedures such as identification of hazards and quantification of risks which are defined in the FSA.

Table 2   History of GBS-SLA

Year	IMO	IACS
~1999	Complete loss accidents of large bulk carriers occurred.	
1999	The Erika broke in two and sank of the coast of Brittany, France.	
2001	The FSA Guidelines were approved in MSC74 and MSPC47(2002) as the IMO Rule-Making Process.	
2002	The oil tanker MV Prestige sank off the coast of Galicia, Spain.	
2003	Development of the GBS was agreed at MSC77.	Development of CSR was agreed in the 47th Council, and development began.
2004	Full-scale discussion to establish GBS began from MSC78.	
2005	GBS-SLA was proposed at MSC80.	CSR was adopted in the 52nd Council.
2006		CSR was enacted.
2010	IMO GBS was adopted in MSC87.	
2012	The SLA-based Interim Guideline work plan was endorsed at MSC90, and draft elements to be considered in working groups were agreed.	
2017	Revisions to FSA Guidelines were approved at MSC98 and MPEC72 (2018).	
2018	· Application of the corresponding steps of the FSA Guidelines was discussed at MSC99. · The draft of the Interim Guideline was approved, and agreement was reached on preparation of the related MSC Circular.	
2019	The Interim Guideline was approved at MSC100.	

4.2   Acceptance Criteria for Fatigue

The principle of risk-based design is that the target reliability is determined based on risk criteria. As one example of structural rule development based on this principle, this section introduces the method for determining the acceptance criteria for fatigue crack damage of hull structures.

Since a hull structure can be regarded as a large-scale welded structure, it contains many welded joints. This means there are multiple evaluation points for fatigue strength in the hull structure. Fatigue strength verification is performed for each of these points using the design S-N diagram. In general, this verification is based on the degree of cumulative fatigue damage D, and is formulated as follows in the Comprehensive Revision of Part C of the ClassNK Rules:

$$\eta \cdot D \leq 1 \tag{28}$$

where η is a correction factor which varies depending on the evaluation point and is determined by whether the point is related to the functionality of the compartment.

For example, let us consider the criteria for fatigue strength using the risk-based design based on Eq. (28). It is assumed that cumulative fatigue damage can be represented by the design vector $\boldsymbol{d}$ and random vector $\boldsymbol{x}$, and the target reliability index for a certain part is β^{Tar}. Then, a constraint using reliability is formulated as follows:

$$P[g(\boldsymbol{d}, \boldsymbol{x}) \leq 0] \leq \Phi(-\beta^{\text{Tar}}) \tag{29A}$$
$$\text{where: } g(\boldsymbol{d}, \boldsymbol{x}) = 1 - D(\boldsymbol{d}, \boldsymbol{x}) \tag{29B}$$

As mentioned in the previous chapter, the left side of Eq. (29A), reliability analysis, is difficult to solve analytically. In addition, repeated reliability analyses for each target part are practically complicated and time-consuming in the practical design process. Considering these points, the Partial Safety Factor (PSF) is often adopted for structural rules and standards from the viewpoint of ease of use by general designers. As a very simple example for understanding the PSF, it is assumed that a constraint equal to Eq. (29A) can be obtained as follows by using the expected value vector $\boldsymbol{\mu}$ and the PSF for fatigue strength η_{PSF}.

$$g_{\mathrm{PSF}}(\boldsymbol{d}, \boldsymbol{\mu}) = 1 - \eta_{\mathrm{PSF}} \cdot D(\boldsymbol{d}, \boldsymbol{\mu}) \geq 0 \tag{30}$$

where the PSF η_{PSF} is evaluated in accordance with the target reliability index β^{Tar}, and is organized in the form of a partial safety factor table in rules and standards. One method for evaluating the PSF uses the MPP, as mentioned in Chapter 3.

The next problem is how target reliability should be determined. In reliability-based design, designers are allowed to determine the target reliability based on their individual experience. However, when rationality and transparency are required, for example, in ship structural rules, the target reliability should be determined by the risk-based design approach. On the other hand, if the target is fatigue crack failure, the direct effect on the total hull structure is small, but since compartment functions may be lost, it is necessary to consider risk from the viewpoint of maintaining the functions of compartments. In other words, it is necessary to conduct a risk assessment for each member and determine the target reliability corresponding to the risk level as shown in Fig. 5. Use of this concept may also make it possible to identify members that do not require a detailed evaluation.
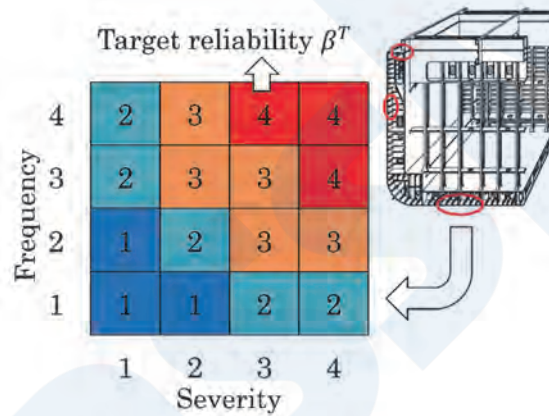

Fig. 5　Risk assessment and determination of the target reliability index for each part

In the concept of risk-based design, the most important task is to create and organize a database. For example, focusing on the watertightness of compartments, it is possible to generalize the data by organizing the degree to which fatigue crack failures that led to loss of watertightness occurred in the past, and recording this information together with related data such as the crack dimensions. Based on this, it is also possible to identify members that lose watertightness easily and the severity of the problem. If necessary, a formula for estimating severity should also be studied.

If this information is arranged in the form of a PSF table, the criteria for fatigue strength using the concept of the risk-based design can be introduced through this process. However, it can be assumed that many technical issues will arise when actually implementing the process described in this paper. The next section discusses those issues and briefly introduces the initiatives of ClassNK in this connection.

4.3　Technical Issues and Initiatives of ClassNK

4.3.1　Collection of Risk Information

As mentioned above, creating a high-quality database is important for using the concept of risk-based design. Focusing on this database, one issue is what items should be used in the classification and recording of accident data. Careful planning and the knowledge of experts are required in order to determine the number of input variables and prerequisites necessary in the severity estimation formula which is constructed after creating the database. Collecting the widest possible range of data and updating the database with appropriate content are also important for maintaining database quality. This will require the development of an environment in which data sharing and reporting are possible in society as a whole.

ClassNK is examining databasing of the information which it acquires through classification surveys and expansion of this to various services. As part of this, we are studying extraction and organization of data specific to risk information and activities to utilize that data in risk assessments and setting of risk criteria. In addition, we are also examining vulnerability reports, which are a framework for obtaining information from a wide range of sources. In this connection, Yamada and Kajita have reported on a framework for collecting and utilizing risk-specific information in the entire maritime cluster in this issue of ClassNK Technical Journal.

4.3.2 Uncertainty Quantification

Uncertainty quantification is important since risk-based design is based on the concept of the structural reliability theory. In particular, in the design of a hull structure, it must be remembered that the uncertainty of the stresses affecting a ship varies greatly depending on the route and weather conditions. Epistemic uncertainty is reduced by utilizing data, and a highly accurate analysis that is closer to reality can be expected.

ClassNK has studied the following topics as research for establishing highly accurate analysis and evaluation techniques.

✓ Research to identify the oceanographic conditions that ships encounter when navigating in actuals seas with high accuracy by using Automatic Identification System (AIS) data, and quantitative assessment of the effect of maneuvering.

✓ Research to reduce wave height error caused by tidal currents.

✓ Research on equations for estimating collapse strength after elastic buckling with high accuracy based on a physically meaningful background.

ClassNK also conducts daily activities to expand this research to the development of risk-based structural rules based on these activities.

5. CONCLUSION

This paper introduced the structural reliability theory, which is the basis of risk-based design, and discussed the difference between reliability-based and risk-based design by using a design optimization problem. As further developments of risk-based design, after touching on GBS-SLA, which is a guideline for the development of structural rules, an example of the development of acceptance criteria for fatigue using the concept of risk-based design and related technical issues were also discussed. The author hopes this paper will be of assistance for incorporation in risk-based design.

ACKNOWLEDGMENT

REFERENCES

1) S. Sakai and H. Kobayashi: Risk-based design, Journal of the Japan Society of Mechanical Engineers, Vol. 106, No. 1020 (2003), pp. 853-856 (in Japanese)

2) IMO: MSC. 1/Circ. 1596 (2019), Interim guidelines for development and application of IMO Goal-Based Standards Safety Level Approach

3) IMO: MSC-MEPC. 2/Circ. 12/Rev. 2 (2018), Revised Guidelines for Formal Safety Assessment (FSA) for Use in the IMO Rule Making Process

4) JISZ8115:2019 (in Japanese)

5) S. K. Choi, R. V. Grandhi and R. A. Canfield: Reliability-based Structural Design, Springer, 2007

6) M. Ichikawa: Structural reliability engineering－Reliability method for strength design and life prediction－ (Second Ed.), Kaibundo, 1996 (in Japanese)

7) Y. Murotsu, S. Shaowen and M. Yonezawa: System reliability engineering, Kyoritsu shuppan, 1996 (in Japanese)

8) (For example) H. Konno and H. Yamashita: Non-linear programming, Nikkagiren, 1978 (in Japanese)

9) Y. Gon, H. Tanaka, M. Ito and N. Kogiso: Proposal and evaluation of modified response surface single loop method for reliability-based design optimization, Transactions of the JSME (in Japanese), Vol. 85, No. 874 (2019), DOI: 10.1299/transjsme.19-00027

10) Der Kiureghian and O. Ditlevsen: Aleatory or epistemic? Does it matter?, Structural Safety, Vol. 31, No. 2 (2009), pp. 105-112.

11) Soize: Uncertainty Quantification, Springer, 2017

Development of Local Scantling Formulae for Plate Members

Tetsuo OKADA[*]

1. INTRODUCTION

Plate members are one of the most essential elements in a ship structure consisting of stiffened panels. Plates are subjected to bending due to lateral pressure from water pressure, cargoes, etc. In-plane stresses also act on plates used in stiffeners, primary supporting members and the members of hull girders, and the magnitude of that stress is particularly remarkable for bending and shearing of hull girders. In the design of plate members, it is necessary to evaluate various damage modes, including bending under lateral pressure and buckling and yielding under in-plane loading. In particular, however, local strength equations for bending due to lateral pressure are extremely important for determining the initial plate thickness in the earliest stage of basic design [1].

Theories of the strength of plate members for out-of-plane (lateral) loading have been established based on plastic design, rigid-plastic analysis and other approaches [2][3], and simplified plate local scantling formulae based on those theories are provided in ship classification rules. The former Rules of Nippon Kaiji Kyokai (ClassNK) were based on safety factors which were given empirically for 3-point plastic hinge formation of a plate strip between stiffeners [4], and considered the reduction of fully plastic moment under the simultaneous action of lateral loading and in-plane stress by using the von Mises yield criterion for transversely framed structures and Tresca's yield criterion for longitudinally framed structures [5]. In the Common Structural Rules (CSR) [6], correction is performed by using a permissible bending stress coefficient set by an elasto-plastic FEM analysis, in which in-plane stress is also made to act simultaneously based on the formation of a 3-point plastic hinge. The safety of these scantling formulae has been confirmed from the actual track records over many years. However, for application to more complex combinations of structural behaviors and loads, reviewing those formulae to develop scantling formulae which have a theoretical backing and a clearer correspondence with damage was an issue. This paper presents an outline of the following items, which were carried out as part of that review [7][8][9].

- As the basic theory that serves as the foundation for the scantling formulae, the reduction of the fully plastic moment by superimposition of bending and in-plane stress was expressed by the von Mises yield criterion for both the transversely framed and longitudinally framed structural systems. Furthermore, theoretical study by obtaining the 2-point and 3-point plastic hinge formation loads, also considering the additional lateral load (term proportional to the curvature of plate bending) generated accompanying in-plane stress, was adopted as a basis.

- The influence of in-plane stress on the lateral pressure that causes a certain designated residual deflection in analysis by elasto-plastic FEM was investigated in detail and compared with the results by the theoretical equations, and a rational in-plane stress influence factor was proposed for plate members of laterally and longitudinally framed structures.

- In the conventional ship classification society rules, the aspect ratio (ratio of the lengths of the longer and shorter edges) was considered independently from the effect of in-plane stress. However, in cases where in-plane stress influence factors are differentiated for a transversely framed structure and a longitudinally framed structure, discontinuity arises when the aspect ratio is larger or smaller than 1, and it is not possible to reflect the actual phenomena. Therefore, an equation for interpolation of the in-plane stress factor between lateral and longitudinal framing systems was proposed for small aspect ratios.

[*] Faculty of Engineering, Yokohama National University

2. THEORETICAL EQUATION FOR PLATE BENDING STRENGTH CONSIDERING INFLUENCE OF IN-PLANE STRESS

2.1 Influence of In-Plane Stress on Fully Plastic Moment

2.1.1 Transversely Framed Structures

Chapter 2 and Chapter 3 consider the case of plates with an extremely large aspect ratio, and therefore treat bending of plates as bending of a plate strip. First, as shown in Fig. 1, the case in which a member receives in-plane stress in the direction perpendicular to the longer edge of the plate as a transversely framed structure is considered. The object of study is the bending behavior of the portion of the plate strip indicated by the hatching, whose span as a beam is assumed to be the spacing between stiffeners.
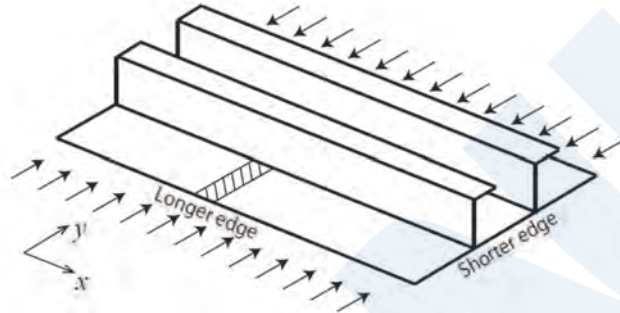
Fig. 1　Model of plate bending (transversely framed structure)

In this case, because bending stress and in-plane stress act in the same direction, the fully plastic moment M_p decreases according to Eq. (1) in comparison with the case without in-plane stress. The former ClassNK Rules considered the influence of in-plane stress based on this equation [5].

$$M_P = \frac{\alpha \sigma_Y t^2}{4}\left\{1 - \left(\frac{\sigma_y}{\sigma_Y}\right)^2\right\} \qquad (1)$$

t : plate thickness
σ_y : in-plane stress acting in y direction
σ_Y : specified yield stress of material
α : Because the direction orthogonal to the stress perpendicular to the y direction is constrained, α is considered as a coefficient which expresses the fact that stress perpendicular to the y direction exceeding the specified yield stress is generated when the material yields by the von Mises yield criterion, and is given by Eq. (2):

$$\alpha = \sqrt{\frac{1}{1 - v_p + v_p{}^2}} = \frac{2\sqrt{3}}{3} = 1.15 \qquad (2)$$

v_p : Poisson's ratio in plastic state; $v_p = 0.5$

From Eq. (1), the effect of the action of in-plane stress on the fully plastic moment can be obtained from the following equation as the ratio of M_p and the fully plastic moment M_{P0} when in-plane stress does not act.

$$\frac{M_P}{M_{P0}} = 1 - \left(\frac{\sigma_y}{\sigma_Y}\right)^2 \qquad (3)$$

Because the required plate thickness t is inversely proportional to the square root of this, it is obtained as a ratio to t_0 when an axial load does not act as follows:

$$\frac{t}{t_0} = \frac{1}{\sqrt{1 - \left(\frac{\sigma_y}{\sigma_Y}\right)^2}} \qquad (4)$$

Fig. 2 shows this, together with the requirement in the CSR. It can be understood that the CSR requirement shown by the thin broken line is a considerable larger factor than Eq. (4).
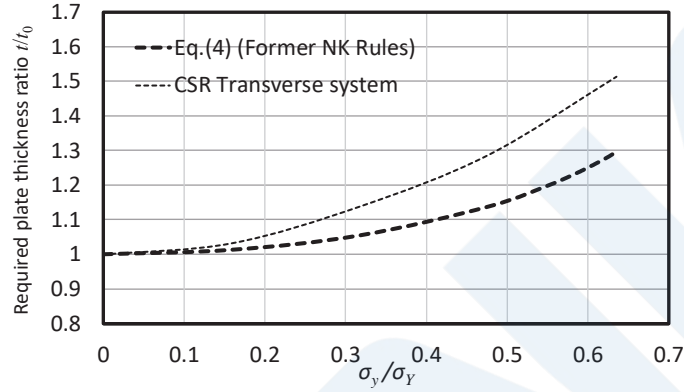

Fig. 2   Required plate thickness ratio depending on in-plane stress (transversely framed structure)

2.1.2   Longitudinally Framed Structures

In longitudinally framed structures, in-plane stress acts in the direction parallel to the stiffeners in Fig. 1, and in-plane stress and bending stress are orthogonal. In the former ClassNK Rules, the influence factor was formulated according to Tresca's yield criterion. Here, however, same as the transversely framed structure, an influence factor was newly derived using the von Mises yield criterion.

Assuming σ_{yu} is the bending stress of the plate upper surface, σ_{yl} is the bending stress of the plate lower surface, and σ_x is the in-plane stress acting in the x direction, the von Mises yield criteria for the plate upper and lower surfaces are given by the following Eqs. (5) and (6), respectively.

$$\sigma_{yu}{}^2 - \sigma_{yu}(\sigma_x + v_p\sigma_{yu}) + (\sigma_x + v_p\sigma_{yu})^2 = \sigma_Y{}^2 \qquad (5)$$

$$\sigma_{yl}{}^2 - \sigma_{yl}(\sigma_x + v_p\sigma_{yl}) + (\sigma_x + v_p\sigma_{yl})^2 = \sigma_Y{}^2 \qquad (6)$$

Next, if η is the range of σ_{yu} when a plastic hinge forms for the given plate thickness, the condition at which the axial load in the y direction becomes 0 is given as follows:

$$\sigma_{yu} \cdot \eta t + \sigma_{yl} \cdot (1 - \eta)t = 0 \qquad (7)$$

$$\therefore \sigma_{yu} = -\frac{1 - \eta}{\eta}\sigma_{yl} \qquad (8)$$

Substituting Eq. (8) into Eq. (5), and arranging the equation using $v_p = 0.5$,

$$\frac{3}{4}\left(\frac{1 - \eta}{\eta}\right)^2 \sigma_{yl}{}^2 + \sigma_x{}^2 = \sigma_Y{}^2 \qquad (9)$$

On the other hand, Eq. (6) can be transformed to,

$$\frac{3}{4}\sigma_{yl}^2 + \sigma_x^2 = \sigma_Y^2 \qquad (10)$$

To satisfy Eq. (9) and Eq. (10) simultaneously, it can be understood that $\eta = 1/2$, and from Eq. (8), $\sigma_{yu} = -\sigma_{yl}$. Let's consider the meaning of this on the von Mises yield criterion curve in Fig. 3. If bending is applied gradually from a condition (point A) in which only an axial stress $\sigma_x(>0)$ acts, the lower surface will yield first (point B), but the Poisson's ratio changes to 0.5 due to plasticizing before full section yielding is achieved, and $\sigma_{yu} = -\sigma_{yl}$ irrespective of the value of σ_x. However, this is the case where σ_x is maintained. In reality, if bending is applied up to full section yielding, σ_x will be released from this position, the one-dot chain line will shift to the left, and the absolute values of σ_{yu} and σ_{yl} can increase to $\alpha\sigma_Y$.
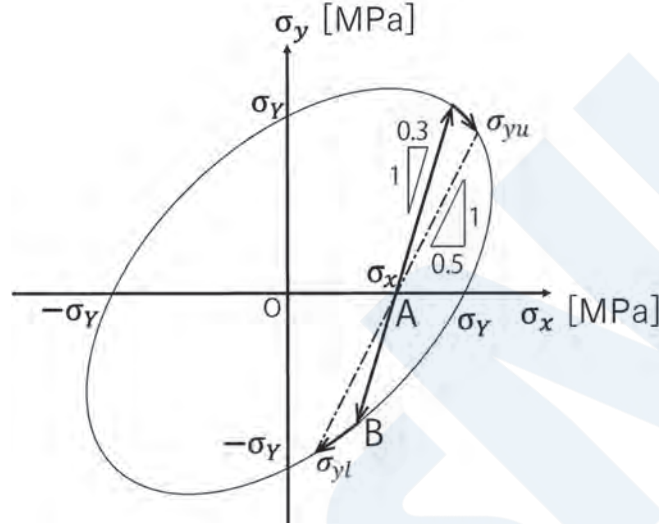

Fig. 3　Von Mises yield curve for plate bending in longitudinally framed structure

The following solution is obtained when Eqs. (9) and (10) are solved for σ_{yl}.

$$\sigma_{yl} = \frac{2\sqrt{3}}{3}\sqrt{\sigma_Y^2 - \sigma_x^2} = \alpha\sqrt{\sigma_Y^2 - \sigma_x^2} \qquad (11)$$

Therefore, the fully plastic moment M_p is given by Eq. (12).

$$M_P = \sigma_{yl} \cdot \frac{t}{2} \cdot \frac{t}{2} = \frac{\alpha\sigma_Y t^2}{4}\sqrt{1 - \left(\frac{\sigma_x}{\sigma_Y}\right)^2} = M_{P0}\sqrt{1 - \left(\frac{\sigma_x}{\sigma_Y}\right)^2}$$

$$\therefore \frac{M_P}{M_{P0}} = \sqrt{1 - \left(\frac{\sigma_x}{\sigma_Y}\right)^2} \qquad (12)$$

Because the required plate thickness t is inversely proportional to the square root of Eq. (12), the ratio of t and the required thickness t_0 when an axial load does not act on the member is as follows:

$$\frac{t}{t_0} = \frac{1}{\left\{1 - \left(\frac{\sigma_x}{\sigma_Y}\right)^2\right\}^{\frac{1}{4}}} \qquad (13)$$

Fig. 4 shows the required plate thickness ratio according to Eq. (13) (red solid line) in comparison with the ratios in the former ClassNK Rules (black bold broken line) and CSR (black thin broken line). The in-plane stress influence factor given by the

ClassNK equation based on Tresca's yield criterion shows there is no influence of in-plane stress until the in-plane stress reaches $0.5\,\sigma_Y$, and the influence rises sharply after exceeding that value. Likewise, the influence of in-plane stress in the CSR is also zero until in-plane stress reaches $0.2\,\sigma_Y$, but then takes a value close to that given by the above Eq. (13), even though the formulation is different.

Table 1 summarizes the influence of in-plane stress on the fully plastic moment obtained by the von Mises yield criterion and the plate thickness ratios based on it.
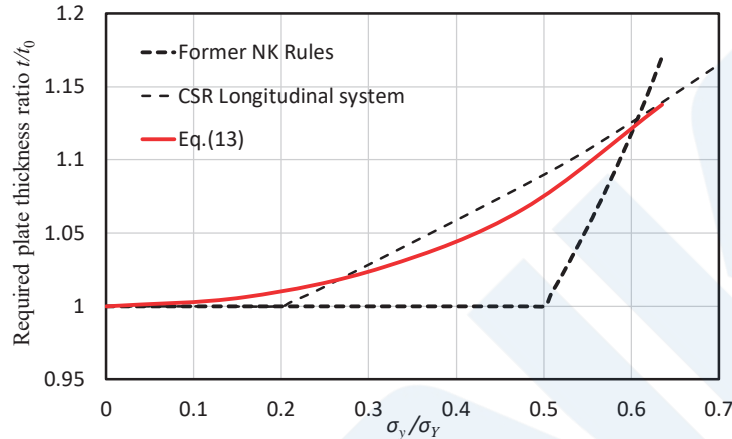
Fig. 4　Required plate thickness ratio by in-plane stress (longitudinally framed structure)

Table 1　Influence of in-plane stress on fully plastic moment

	Strength ratio	Required thickness ratio (Inverse square root of strength ratio)
Transversely framed structure (In-plane stress perpendicular to the longer edge)	$\dfrac{M_P}{M_{P0}} = 1 - \left(\dfrac{\sigma_y}{\sigma_Y}\right)^2$	$\dfrac{t}{t_0} = \dfrac{1}{\sqrt{1 - \left(\dfrac{\sigma_y}{\sigma_Y}\right)^2}}$
Longitudinally framed structure (In-plane stress parallel to the longer edge)	$\dfrac{M_P}{M_{P0}} = \sqrt{1 - \left(\dfrac{\sigma_x}{\sigma_Y}\right)^2}$	$\dfrac{t}{t_0} = \dfrac{1}{\left\{1 - \left(\dfrac{\sigma_x}{\sigma_Y}\right)^2\right\}^{1/4}}$

2.2　Influence of Additional Lateral Loading Accompanying In-Plane Stress

2.2.1　Formulation Considering Additional Lateral Loading

In transversely framed structures, the influence of additional lateral loading generated by in-plane stress is remarkable. To formulate this influence, a both-end fixed beam on which a tensile axial load N and a uniformly-distributed load w act, as shown in Fig. 5, will be considered. At this time, the equation related to deflection v considers the term $N\,d^2v/dx^2$ for additional lateral loading term associated with the axial load, and is as follows, where E is young's modulus and I is the moment of inertia of area.

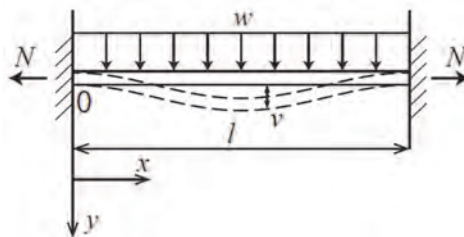$$EI\frac{d^4v}{dx^4} = w + N\frac{d^2v}{dx^2} \qquad (14)$$

Fig. 5　Bending of plate under tensile axial load

If this equation is solved for the appropriate boundary condition, the load w_{2H-t} necessary for the formation of a 2-point plastic hinge and the deflection v_{2H-t} at that time, and the load w_{C-t} necessary for the formation of a 3-point plastic hinge and the accompanying deflection v_{C-t} is obtained as follows:

$$w_{2H-t} = \frac{2NM_P(e^{\beta l} - 1)}{EI(\beta l + \beta l e^{\beta l} - 2e^{\beta l} + 2)} \tag{15}$$

$$v_{2H-t} = \frac{w_{2H-t}l(1 - e^{\frac{\beta l}{2}})}{2\beta N(1 + e^{\frac{\beta l}{2}})} + \frac{w_{2H-t}l^2}{8N} \tag{16}$$

$$w_{C-t} = \frac{NM_P}{EI}\left(\frac{1 + e^{\frac{\beta l}{2}}}{1 - e^{\frac{\beta l}{2}}}\right)^2 \tag{17}$$

$$v_{C-t} = -\frac{\frac{M_P}{EI} + \frac{w_{C-t}}{N}}{\beta^2(1 + e^{\beta l})}\left(e^{\frac{\beta l}{2}} - 1\right)^2 + \frac{w_{C-t}l^2}{8N} \tag{18}$$

where, $\beta = \sqrt{\frac{N}{EI}}$

When a compressive axial load acts, solution of an equation in which the signs of the term $N\, d^2v/dx^2$ in Eq. (14) are reversed, where compression is taken as positive, gives the load w_{2H-c} necessary for the formation of a 2-point plastic hinge and the deflection v_{2H-c} at that time, and the load w_{C-c} necessary for the formation of a 3-point plastic hinge and the deflection v_{C-c} at that time, as follows.

$$w_{2H-c} = \frac{2NM_P(-1 + \cos\beta l)}{EI(\beta l \cdot \sin\beta l - 2 + 2\cos\beta l)} \tag{19}$$

$$v_{2H-c} = \frac{w_{2H-c}l \cdot \sin\frac{\beta l}{2}}{2\beta N(1 + \cos\frac{\beta l}{2})} - \frac{w_{2H-c}l^2}{8N} \tag{20}$$

$$w_{C-c} = \frac{NM_P}{EI}\frac{1 + \cos\frac{\beta l}{2}}{1 - \cos\frac{\beta l}{2}} \tag{21}$$

$$v_{C-c} = \frac{1}{\beta^2}\left(\frac{w_{C-c}}{N} - \frac{M_P}{EI}\right)\frac{1 - \cos\frac{\beta l}{2}}{\cos\frac{\beta l}{2}} - \frac{w_{C-c}l^2}{8N} \tag{22}$$

It may be noted that the Euler buckling load when the member is regarded as a both-end simply supported beam is $N_E = \pi^2 EI/l^2$, and the corresponding β is $\beta = \pi/l$. From Eq. (22), it can be understood that deflection diverges at this time.

2.2.2 Parametric Study of Influence of In-Plane Stress on Plate Bending Strength

The ratios of strength (ratio of the 2-point and 3-point plastic hinge formation loads) with and without the action of in-plane stress were obtained using Eqs. (15), (17), (19) and (21). Figs. 6 and 7 show the results for tensile in-plane stress, and Figs. 8 and 9 show the results for compressive in-plane stress. In these calculations, $l = 800$ mm, $E = 206\,000$ MPa and $\sigma_Y = 315$ MPa. The black broken lines show the strength decrease when the influence of the additional lateral loading accompanying in-plane stress is not considered, in other words, the strength decrease according to Eq. (3).

From Figs. 6 and 7, under the action of tensile in-plane stress, it can be understood that the strength increases due to the effect of additional lateral loading, and that effect becomes more remarkable as the plate thickness becomes thinner. Moreover, that effect is also larger in 3-point plastic hinge formation than in 2-point plastic hinge formation. Regarding the 3-point plastic hinge load, almost no strength decrease can be seen up to approximately 0.5 σ_Y when the plate thickness is 25 to 30 mm and up to about 0.8 σ_Y when the plate thickness is 15 mm.

From Figs. 8 and 9, under the action of compressive in-plane stress, strength decreases due to the influence of additional lateral loading, and that effect becomes more pronounced as the plate thickness decreases. In the case of the 2-point plastic hinge formation load, strength decreases almost linearly with respect to in-plane stress (red solid line) when the plate thickness is approximately 20 mm. Similarly, for the 3-point plastic hinge formation load, a nearly linear decrease in strength against in-plane stress (red solid line) is observed when the plate thickness is approximately 25 mm. When the plate thickness is less than the above value, the strength is further reduced. However, because this thinner plate thickness is supposed to be increased substantially by the buckling criteria separately, the red lines can be considered to be the substantial lower limit of the strength decrease. Therefore, the required plate thickness equation, Eq. (23), which is based on the linear strength reduction shown by the red lines and (strength ratio) = $1 - \sigma_y / \sigma_Y$, is one guideline for the in-plane stress influence factor in transversely framed structures in which compressive in-plane stress acts.

$$\frac{t}{t_0} = \frac{1}{\sqrt{1 - \dfrac{\sigma_y}{\sigma_Y}}} \qquad (23)$$
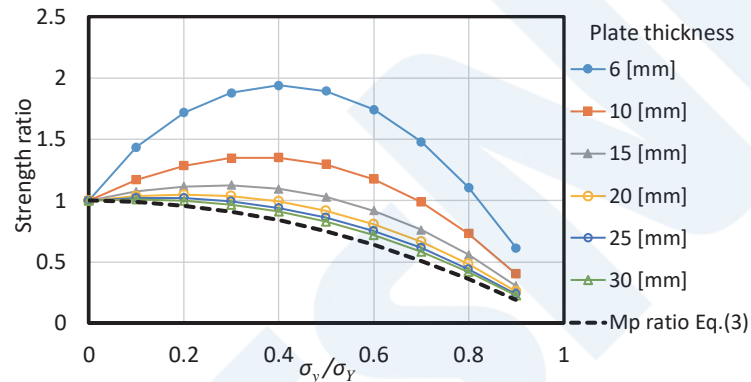

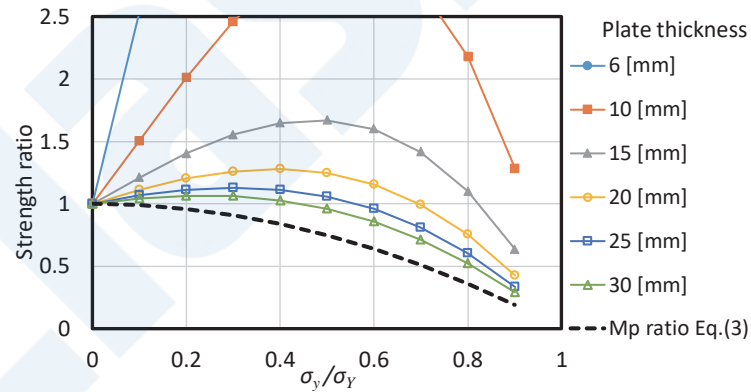Fig. 6   2-point plastic hinge formation load ratio (tensile in-plane stress)

Fig. 7   3-point plastic hinge formation load ratio (tensile in-plane stress)
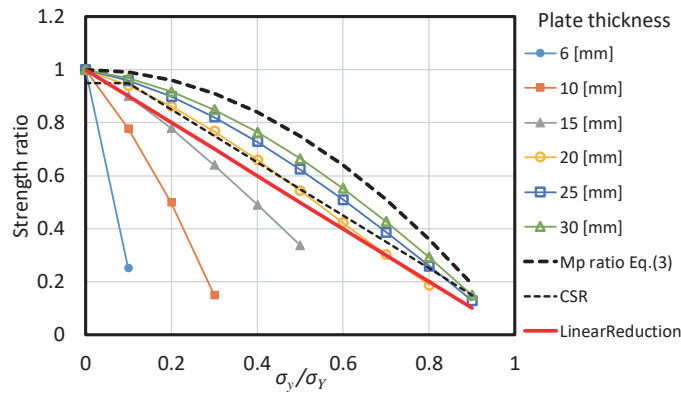
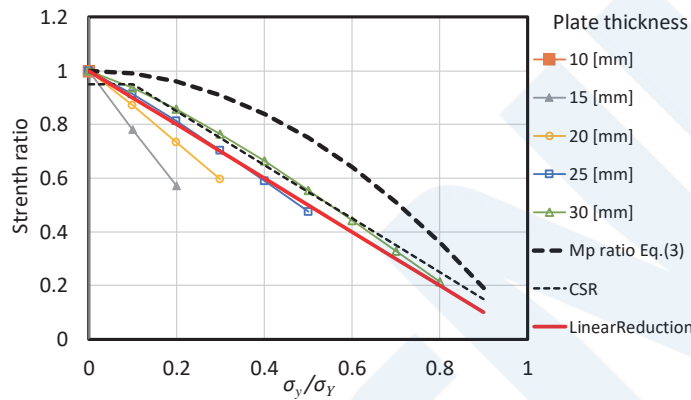Fig. 8　2-point plastic hinge formation load ratio (compressive in-plane stress)

Fig. 9　3-point plastic hinge formation load ratio (compressive in-plane stress)

2.3　Verification of Theoretical Equations by Elasto-Plastic FEM

In this section, the theoretical equations derived up to the previous section will be verified by elasto-plastic FEM. Fig. 10 shows the FEM model. To eliminate the influence of the aspect ratio in accordance with the formulation up to the previous section, a sufficiently long panel with dimensions of 800 mm x 8 000 mm was assumed, and a 2 longitudinal space x 2 transverse space member was modeled. At the center of the long side (point A), the mesh was subdivided so that the element side length was 2.5 mm in order to detect the stress and bending moment. In addition, the displacement is detected at the center of the panel (point B). The analysis was conducted by the implicit method of LS-DYNA using Belytschko-Tsay shell elements with 6 integration points in the plate thickness direction, assuming Young's modulus = 206 000 MPa, Poisson's ratio = 0.3, tangent modulus = 0 and yield stress = 315 MPa. To model an infinitely continuing stiffened plate, a periodic boundary condition was adopted all around the model. As the loading procedure, after first applying various in-plane loads, lateral pressure loading was applied by incremental loading to the specified lateral pressure, after which both the lateral pressure and the in-plane load were removed (unloaded), and the stresses, bending moments and deflections at points A and B in this process and the residual defection after unloading were observed.


Fig. 10　Analysis model

2.3.1　Case without In-Plane Stress
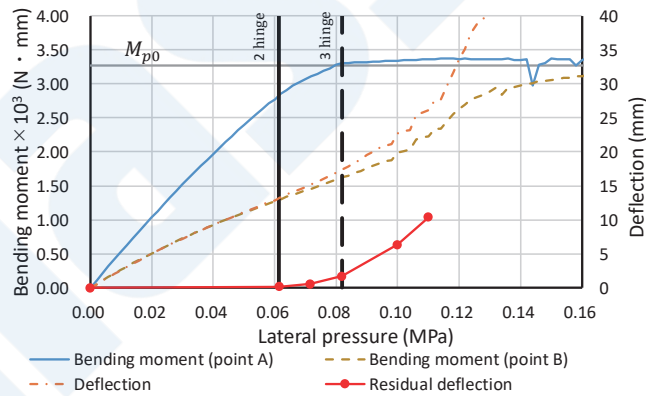
Fig. 11 shows the transition of the bending moment, deflection and residual deflection at points A and B with respect to the increment of lateral pressure for the plate thicknesses of 20 mm, 14 mm and 6 mm. In this figure, the vertical solid lines and vertical broken lines represent the 2-point plastic hinge formation load and the 3-point plastic hinge formation load, respectively.
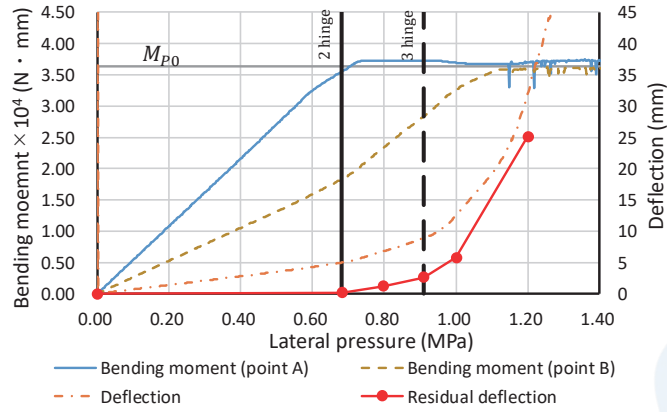
(1) Plate thickness: 20 mm
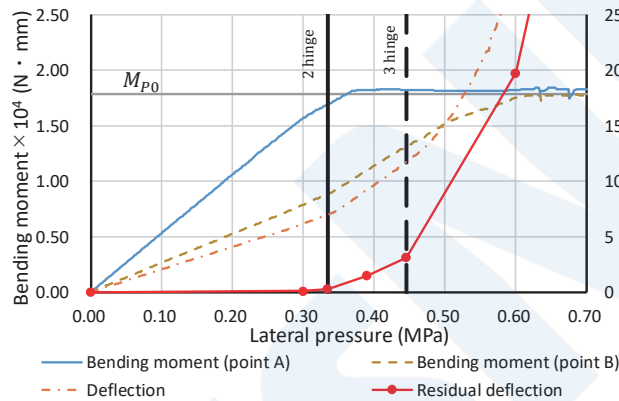
(2) Plate thickness: 14 mm


(3) Plate thickness: 6 mm

Fig. 11　Transitions of bending moment and deflection by lateral pressure

　　The bending moment at the center of the long side (point A) reaches a plateau at the fully plastic moment M_{P0}, and the lateral pressure at this time is roughly in agreement with the calculated 2-point plastic hinge formation load, excluding the case of the 6 mm plate thickness. On the other hand, although the bending moment in the panel center (point B) also reaches a plateau at M_{P0}, a substantially larger load than the 3-point plastic hinge formation load is required in order to reach M_{P0}. This tendency is particularly remarkable when the plate thickness is thin, and furthermore, when the plate thickness is 6 mm, a slight delay in 2-point plastic hinge formation is observed. These tendencies are the result of membrane stress supporting the lateral load. Although the effect is slight until formation of a 2-point plastic hinge, these effects cannot be ignored in 3-point plastic hinge formation. When residual deflection is observed, large growth of residual deflection begins regardless of the plate thickness if the applied load is larger than the 2-point plastic hinge formation load. Based on these facts, it appears to be appropriate to use

2-point plastic hinge formation as a criterion for establishing strength standards based on residual deflection criteria, as described in the following.

2.3.2　Case Where In-Plane Stress Acts on Transversely Framed Structure

Figs. 12 and 13 show the bending moment at the center of the long side (point A) and the center of the panel (point B) for the cases where compressive in-plane stress and tensile in-plane stress act on a structure, respectively. Here, the plate thickness is 20 mm.
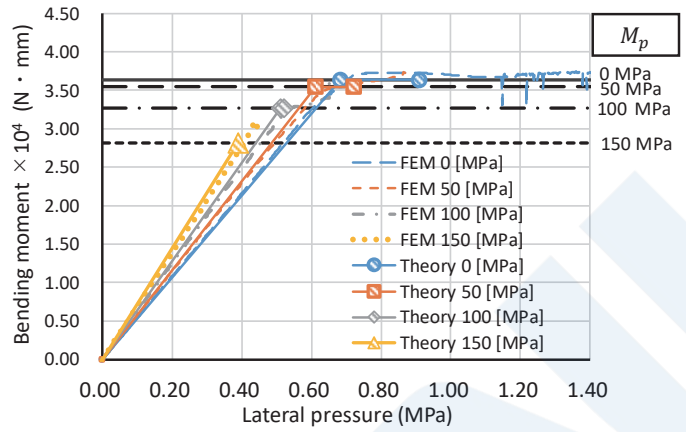
(1) Center of long side (point A)
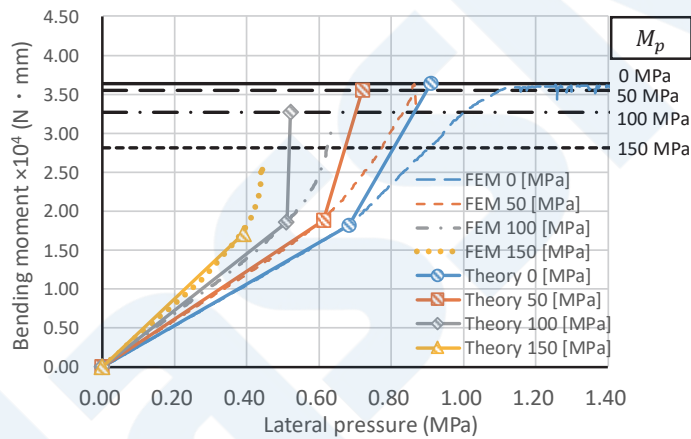
(2) Center of panel (point B)

Fig. 12　Transition of bending moment when compressive in-plane stress acts on a transversely framed structure

(1) Center of long side (point A)
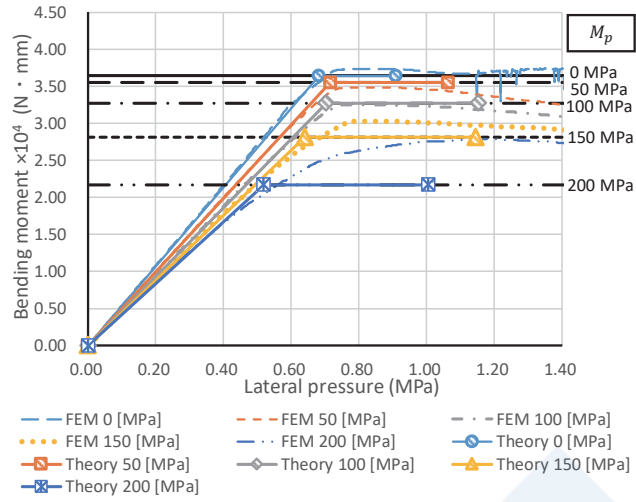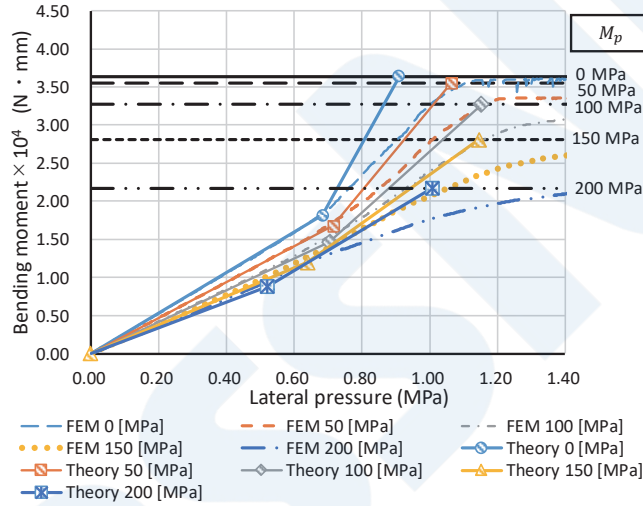

(2) Center of panel (point B)

Fig. 13　Transition of bending moment when tensile in-plane stress acts on a transversely framed structure

In these figures, the broken lines and one-dot chain lines show the FEM results, and the solid lines show the theoretical calculations derived in the previous section. The several black horizontal lines in the figures are the fully plastic moment corresponding to the respective in-plane stresses obtained by Eq. (3). The markers attached to the theoretical calculation results are the positions of 2-point plastic hinge and 3-point plastic hinge formation given by Eqs. (15), (17), (19) and (21), respectively. Comparing the FEM and theoretical equation results, the two are in good agreement until formation of the 2-point plastic hinge, but after that point, the results diverge due to the effect of membrane stress. When compressive in-plane stress acts, the slope of the graphs becomes larger due to the effect of the additional lateral loading associated with the increase in in-plane stress. Together with the decrease in the fully plastic moment M_p accompanying in-plane stress, this greatly reduces the 2- and 3-point plastic hinge formation loads. Conversely, when tensile in-plane stress acts, the slope of the graphs decreases as the in-plane stress increases. In this case, with the balance of the strength increase due to the decrease in the slope and the strength decrease due to the decrease in M_p, a tendency in which strength increases once accompanying an increase in in-plane stress and then begins to decrease can also be observed from the graphs.

2.3.3　Case Where In-Plane Stress Acts on Longitudinally Framed Structure

Next, Fig. 14 shows the transition of the bending moment at the center of the long side (point A) when compressive in-plane stress acts on a longitudinally framed structure. The several black horizontal lines in the figure are the fully plastic moment corresponding to the in-plane stresses obtained by Eq. (12) for a longitudinally framed structure. Because the effect of in-plane stress on the fully plastic moment is small compared with that in a transversely framed structure, the amount of decrease in the

fully plastic moment due to in-plane stress is small in comparison with Fig. 12 and Fig. 13, which were based on Eq. (3). Since additional lateral loading due to in-plane stress does not act on a longitudinally framed structure, the slopes of the various lines are substantially identical regardless of the magnitude of the in-plane stress. Although the figure for the panel center (point B) is omitted here, almost no difference due to the action of in-plane stress was observed at the panel center and under the action of tensile in-plane stress.
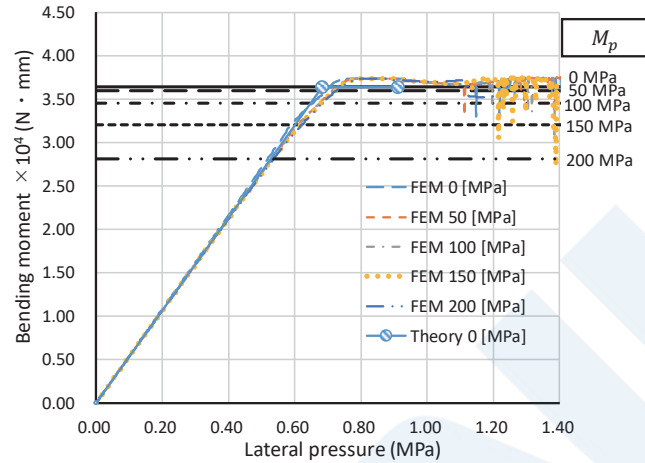

Fig. 14 Transition of bending moment at center of long side (point A) when compressive in-plane stress acts on a longitudinally framed structure

It is conceivable that a plastic hinge forms at point A when the lines in Fig. 14 reach the horizontal line representing the fully plastic moment corresponding to each in-plane stress. However, even under the action of in-plane stress, it can be seen that the bending moment calculated by FEM passes through the corresponding theoretical fully plastic moment and becomes a plateau on reaching the value M_{P0}, that is, the fully plastic moment without in-plane stress. This suggests the possibility that the fully plastic moment can substantially be supported in this cross section in case in-plane stress does not act, and the effect of in-plane stress on strength is extremely small in a longitudinally framed structure. In order to examine the reason for this, Fig. 15 shows the stress history of the upper surface and lower surface at point A when lateral pressure was gradually applied to a panel under the action of tensile in-plane stress of 200 MPa. Here, light blue shows the stress in the x direction, orange shows the stress in the y direction, black represents the von Mises stress, and the solid lines and broken lines show the values for the top surface and the bottom surface, respectively.
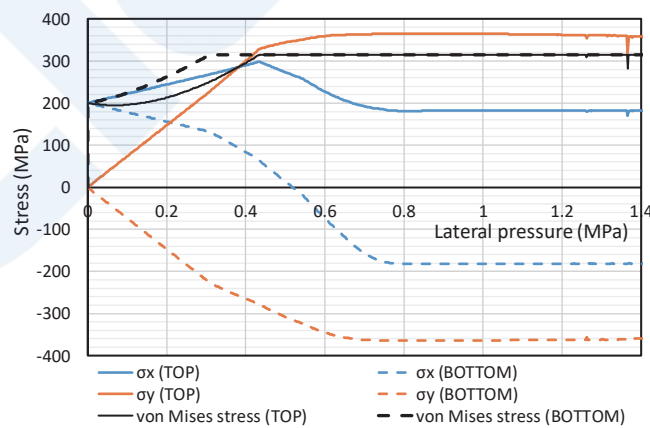
Fig. 15 Transition of surface stress condition at point A (longitudinally framed structure, tensile stress: 200 MPa)

When application of lateral pressure begins, y-direction bending stress is generated in opposite directions on the top and bottom surfaces, and the x-direction stress changes from the initial value of 200 MPa by an amount equivalent to the value obtained by multiplying that stress by the Poisson's ratio of 0.3. The slope of the bottom surface stress changes accompanying

yielding of the bottom surface at the lateral pressure of 0.31 MPa, and next, the top surface yields at the lateral pressure of 0.43 MPa, and the slope of the top surface stress also changes. When further lateral pressure is applied, the in-plane stress is released and the x-direction stress settles to v_p (= 0.5) ・ σ_y, while σ_y continues to increase even after yielding and reaches α (= 1.15) ・ σ_Y when the lateral pressure is about 0.78 MPa. This condition is shown on the von Mises stress criterion curve in Fig. 16. That is, when further lateral pressure is applied after yielding of the bottom surface (●) and the top surface (■), it can be understood that the phenomenon observed in Fig. 3 where Poisson's ratio changes to 0.5 while maintaining the in-plane stress in the x direction does not occur, but instead the stress moves in the direction where the x-direction in-plane stress will be released.
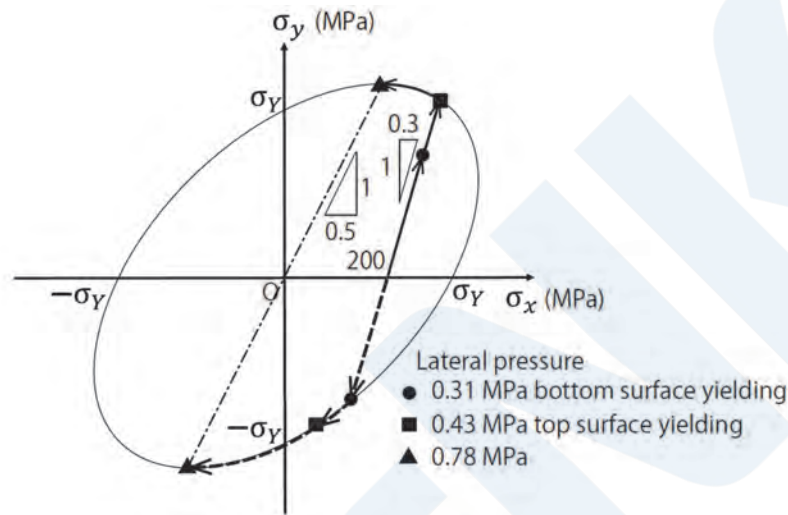

Fig. 16　Von Mises yield criterion curve for plate bending in a longitudinally framed structure (transition of stress in FEM results)

This fact means that the influence of in-plane stress on plate bending strength is eliminated if an extremely large lateral load is applied. However, at the timing of 2-point plastic hinge formation (calculated: 0.527 MPa), the x-direction in-plane stress still has not been released, and residual deflection begins to increase by the formation of the 2-point plastic hinge. Based on these facts, it is thought to be appropriate to consider the decrease in the fully plastic moment due to in-plane stress when placing the plate strength criterion on 2-point plastic hinge formation.

3.　SERIES ANALYSIS OF ELASTO-PLASTIC FEM BASED ON RESIDUAL DEFLECTION CRITERION

As also pointed out by Hughes et al. [10] [11], because plate members which are subjected to lateral pressure have extremely large ultimate strength due to the effect of membrane stress, etc., an index based on the serviceability like residual deflection is useful as a design criterion. Therefore, in this chapter, series calculations by elasto-plastic FEM were carried out using residual deflection as a criterion, the effect of in-plane stress on plate bending strength was arranged, and a comparative study with the equations derived in Chapter 2 was conducted. The FEM model used here was the same as that used in Chapter 2, and we obtained the lateral pressure which causes the specified residual deflection by iterative FEM calculations at each level of in-plane stress. Since residual deflection began to increase when the load exceeded a load equivalent to 2-point plastic hinge formation regardless of the plate thickness, as in Chapter 2, it was considered appropriate to use 2-point plastic hinge formation as a strength criterion. Therefore, residual deflection of 0.26 mm which was generated when the 2-point plastic hinge formation load was applied to a 14-mm plate without in-plane stress was adopted as a common criterion.

3.1　Results of Analysis of Transversely Framed Structure

Fig. 17 shows the relationship between the plate thickness and lateral pressure when residual deflection is 0.26 mm for the case where compressive in-plane stress acts on a transversely framed structure. When in-plane stress increases, the lateral pressure decreases remarkably at the same plate thickness, and conversely, the plate thickness for the same lateral pressure increases remarkably. Fig. 18 shows the result of plotting the strength ratio with respect to the case without in-plane stress,

where in-plane stress is shown on the horizontal axis. The FEM results show a tendency which is consistent with the graph of the strength ratio for the 2-point plastic hinge formation load shown in Fig. 8. The linear strength decrease equation (shown by the red solid line) covers the FEM results on the safe side. For reference, if the same calculation is performed with residual deflection set to 4 mm, the effect of in-plane stress becomes more pronounced, and the results approach the graph of the theoretical values of the strength ratio for the 3-point plastic hinge formation load shown in Fig. 9. Fig. 19 shows the relationship between compressive in-plane stress and the required plate thickness ratio. The required plate thickness ratio in the FEM result is larger than that by Eq. (4) in the former ClassNK Rules, and deviates both above and below the required values in the CSR. Although the required plate thickness ratio when lateral pressure is small (i.e., when the plate thickness is small) is larger than the CSR requirement, the linear strength decrease equation (Eq. (23); red solid line) covers the FEM results on the safe side.
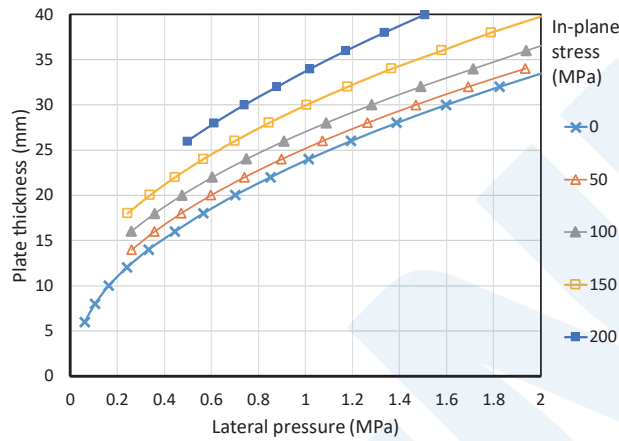

Fig. 17　Relationship between plate thickness and lateral pressure (transversely framed structure, compressive in-plane stress)
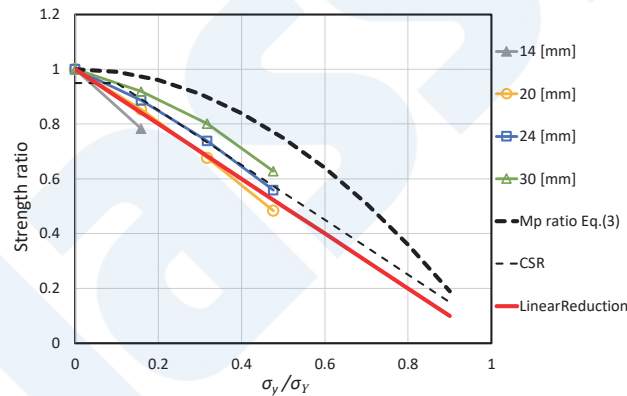

Fig. 18　Relationship between compressive in-plane stress and strength ratio (transversely framed structure)
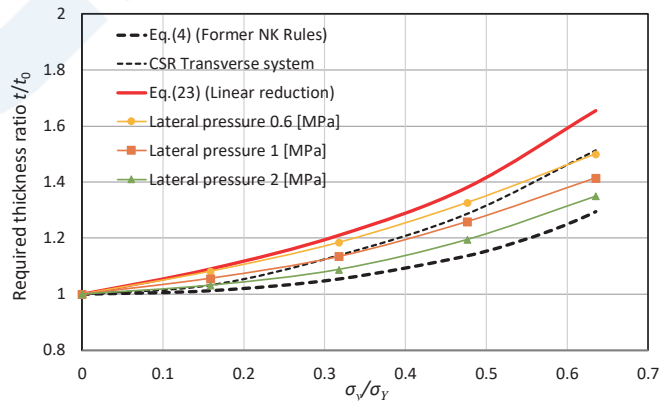

Fig. 19　Relationship between compressive in-plane stress and required plate thickness ratio (transversely framed structure)

Next, Fig. 20, Fig. 21 and Fig. 22 show similar figures for the case where the in-plane stress is tensile stress. Fig. 20 shows that the variation of each line due to the difference in the in-plane stress is smaller than that in Fig. 17, indicating that the influence of tensile in-plane stress on strength is small. In particular, when lateral pressure is small, in other words, when the plate thickness is small, a range where strength increases due to the action of tensile in-plane stress is observed. Here, it was found that Fig. 21, which shows the strength ratio for cases without the action of in-plane stress, displays a tendency which is in agreement with the graph of the theoretical values of the strength ratio for the 2-point plastic hinge formation load under the action of tensile in-plane stress in Fig. 6. In this case, the fully plastic moment ratio (Eq. (3), bold black broken line) based on the von Mises yield criterion adopted in the former ClassNK Rules covers the FEM results on the safe side. It should be noted that the influence of in-plane stress becomes more remarkable when the same calculation is performed with the residual deflection set to 4 mm for reference, and the result approached the graph of the theoretical values of the strength ratio for the 3-point plastic hinge formation load in Fig. 7. In the relationship between tensile in-plane stress and the required plate thickness in Fig. 22, the required plate thickness ratio in the FEM results falls even further below that of the former ClassNK Rules (Eq. (4), bold black broken line), which has the smallest required plate thickness ratio, and this covers the FEM results on the safe side. The strength increases due to tensile in-plane stress when lateral pressure is small (i.e., when the plate thickness is small), and the required plate thickness ratio falls below 1.0. This tendency becomes more remarkable in the calculation when the residual deflection criterion is set to 4 mm, and a strength decrease is not observed in almost all cases. However, with the criterion of 0.26 mm, which is equivalent to 2-point plastic hinge formation, that is, the point where growth of residual deflection begins, a clear effect on in-plane stress is observed, as can be seen in Fig. 22. Therefore, the design will be on the dangerous side if this effect is ignored.

To summarize the influence of compressive and tensile in-plane stress on transversely framed structures, the required plate thickness ratio given by the FEM results is covered on the conservative side by Eq. (23) using the linear strength decrease in the case of compressive in-plane stress, and by Eq. (4), which is based on the von Mises yield criterion, in the case of tensile in-plane stress. In this case, the safety margin for compression increases when the plate thickness is large, while the safety margin for tension increases when the plate thickness is small.
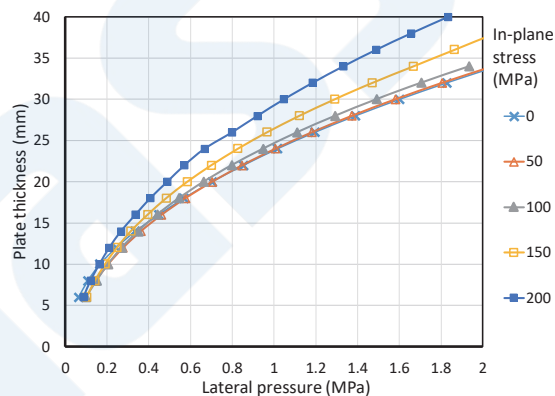

Fig. 20 Relationship of plate thickness and lateral pressure (transversely framed structure, tensile in-plane stress)
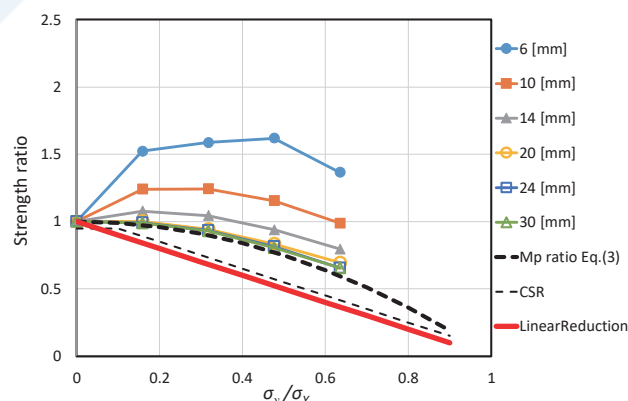
Fig. 21 Relationship of tensile in-plane stress and strength ratio (transversely framed structure)
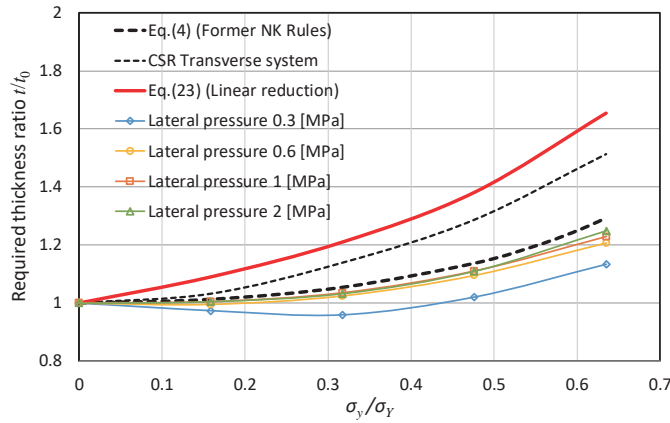
Fig. 22   Relationship of tensile in-plane stress and required plate thickness ratio (transversely framed structure)

3.2   Results of Analysis for Longitudinally Framed Structures

Similar figures for the case where compressive in-plane stress acts on a longitudinally framed structure are shown in Fig. 23, Fig. 24 and Fig. 25. As can be seen in Fig. 23, the influence of in-plane stress is quite small, but occurs in the same manner regardless of the level of lateral pressure. As shown in the strength ratio in Fig. 24, the influence of in-plane stress is disregarded up to $0.5\sigma_Y$ in the former ClassNK Rules and up to $0.2\sigma_Y$ in the CSR. However, the FEM results show a slight decreasing tendency from the stage where in-plane stress is small, and Eq. (12) (red solid line), which is based on the von Mises yield criterion, expresses that tendency well on the safe side. Likewise, in Fig. 25, which is arranged by the required plate thickness, Eq. (13) (red solid line) based on the von Mises yield criterion also covers the FEM results on the safe side.

The case of tensile in-plane stress gave results that were substantially the same as the case of compression. Moreover, if summarized using the 4 mm residual deflection criterion, the influence of in-plane stress is small to a level that is almost negligible. This is considered to be the result of a phenomenon in which in-plane stress is released from the plastic hinge formation site, as explained in Section 2.3.3.
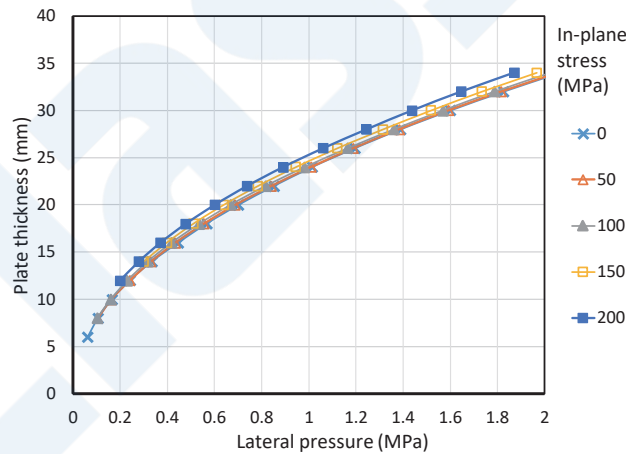
Fig. 23   Relationship of plate thickness and lateral pressure (longitudinally framed structure, compressive in-plane stress)
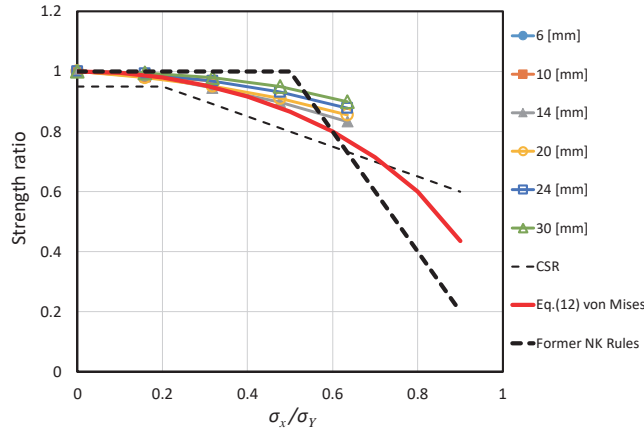
Fig. 24   Relationship of compressive in-plane stress and strength ratio (longitudinally framed structure)
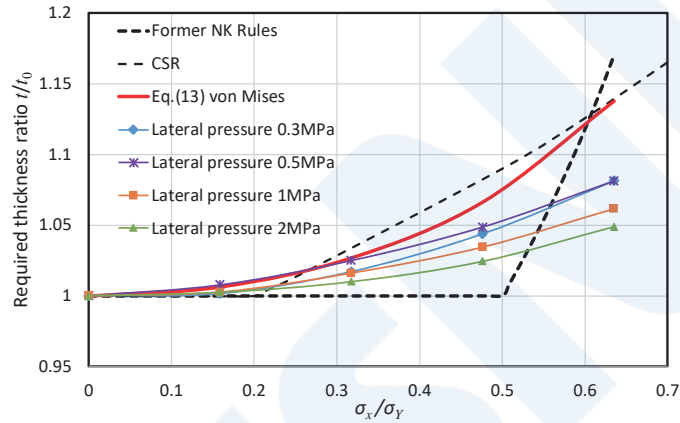
Fig. 25   Relationship of compressive in-plane stress and required plate thickness ratio (longitudinally framed structure)

Table 2   In-plane stress influence factors (strength ratio) and required plate thickness ratio

		Applied criterion	In-plane stress influence factor C_a (Strength ratio)	Required thickness ratio t/t_0
Longitudinally framed structure		Von Mises criterion with orthogonal in-plane and bending stress	$\sqrt{1-\left(\dfrac{\sigma_x}{\sigma_Y}\right)^2}$ (12)	$1\Big/\left(1-\left(\dfrac{\sigma_x}{\sigma_Y}\right)^2\right)^{1/4}$ (13)
Trans-versely framed structure	Tension	Von Mises criterion with parallel in-plane and bending stress	$1-\left(\dfrac{\sigma_y}{\sigma_Y}\right)^2$ (3)	$1\Big/\sqrt{1-\left(\dfrac{\sigma_y}{\sigma_Y}\right)^2}$ (4)
	Compression	Linear strength reduction	$1-\dfrac{\lvert\sigma_y\rvert}{\sigma_Y}$	$1\Big/\sqrt{1-\dfrac{\lvert\sigma_y\rvert}{\sigma_Y}}$ (23)

3.3   Summary of In-Plane Stress Factors

Based on the results presented above, Table 2 summarizes the strength ratios and scantling formulae (required plate thickness ratios) which are capable of covering the FEM results on the safe side. These are the von Mises yield criterion (Eq. (13)) for cases where in-plane stress and bending stress act orthogonally for longitudinally framed structures, the von Mises yield criterion (Eq. (4)) for cases where in-plane stress and bending stress act in the same direction for transversely framed structures under tension, and the linear strength decrease criterion (Eq. (23)) for transversely framed structures under compression.

4. COMBINED INFLUENCE OF IN-PLANE STRESS AND ASPECT RATIO

Up to the previous chapter, cases in which the aspect ratio of plate members was sufficiently large were examined, and it was shown that the influence of in-plane stress differs greatly in longitudinally framed structures and transversely framed structures. However, if the same in-plane stress influence factors are also applied to cases where the aspect ratio is small, the results will be irrational, since the required plate thickness becomes discontinuous depending on whether the aspect ratio is larger or smaller than 1.0. In reality, in such cases, it is thought that an intermediate in-plane stress influence between that of a longitudinally framed structure and a transversely framed structure acts on the member.

On the other hand, an aspect ratio correction factor is introduced in the scantling formulae in the CSR and other standards in order to consider the strength increase when the aspect ratio of a plate member is small, but this is treated independently from the in-plane stress factor. Therefore, this chapter will examine a method for rationally interpolating the in-plane stress influence factor between those of a longitudinally framed structure and a transversely framed structures, and a combined influence factor of this interpolated in-plane stress influence factor and the aspect ratio correction factor.

4.1 Derivation of Combined Influence Factor

In cases where in-plane stress acts, strength decreases by the ratio C_a as shown in Table 2, depending on whether the structure is longitudinally framed or transversely framed and whether the in-plane stress is compressive or tensile. These C_a ratios can all be expressed by generalization to the form of Eq. (24). Therefore, the influence of in-plane stress for small aspect ratios is considered to be expressed rationally by appropriately correcting α and β in Eq. (24) between the longitudinally framed structure and transversely framed structure.

$$C_a = \left\{ 1 - \left(\frac{|\sigma_{BM}|}{\sigma_Y} \right)^\alpha \right\}^\beta \tag{24}$$

Here, σ_{BM} is the hull girder vertical bending stress. In this chapter, only the hull girder vertical bending stress will be considered as the in-plane stress. Based on this assumption, when the aspect ratio is large, in a longitudinally framed structure, $\alpha = 2$, $\beta = 1/2$, and in a transversely framed structure, $\alpha = 2$, $\beta = 1$ when the in-plane stress is tensile and $\alpha = 1$, $\beta = 1$ when the in-plane stress is compressive.

Next, regarding the aspect ratio correction factor, in the previous chapter, 2-point plastic hinge formation was adopted as the criterion for the in-plane stress influence factor. Therefore, here, the aspect ratio correction factor will be studied based on plate elastic bending theory. Using the series solutions [12] of the bending moments at the center of the long side and center of the short side of a rectangular plate with a finite aspect ratio and four fixed sides subjected to a uniformly distributed load, an approximate expressions for the required plate thickness ratio to the required plate thickness t_∞ when the aspect ratio $= \infty$ and the short side length is the same were obtained as shown in Eqs. (25) and (26).

$$C_{Aspect-L} = \min\left(1.07 - 0.28\left(\frac{\min(l,s)}{\max(l,s)}\right)^2, 1\right) \tag{25}$$

$$C_{Aspect-S} = \min\left(0.84 - 0.05\left(\frac{\min(l,s)}{\max(l,s)}\right)^4, 0.828\right) \tag{26}$$

Here, l and s are the side length in the ship longitudinal direction and transverse direction, and $C_{Aspect-L}$ and $C_{Aspect-S}$ are the required plate thickness ratio considering the influence of the aspect ratio at the center of the long side and the short side, respectively. Because $C_{Aspect-L}$ is always larger than $C_{Aspect-S}$ when in-plane stress does not act, $C_{Aspect-L}$ is adopted as the basis for the aspect ratio correction factor.

Next, the influence of in-plane stress on this will be considered. In a longitudinally framed structure, the influence of the in-plane stress on the center of the short side is larger than the influence on the center of the long side, which means a plastic hinge forms first on the center of the short side when the in-plane stress is large. If the structure is longitudinally framed, the influence

of additional lateral loading accompanying in-plane stress is assumed to be small even if the aspect ratio is small. Then, we examine the strength decrease expressed by Eq. (12) at center of the long side, and the strength decrease expressed by Eq. (3) at the center of the short side. Fig. 26 shows the required plate thickness ratio to the required plate thickness $t_{0\infty}$ when the aspect ratio $= \infty$ and the in-plane load is zero for aspect ratios in the range of 0.5 to 1.0 in a longitudinally framed structure. The black lines and red lines show the required plate thickness ratio based on bending at the center of the long side and bending at the center of the short side, respectively. The broken lines indicate the required plate thickness ratio when in-plane stress is zero (i.e., the above-mentioned Eqs. (25) and (26)), and the solid lines are the required plate thickness ratio when the in-plane stress $\sigma_{BM} = 0.5\sigma_Y$ acts.

As the aspect ratio approaches 1.0, the required plate thickness ratio with respect to t_{∞} decreases in accordance with Eq. (25), as shown by the black broken line, and plastic hinges form simultaneously at the centers of the long side and the short side at the aspect ratio of 1.0. On the other hand, if in-plane stress acts on the member, the influence on the center of the short side is larger, and as a result, in this case, a plastic hinge forms first at the center of the short side at about $s/l > 0.83$. Based on the above, we tried setting α and β so that $\alpha = 2$ and $\beta = 1$ when the aspect ratio is 1.0. In this case, when the aspect ratio changes from 1.0 in a longitudinally framed structure, the result is an interpolation that takes the envelope of the two solid lines in Fig. 26 on the safe side. When the aspect ratio changes from 1.0 in a transversely framed structure and if the in-plane stress is compressive, the result is an interpolation in which the influence of additional lateral loading which is not considered when the aspect ratio is 1.0 appears progressively as the aspect ratio s/l becomes larger.
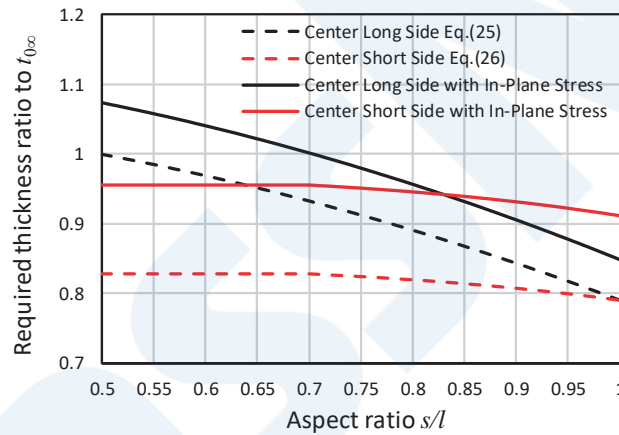
Fig. 26   Relationship of aspect ratio and required plate thickness ratio

Based on these points, when the influence of in-plane stress of a longitudinally framed structure is applied to aspect ratios of $s/l < 0.5$ and the influence of in-plane stress of a transversely framed structure is applied to $s/l > 2.0$, and linear interpolations are performed between $0.5 \leq s/l < 1.0$ and between $1.0 \leq s/l \leq 2.0$, α and β can be set as shown in Table 3.

Table 3   Interpolation of parameters α and β

	In-plane stress	s/l	α	β
Longitudinally framed structure	Common to tensile and compressive	$\dfrac{s}{l} \leq 0.5$	2	0.5
		$0.5 \leq \dfrac{s}{l} \leq 1$	2	$\dfrac{s}{l}$
Transversely framed structure	Tensile	$1 \leq \dfrac{s}{l}$	2	1
	Compressive	$1 \leq \dfrac{s}{l} \leq 2$	$2\dfrac{l}{s}$	1
		$2 \leq \dfrac{s}{l}$	1	1

On this assumption, the combined influence factor of the in-plane stress influence factor and the aspect ratio correction factor can be expressed by the following equation:

$$\frac{t}{t_{0\infty}} = \frac{C_{Aspect-L}}{\sqrt{C_a}} = \frac{\min\left(1.07 - 0.28\left(\frac{\min(l,s)}{\max(l,s)}\right)^2, 1\right)}{\sqrt{\left\{1 - \left(\frac{|\sigma_{BM}|}{\sigma_Y}\right)^\alpha\right\}^\beta}} \qquad (27)$$

4.2　Verification of Aspect Ratio Influence by Elasto-Plastic FEM

Here, as in Chapter 3, the plate thickness that gives residual deflection of 0.26 mm at each level of lateral pressure was obtained by repeated FEM calculations. The FEM model was the same as that used in Chapter 3, and the length of the short side was kept at 800 mm when changing the aspect ratio.

Fig. 27 shows the calculated results of the influence of the aspect ratio on the required plate thickness ratio when the in-plane stress is zero. The horizontal axis shows the aspect ratio s/l expressed on a logarithmic scale. The left half of the figure corresponds to a longitudinally framed structure, and the right half to a transversely framed structure. The black broken line and red solid line are the aspect ratio influence by Eq. (25) and the CSR method, respectively. The influence of the aspect ratio appears remarkably as the acting lateral pressure decreases, and Eq. (25), which is proposed in this paper, covers the FEM results on the safe side. Although the results by the correction equation according to the CSR also contain some points that are slight on the dangerous side, overall, those results are in good agreement with the FEM results.
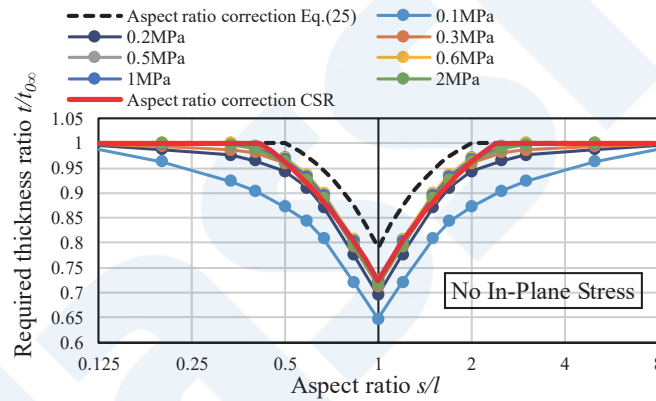
Fig. 27　Influence of aspect ratio without in-plane stress

Next, the calculated results of the aspect ratio influence with in-plane stress are shown in Fig. 28. The three figures on the left are cases of compressive in-plane stress, the three on the right are cases of tensile in-plane stress, where the magnitude of the in-plane stress, in order from the top, is 0.3 σ_Y, 0.5 σ_Y and 0.7 σ_Y. When the in-plane stress is compressive and the plate thickness is thin, there were cases where the calculation could not be continued due to buckling; those results are not included here (this occurred particularly in cases such as large in-plane stress in a transversely framed structure and a lateral pressure of 0.3 MPa or less, etc.). In addition, although calculation was possible, cases where the Euler buckling stress was less than the in-plane stress are indicated by the triangular markers (▲). In this figure, the black solid lines are the required plate thickness ratio according to Eq. (25), which does not consider the influence of in-plane stress, and the black broken lines are the required plate thickness ratio according to Eq. (27), which includes the influence of in-plane stress in this Eq. (25).

The black broken lines generally cover the FEM results to the safe side. In the case of compressive in-plane stress, the results partially exceed the black broken lines, but since these points are thought not to satisfy the Euler buckling stress (shown by the ▲ marker), or to be close to that condition, it is thought that these should be covered by a separate buckling criterion. Between $0.5 \leq s/l < 1.0$ in the longitudinally framed structure, a phenomenon in which the required plate thickness ratio increases once as the aspect ratio approaches 1.0 can be observed, particularly when the lateral pressure is small. Although the additional lateral loading associated with in-plane stress is disregarded in longitudinally framed structures, in actuality, some influence of

additional lateral loading occurs when the aspect ratio is near 1.0, and this is thought to be the cause of such behavior. Moreover, the fact that the graphs of the required plate thickness ratio shift to the opposite (lower) side at the corresponding locations when in-plane stress is tensile also support this conclusion. Based on the above, for tensile in-plane stress, a quite conservative assessment is obtained when the lateral pressure is small. Overall, however, the Eq. (27) proposed here gives a conservative assessment of the FEM results, and therefore can be considered a valid criterion.

5.　CONCLUSION

This paper introduced the main content studied in connection with local strength formulae for plate members, which are the most basic element of ships, in the comprehensive revision of Part C of ClassNK's "Rules and Guidance for the Survey and Construction of Steel Ships." As a result, it is thought that the initial goal of revising these formulae as scantling formulae which are backed by theoretical equations and have a clearer correspondence with damage has been achieved to some extent.

While scantling formulae for plate members are fundamental, they are also affected in a complex manner by a variety of factors, and it is essential to develop formulae that are as simple as possible while quantitatively verifying the effects of the main factors. A more detailed analysis of cases where members are subjected to biaxial in-plane stress or shear stress, cases of initial irregularities such as plate distortion caused by welding, and the like, and study of how those problems can be covered by the equations in the Rules, are issues for the future.

(1)

Compressive in-plane stress $0.3\sigma_Y$

Required thickness ratio $t/t_{0\infty}$

Aspect ratio s/l

(4)

Tensile in-plane stress $0.3\sigma_Y$

Required thickness ratio $t/t_{0\infty}$

Aspect ratio s/l

(2)

Compressive in-plane stress $0.5\sigma_Y$

Required thickness ratio $t/t_{0\infty}$

Aspect ratio s/l

(5)

Tensile in-plane stress $0.5\sigma_Y$

Required thickness ratio $t/t_{0\infty}$

Aspect ratio s/l

(3)

Compressive in-plane stress $0.7\sigma_Y$

Required thickness ratio $t/t_{0\infty}$

Aspect ratio s/l

(6)

Tensile in-plane stress $0.7\sigma_Y$

Required thickness ratio $t/t_{0\infty}$

Aspect ratio s/l

Eq.(25) with in-plane stress — — — Eq.(27) without in-plane stress
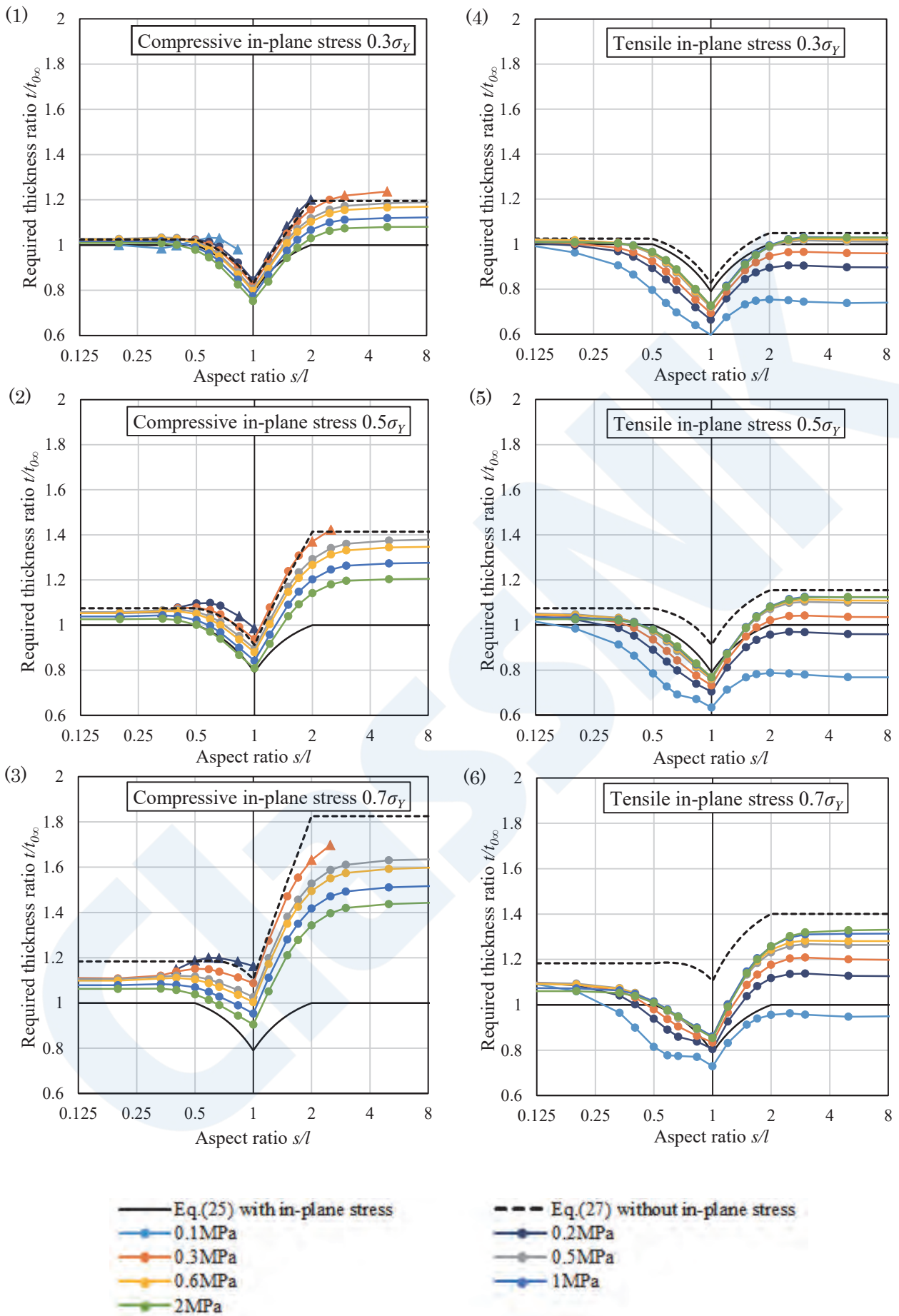0.1MPa   0.2MPa
0.3MPa   0.5MPa
0.6MPa   1MPa
2MPa

Fig. 28　Relationship of aspect ratio and required plate thickness ratio under action of in-plane stress

REFERENCES

1) Okumoto, Y., Takeda, Y., Mano, M., Okada, T.: Part II, Chapter 5 Design of plates, in Design of ship hull structures – A practical guide for engineers, Springer, 2009

2) Yamamoto, Y.: Elasticity and Plasticity, Asakura Publishing Co., Ltd., 1961

3) Jones, N.: Plastic behavior of ship structures, Transactions of the Society of Naval Architects and Marine Engineers, pp.115-145, 1976

4) Nippon Kaiji Kyokai (ClassNK): 1980 Commentary on Revisions of Rules and Guidance for the Survey and Construction of Steel Ships, Transactions of Nippon Kaiji Kyokai No. 172, 1980

5) Nippon Kaiji Kyokai (ClassNK): 1961 Commentary on Revisions of Rules and Guidance for the Survey and Construction of Steel Ships, Transactions of Nippon Kaiji Kyokai No. 67, 1961

6) International Association of Classification Societies: Common structural rules for bulk carriers and oil tankers – technical background rule reference, 2020

7) Naruse, Y., Kim, M., Umezawa, R., Ishibashi, K., Koyama, H., Okada, T., Kawamura, Y.: Scantling evaluations of plates and stiffeners based on elasto-plastic analysis under axial loads and lateral pressures, In: Practical design of ships and other floating structures - proceedings of the 14th international symposium, PRADS2019, September 22-26, 2019, Volume II, Yokohama, Japan: Springer, pp. 100-127, 2021

8) Umezawa, R., Naruse, Y., Okada, T., Kawamura, Y., Ishibashi, K., Koyama, H.: A study on scantling formulae of plate members due to lateral pressure under the effect of axial loads, Marine Structures 80, 103099, 2021

9) Yamada, M., Okada, T., Naruse, Y., Kawamura, Y., Hayakawa, G., Ishibashi, K., Koyama, H.: Influence of plate aspect ratio on the axial load effect on the plate strength against lateral pressure, 15th International Symposium on Practical Design of Ships and Other Floating Structures, PRADS2022, Dubrovnik, Croatia, October 9th –13th, 2022

10) Hughes, O. F. et al.: Ship structural analysis and design, The Society of Naval Architects and Marine Engineers, 2010

11) Hughes, O. F.: Design of laterally loaded plating – uniform pressure loads, Journal of Ship Research, 25(2), pp.77-89, 1981

12) Timoshenko, S., Woinowsky-Krieger, S.: Theory of plates and shells, McGraw-Hill Book Company, New York, 2nd Edition, 1959

World's First Zero Emission Battery-Propelled Tanker
and Outlook for the Future

Yuki HIRAMATSU[*], Tatsuya ONODERA[*]

1.　INTRODUCTION

Reduction of emissions of greenhouse effect gases (GHG) as a measure against global warming is an urgent challenge. In ships as well, in order to reduce GHG further toward the achievement of GHG emission targets, it will be necessary not only to improve ship geometry and the efficiency of unit components such as engines and propellers, but also to change the thinking on the energy used in ships as a whole, including onboard energy use. One such approach is hybrid propulsion systems and battery propulsion systems, which are already increasingly used in automobiles.

Kawasaki Heavy Industries, Ltd. recently delivered a large-capacity battery propulsion system for coastal ships for the world's first zero-emission battery-propelled tanker, the "Asahi" (see Fig. 1), which was ordered by Asahi Tanker Co., Ltd. (hereinafter, the Owner) and completed at the end of March 2022. This ship was constructed by Koasangyo Co., Ltd. (hereinafter, the Shipyard) and is now operating as a bunkering ship (ship fuel supply vessel) sailing in Tokyo Bay. This paper introduces the background, overview and features of the battery propulsion system and the outlook for the future.

Fig. 1　Battery-propelled tanker "Asahi"

2.　BACKGROUND OF DEVELOPMENT

2.1　Background of Development

In April 2018, the IMO (International Maritime Organization) adopted the Initial IMO Strategy on the reduction of GHG from ships in international shipping, and has set a target of reducing GHG emissions by 50% from the 2008 level by 2050 and further achieving zero GHG emissions by the earliest possible date in the present century. In a related development, various countries also announced their aim of achieving carbon neutrality in international shipping in 2050 at the COP26 meeting held in England in November 2021. As these moves indicate, the momentum toward GHG reduction in ships is accelerating worldwide.

In Japan, former Prime Ministry Suga announced a target of net-zero GHG emissions in 2050, with a reduction of 46% from the 2013 level to be achieved by 2030. Based on this, in August 2021 Japan's Ministry of Land, Infrastructure, Transport and Tourism (MLIT) raised the CO_2 reduction target for coastal ships in fiscal year 2030 from a 15% reduction to a 17% reduction against FY 2013.

To accelerate energy conservation and CO_2 emission saving in coastal ships, MLIT established an energy conservation rating system for coastal ships which evaluates the energy conservation and CO_2 emission saving performance of ships and began full-scale operation of this system in March 2020 [*1]. Thus, the momentum of GHG reduction is also increasing in the coastal shipping

sector.

2.2　Energy Use in Ships

The energy used by ships can be divided into two types, propulsion power and onboard electric power for pumps, lighting, control use, etc. Propulsion power (thrust) is supplied by the main engine, while onboard electric power is supplied by generators. As shown in Fig. 2, these two types of power are generally used in a completely separated manner. Although depending on the application and size of the ship, the main engine unit is frequently substantially larger than the generator unit and also has higher efficiency.
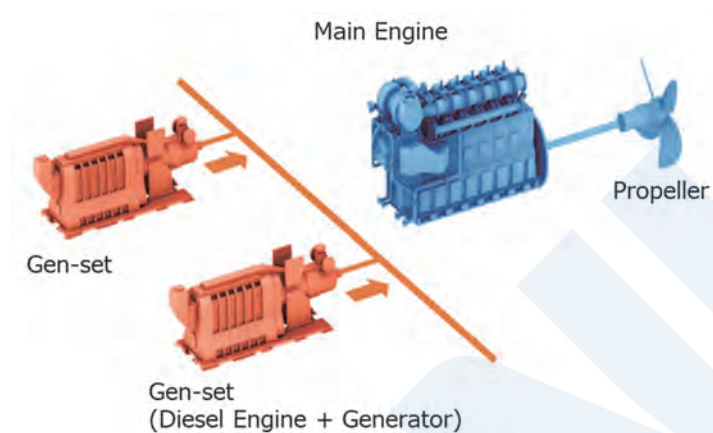
Fig. 2　General energy system of ship

Since the cost of the fuels consumed by the main engine and generators occupy a large part of the cost of ship operation, reduction of fuel costs has attracted great interest. Ongoing research and development on ship propulsion performance is being carried out, including ship geometries that reduce propulsion resistance, improvement of the performance and efficiency of the main engine and propeller, and accessory items to improve above performances. However, in some cases different companies are responsible for the hull (shipyard), the main engine (main engine maker) and the propeller (propeller maker), and as a general practice, improvement activities for each are only carried out for the simple unit component.

2.3　Energy Use in Ships

In these circumstances, the Kyoto Protocol of 1997 led to heightened awareness of the environment, and the price of crude oil rose sharply from around 2005 and has remained high since that time. Against this background, efforts were made to reduce fuel costs and conserve energy in the total ship, rather than in the individual component parts. There were attempts to couple the two energy sources, that is, the main engine for ship propulsion and the generators for onboard power, from an electrical view point and optimize the operation of the main engine and generators considering the power required in the total ship. This system configuration is called a hybrid propulsion system because propulsion power is supplied by two power sources, that is, the main engine and the generators (Fig. 3).

Fig. 3　Hybrid propulsion system

2.4 Trend toward Environment-Friendly Systems Incorporating Batteries

In addition to the hybrid propulsion system described above, lithium-ion batteries (LiBs), which are widely used in industrial applications and electric vehicles (EVs), are now also available for ship use. A battery hybrid propulsion system (Fig. 4) is a system that combines a marine LiB and a conventional hybrid propulsion system.
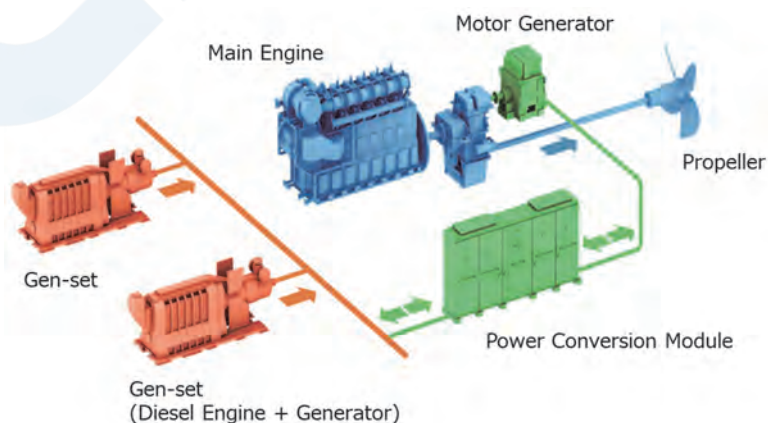
While a ship is navigating with energy supplied by the battery, it discharges zero exhaust gas, enabling local "zero emission navigation," for example, in ports and harbors.
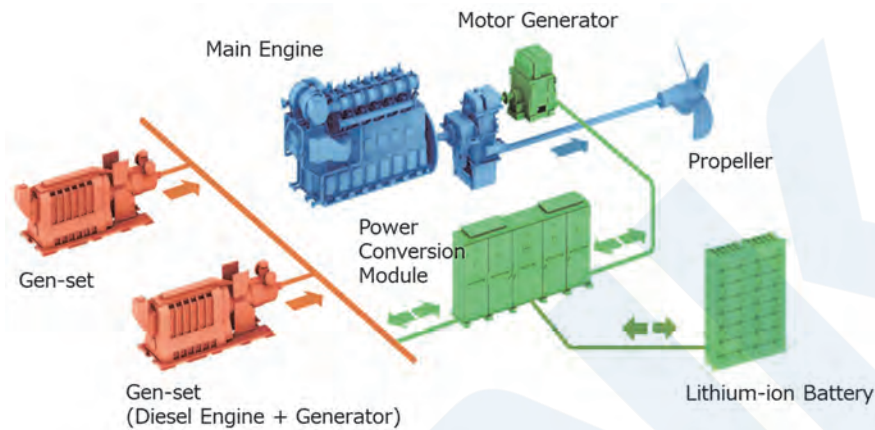
Fig. 4　Battery hybrid propulsion system

In a pure battery propulsion system (Fig. 5), the main engine and main generators are eliminated from the equipment configuration in Fig. 4. Because a pure battery propulsion system does not use internal combustion engines, it is an extremely environment-friendly system which makes it possible to realize zero emissions in all operations.
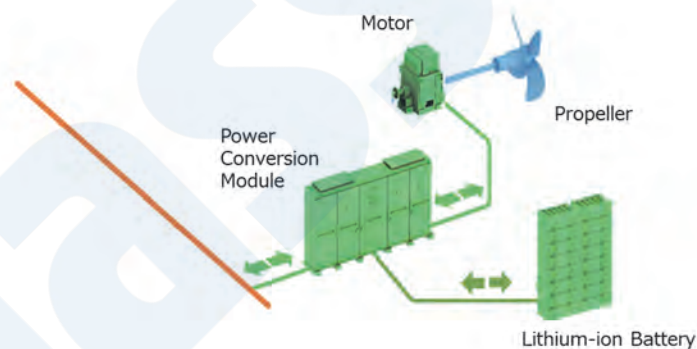
Fig. 5　Battery propulsion system

2.5 Initiatives of Kawasaki Heavy Industries

Kawasaki Heavy Industries has designed and manufactured various types of marine propulsion equipment, such as engines for use as main engines and generator engines, variable pitch propellers, and a fully azimuth-steerable 360° rotating-type thruster called the Kawasaki Rexpeller®, which can generate thrust in any desired direction. Although the company contributed to ship energy conservation and CO_2 emission saving by increasing the performance and improving those equipment, it also developed and commercialized the Kawasaki Hybrid Propulsion System beginning in 2014. Development was carried out prioritizing the power management technology, which optimally controls multiple energy sources, including the main engine, generators, batteries, etc., and battery management technology, which is currently indispensable for zero emission operation, and a system package that achieves economic effects and exhaust gas reduction while also securing the necessary power and power source quality is proposed.

Environment-friendly propulsion systems are available in multiple patterns, as outlined above. Since the most suitable system will differ depending on the vessel size and operation, it is important to take a comprehensive view of the ship as a whole,

including its role and operation, the effects that the owner hopes to achieve, etc. Kawasaki Heavy Industries communicates fully with the ship's owner in order to optimize the concept at an early stage.

3.　OVERVIEW AND FEATURES OF THE ZERO-EMISSION BATTERY-PROPELLED TANKER "ASAHI"

3.1　Features of Battery Propulsion System

As benefits of battery propulsion systems, both GHG emissions such as carbon dioxide (CO_2) and pollutants such as nitrogen compounds (NOx), sulfur compounds (SOx) and soot and smoke (particulate matter: PM) can be substantially reduced. Other benefits of battery propulsion systems include improvement of the living environment for the crew by reduction of noise and vibration because the ship does not have a main engine, and improvement of the environment around the port.

On the other hand, because the batteries employed in battery propulsion systems have a much smaller energy density than the heavy oil used as a general marine fuel, the cruising distance (range) is an issue. In terms of the system configuration, a battery propulsion system appears simple, but actual operation is a challenging endeavor. In fact, system configurations that supply all of the energy required for ship operation using only batteries have only been adopted in some limited types of ships, such as short distance ferries serving regular routes.

3.2　Study of Specifications of the "Asahi"

Operation of a bunkering ship broadly consists of four types of operation: ① Cargo handling work (taking on fuel oil on the bunkering ship, supplying the fuel oil to other ships), ② Voyaging to fuel oil loading and bunkering locations (navigation), ③ Entering/leaving port, berthing/deberthing, coming alongside/leaving the ship being fueled and ④ Anchorage (waiting while in service, mooring). The main equipment used in these respective operations is as follows.

Table 1　Main equipment in each operation

① Cargo handling	Cargo pump (when fueling other ships), controllers and other onboard equipment
② Navigation	Thrust (propeller), onboard equipment
③ Entering/leaving port, berthing/deberthing, coming alongside/leaving	Thrust (propeller), side thrusters, deck machinery
④ Anchorage	(when waiting) Pumps and other onboard equipment, (mooring) cooking equipment and other everyday life devices

The battery capacity, which is the largest factor in a battery propulsion system, was determined by conducting a simulation of energy use. The factors related to battery capacity are the operating time of each of the above operations and the energy consumption of the operation. Because the cargo handling locations are distributed in Tokyo Bay and the number of cargo handling operations in one day differs, various operational patterns must be considered. Therefore, the operational data for an existing ship, navigation distances and other information were obtained from the ship's Owner, updated for the specifications of the new ship, and used as the input data for the simulation. The propulsion performance and a knowledge of batteries are also important elements for determining the battery capacity. In conducting the simulation, we took advantage of the strengths of Kawasaki Heavy Industries as a general heavy industrial manufacturer. Propulsion performance was based the experience of the company's Marine Machinery Business Division, which has delivered a large number of propellers to date, and the battery technology was based on the experience of the Battery Team in the Technology Development Division. The simulation of energy use was carried out based on this information, and the battery capacity necessary for the operation of this ship was determined. In addition, the possibility of actual operation with the calculated battery capacity was also verified.

For battery charging, a plug-in system using land-based power was adopted. In the operation of the ship, the battery is charged while the ship is moored at night after completing the day's operation and returning to port, and the ship then leaves port the next morning. The study of the charging procedure and the power supply capacity required to complete charging while the ship is moored overnight was carried out in cooperation with a land-based equipment company.

Based on the battery capacity determined as described above, the arrangement of the individual batteries in the ship was studied in consultation with the Owner and the Shipyard. Taking advantage of the flexibility of arrangement possible with a

battery propulsion system, the batteries were arranged in two layers on the bow sides, realizing a shipboard layout that can secure the necessary load capacity of fuel for bunkering while also keeping a large living area for the crew.

Since high maneuverability is demanded in a bunkering ship, which frequently performs the operations of entering/leaving port, berthing/deberthing and coming alongside/leaving ships being fueled, a design with 2 azimuth thrusters and 2 side thrusters was proposed for the propulsion equipment. The power of the propulsion equipment was decided considering its arrangement on a vessel with a gross tonnage of 499 tons while maintaining the necessary speed.

Based on the study described above, the following specifications were adopted for the ship.

Table 2　Specifications of "Asahi"

Dimensions	Length overall: 62 m / Beam: 10.3 m
	Draft: 4.15 m
Speed	10 knots (approx.)
Tank capacity	1,277 m^3
Propulsion equipment	Azimuth thruster: 300 kW x 2
	Side thruster: 68 kW x 2
Battery capacity	3,480 kWh

3.3　Large-Capacity Battery Propulsion System

Kawasaki Heavy Industries was responsible for the large-capacity battery propulsion system, which comprises the large-capacity LiBs, main switch board, power management system, power conversion module, main electric motor, azimuth thrusters (Kawasaki Rexpeller®), propulsion control system, side thrusters and other equipment (Fig. 6).
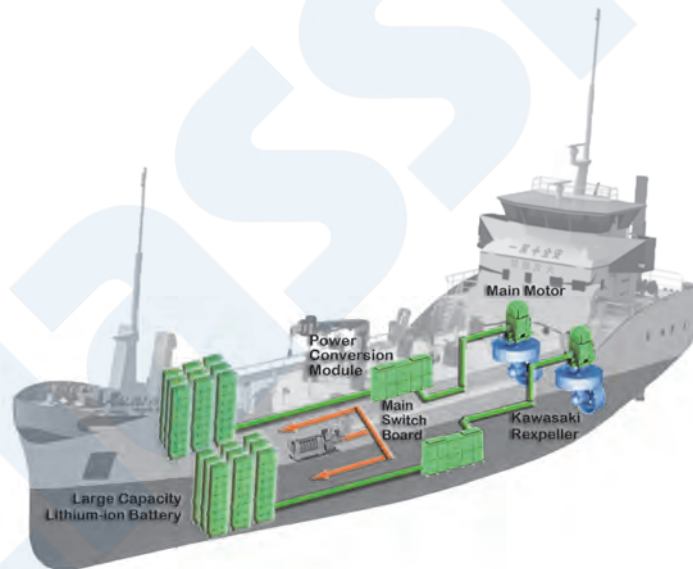
Fig. 6　Large-capacity battery propulsion system

As shown in Fig. 6, the lithium-ion batteries are coupled with the power conversion module, which distributes the power from the LiBs to the main motor and the main switch board for use as propulsion power and onboard power, respectively. As discussed in Section 3.2, this ship has four types of operation, ① Cargo handling, ② Navigation, ③ Entering/leaving port, etc. and ④ Anchorage. The following mode setting is performed for these four operations.

Table 3　Definitions of operational modes

Cargo handling mode	Mode in which fuel is supplied to the ship being fueled by using the cargo pump.
Navigation mode	Mode in which the ship navigates by using the azimuth thrusters.
Entering/leaving port mode	Mode in which the ship enters/leaves port, performs berthing/deberthing and comes alongside/leaves the object ship by using the azimuth thrusters and side thrusters.
Anchorage mode	Mode in which the ship stops the azimuth thrusters and side thrusters and moors.

Smoothly utilizing each of these operations as appropriate is extremely important for the operating efficiency of the ship. Furthermore, it is also necessary to consider the safety aspect so as to ensure that there are no mistakes in the start of operation of the propulsion equipment during cargo handling work. Considering both the operational aspect and the safety aspect, mode switching sequence is set as navigation mode and entering/leaving port mode, in which the propulsion equipment is used, and cargo handling mode, in which mode switching is performed once via the anchorage mode.

The devices used in the four operational modes are different, and large propulsion power is required in the navigation mode, while large onboard power is required in the cargo handling mode and entering/leaving mode. This means it is important to switch the necessary propulsion power and onboard power smoothly based on the operational mode. Since it is a burden to the ship's operator for switching the operating equipment and changing the allocation of power with an awareness of this, the system for this ship is equipped with a function that automatically judges the operational mode and switches the energy distribution automatically. This function is materialized by optimal management of the energy/power flow in the propulsion control system. In the anchorage mode at the mooring point, the batteries are charged by receiving power from an onshore power supply facility.

In addition to operational mode switching and management of propulsion power and onboard power, the propulsion control system also performs integrated control of battery charge/discharge management.

3.4　System Safety

At present, no ClassNK rules have been established for battery-propelled ships at present. Therefore, the battery room and the batteries themselves were designed based on "Guidelines for Large-Capacity Storage Batteries," which has been published by ClassNK. Because Chapter 4.9 of the Guidelines requires a risk assessment for safety, the safety of the system was verified by using HAZID (Hazard Identification). HAZID is one assessment technique for determining how the target system may affect human life and the environment by identifying assumed events (hazards) and studying the safety of the system based on the combination of their frequency of occurrence and degree of effect. In HAZID, the risks in the ship operation condition during normal operation and under abnormal conditions such as fire, etc. is verified, and safety measures are studied. In the HAZID for this ship, the risk assessment was conducted with the participation of the Owner, the basic design company and Kawasaki Heavy Industries, and for a safety assessment from the third-party viewpoint, ClassNK and NK Consulting Service Co., Ltd., which is also a risk assessment facilitator, were also asked to participate.

In the HAZID, hazards related to the ship were identified by the cause of the hazard, which included items related to the lithium-ion storage battery system itself and electrical, thermal and other hazards. The following are examples of representative hazards.

① Overcharging of batteries
② Thermal runaway of batteries [*2]
③ Abnormality of control devices

The validity of the design in the stage prior to the HAZID was evaluated for these hazards, and the necessity of additional safety measures was discussed. As a result, it was confirmed the risk of all hazards could be suppressed to the tolerable range by executing the design at the time of the HAZID with additional safety measures, and the design in which these safety features were confirmed was implemented in the ship.

[*2] Thermal runaway refers to a condition in which a designated internal component in a battery generates heat for some reason, that heat generation triggers heat generation in other components, and the temperature of the battery continues to rise. The main causes are internal short circuit, external short circuit, overcharging, heating from an external source, etc.

3.5　Handling of Batteries and Points to Note

Even in familiar electronic devices such as cellphones, it is known that batteries have a useful life, as they deteriorate with use and their performance gradually declines. Although fewer in recent years, in the past, examples of accidents in which mobile batteries exploded had been reported on television and in other media. The following are points to note when using large-capacity batteries on a ship.

① Temperature management

Proper temperature management of the ambient environment for battery use is important. If proper temperature management is not introduced, early deterioration of the battery is possible, and this may be fatal for the battery propulsion system, which depends on the battery as its main source of electric power. Therefore, we consulted with the Shipyard, air-conditioner manufacturers and others and selected an air-conditioner considering the heat generation from the battery itself and external heat inputs to the battery room.

② Application of the Fire Services Act

Lithium-ion batteries contain a flammable liquid electrolyte that falls under Class IV hazardous materials, Class II petroleum of Japan's Fire Services Act. Appropriate handling in accordance with the Act or local government ordinances must be noted, including handling during storage and ship outfitting work in the shipyard.

③ Fire-extinguishing devices in the battery room

A CO_2 fire extinguishing system was adopted as the fire-extinguishing device in the battery room. To enable sure fire-extinguishing in case a fire occurs, the control location and fire-extinguishing agent storage location were also discussed in the HAZID.

3.6　Features of the "Asahi"

In this ship, we adopted the KICS (Kawasaki Integrated Control System), which enables integrated control of multiple ship-handling elements. The improved ship maneuverability and shorter time required for berthing and deberthing, etc. reduce the energy necessary in ship operation, which in turn makes it possible to reduce the battery capacity in the battery propulsion system. In conventional ship handling, the ship operator must simultaneously operate multiple thrusters in order to move the ship in the intended direction. In response to operation of a joystick and dial, KICS moves the ship in the direction that the joystick is moved and turn the ship in the direction that the dial is turned (Fig. 7). KICS can also calculate the size and direction of the thrust that should be output by multiple thrusters corresponding to the operation of the joystick and dial by the operator and give appropriate commands to the various thrusters. This allows the operator to steer that ship only by intuitive operation, even in operations that are difficult and require care, such as berthing and deberthing.
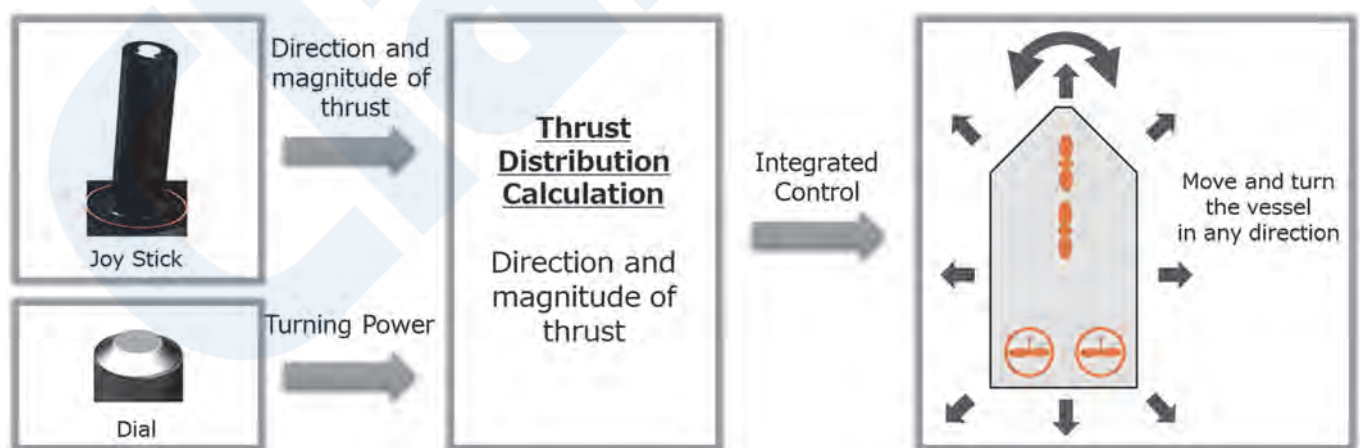
Fig. 7　Overview of KICS

As one more noteworthy feature, the ship's batteries can also be used as an emergency power source during large-scale natural disasters, which was an idea proposed by the owner and e5 Lab. By utilizing the electricity stored in the LiBs on the ship as an emergency power source on land, it is possible to contribute to the business continuity plans (BCP) and life continuity plans (LCP) of regional society. Moreover, because a ship can access locations where electric power is required from the sea under

conditions where the land transportation network is not functioning due to traffic congestion or damaged roadways, this capability will expand the possibilities for responding to states of emergency.

4. OUTLOOK FOR THE FUTURE

4.1 Optimum System Configuration Corresponding to the Ship

Although higher energy densities have been achieved in batteries through technical innovation, the energy density of batteries is still far lower than that of the heavy oil used as a marine fuel. This means there is a limit to the cruising distance of a ship using only batteries, considering the balance with space on the ship. From this viewpoint, hybrid propulsion using a combination of batteries and an internal combustion engine is realistic in certain cases, for example, in ships with comparatively long continuous cruising distances and large ships, in which battery propulsion would only be used when entering and leaving port. In addition to the problems of shipboard space and cruising distance, there are also other elements that should be considered, such as the availability of charging points (or charging interval) and the time required for charging. Thus, it is necessary to study a total solution that includes not only the aspects of ship layout and operation, but also charging facilities on the land side.

Moreover, the types of operations such as cargo handling, work at sea, etc. vary depending on the type of ship, and the optimum size of the main engine, battery capacity and system configuration of each type will also differ. We, Kawasaki Heavy Industries, propose the optimum system for all ship sizes and ship types responding to each type of ship operation and the request of the ship owner.

Battery hybrid and pure battery propulsion systems also have excellent compatibility with engines using LNG, which has been adopted progressively as a low environmental load fuel in recent years, and with engines, fuel cells and other power sources that utilize future fuels such as hydrogen and ammonia, which are expected to be used as decarbonized fuels in the future. It is possible to propose GHG reduction options that also include the future by combining those technologies with the system described here.

4.2 Gas Single-Fuel Fired Engine + Battery Hybrid Propulsion System

Kawasaki Heavy Industries has developed and received its first order for a hybrid propulsion system which combines a marine gas single-fuel fired engine (Fig. 8) and a large-capacity lithium-ion battery. The basic configuration of the hybrid propulsion system consists of the gas single-fuel fired engine and a large-capacity LiB. However, as the system integrator, Kawasaki Heavy Industries also covers the propulsion equipment, such as the gas fuel supply system, variable pitch propeller and side thrusters, as well as other equipment such as the power conversion module, propulsion control system, etc. Optimum operation for CO_2 reduction while maintaining the necessary thrust is achieved by appropriately controlling those systems and equipment corresponding to navigational conditions.

During navigation, propulsion is provided by the gas engine by way of a speed reducer. At the same time, the electric power generated by a shaft generator is used to supply onboard electric power and charge the batteries. This means the gas engine can be operated continuously in the high load region, where it is possible to maintain high thermal efficiency, and separate operation of a generator to supply onboard power, like that on conventional ships, is not necessary. In addition, high-load operation of the gas engine can also be continued during bad weather by properly controlling the balance of thrust and power generation. When entering/leaving port and when the ship is anchored or moored, the gas engine is stopped and during voyage, electrical propulsion power and onboard power are supplied by the charged batteries, thereby achieving zero emission operation.

Fig. 8　Marine gas engine

4.3　Marine Lithium-Ion Capacitor

In battery hybrid and pure battery propulsion systems, the role of power storage systems such as batteries is to supply or store energy for propulsion power and onboard electric power. However, as another role, it is also possible to absorb load fluctuations of the main engine and main generators. That is, fuel economy is improved by assisting main engine load changes, for example, in rapid acceleration, and in compensating for fluctuations in propulsion output during bad weather, etc.

In comparison with heavy oil-fired diesel engines, it is said that the above-mentioned engines that use LNG or future fuels such as hydrogen or ammonia generally have a narrower stable combustion region and are more susceptible to misfiring and knocking due to load fluctuations. For this reason, stabilizing the engine load by using these engines in combination with batteries or some other type of power storage system can contribute to expanding the range of application of these new fuel engines and their operable region.

Kawasaki Heavy Industries was the first to focus on this kind of load fluctuation absorbing application of the power storage system, and developed a power storage system using a marine lithium-ion capacitor (LiC) (Fig. 9)

The LiC is a storage device with a high power density (capable of instantaneously charging/discharging a large amount of electric power) and has an extremely long life when repeatedly charged and discharged. Table 4 shows a comparison of the representative specifications of the LiC and a lithium-ion battery (LiB), which is also a storage device. While the LiB has a high energy density and is suitable for supplying energy over a long period, the battery deteriorates due to repeated charging and discharging, and its power density is low. On the other hand, the LiC has a low energy density and thus is not suitable for supplying energy over an extended period, but it has the benefits of a high power density and extremely long life under repeated charging and discharging. Therefore, while the LiC alone cannot be used in ship propulsion and power supply applications, a large reduction in size, lower cost and long life can be expected by limiting its use to the load fluctuation absorbing function.

Fig. 9　Marine lithium-ion capacitor (LiC)

Table 4　Comparison of LiB and LiC

Item	LiB	LiC	Remarks
Temperature of use environment	15 to 25 °C	5 to 45 °C	
Cycle life	10,000 or less	500,000 or more	Differs depending on test conditions.
Float life	10 years (approx.)	20 years or more	At 25 °C
Charge/discharge rate	3 C (approx.)	100 C	1 C: 100% discharge in 1 hour

5.　CONCLUSION

With the ongoing tightening of regulations on all types of exhaust gases by the IMO (International Maritime Organization), use of clean power sources as an alternative to the heavy oil which is generally used as a ship fuel has attracted large expectations and interest in the shipping industry. One of these clean power sources is battery propulsion systems, which can substantially reduce emissions of carbon dioxide (CO_2), nitrogen oxides (NOx), sulfur oxides (SOx) and particulate matter (PM) during ship operation. Proposing the optimum system, which differs in each ship, and wide dissemination of the system described in this paper will contribute to improvement of the global environment, and Kawasaki Heavy Industries would also like to play a role in those efforts.

In the future as well, Kawasaki Heavy Industries will focus its efforts on supplying systems with excellent environment-friendliness and economy and optimized operation in line with the requests of its customers.

REFERENCES

1)　Asahi Tanker Co., Ltd., Completion of Next-Generation Coastal Electric-Propelled Tanker "Asahi" https://www.asahi-tanker.com/news-release/2022/647/ (accessed August ,1 2022)

2)　Shingo Maekawa, Toward Reduction of Exhaust Gas from Ships – Electrification/Hybridization of Marine Propulsion Systems, Journal of the Japan Institute of Marine Engineering, Vol. 57, No. 2 (2022), pp. 20-24.

Introduction to "Guidelines for Additive Manufacturing (3D Printing)"

Kazunori OTAKI[*]

1. INTRODUCTION

In recent years, the development of metallic products using additive manufacturing (AM) technologies, notably 3D printing, has spread rapidly, and in particular, this technology is used in fields such as automobiles, aerospace, medicine and industrial machinery. One reason for this rapid growth is the molding capability of AM, which makes it possible to produce shapes that were impossible with conventional technologies and is a distinctive feature of AM. Because this capability realizes molding of complex 3-dimensional shapes, grating structures and graded structures and makes it possible to manufacture highly designed products, additive manufacturing is expected to bring about a major revolution in manufacturing in the future.

Additive manufacturing has a long history, dating from the invention of optical modeling using ultraviolet rays and photosensitive resin in Japan at the beginning of the 1980s, and was subsequently commercialized by American and Japanese companies. Although the use of this technology initially concentrated in resin modeling, research on application to metal materials was also begun in the United States, and a large number of AM machines have been developed to date.

Recently, cost reduction and improved productivity have been strongly demanded in all manufacturing industries. AM technology has attracted considerable interest as a breakthrough solution to this problem, as it enables efficient manufacturing and is also a labor-saving process. Since the market scale of AM machines is also increasing by the year, a further expansion of the fields of product manufacturing utilizing AM technology is foreseen in the future, including application to the marine equipment field.

Against this backdrop, as an introduction to additive manufacturing technology, ClassNK prepared "Guidelines for Additive Manufacturing (3D Printing)", which summarizes the terminology, types and characteristics of AM technology, together with the approval requirements for metallic marine equipment manufacturing using AM. The following introduces the content of the Guidelines.

2. INTRODUCTION TO THE GUIDELINES

2.1 Fundamental Knowledge of Additive Manufacturing (Part 1 of the ClassNK Guidelines)

2.1.1 Terminology

Because the terminology used in the Guidelines is the basic terminology of additive manufacturing (hereinafter called "AM") technology, the terminology used in this documents is defined referring to international standards such as ISO and JIS or national standards. Specifically, the standards used as reference are as follows.

(1) ISO/ASTM 52900 : 2015 "Additive manufacturing – General principles – Terminology"

(2) JIS B 9441: 2020 "Additive manufacturing – General principles − Vocabulary and fundamental concepts"

2.1.2 Additive Manufacturing Technologies (AM Technologies)

The seven technologies listed in the following Table 1 have been defined as the basic types of AM technologies. Among these, the AM technologies which are mainly used in manufacturing metallic products are generally the powder bed diffusion (PBD) process and the direct energy deposition (DED) process. However, these Guidelines present the overview, feedstocks and process after lamination for all seven types of AM technology in Table 1. The categorization of the main AM technologies using each feedstock is also shown in Fig. 1.

[*] Rule Development and ICT Division, Machinery Rules Development Department, ClassNK

Table 1　Types of AM technologies

	Additive Manufacturing Technology
1	Binder Jetting：BJT
2	Material Jetting：MJT
3	Powder Bed Fusion：PBF
4	Directed Energy Deposition：DED
5	Sheet Lamination：SHL
6	Vat Photopolymerization：VPP
7	Material Extrusion：MEX
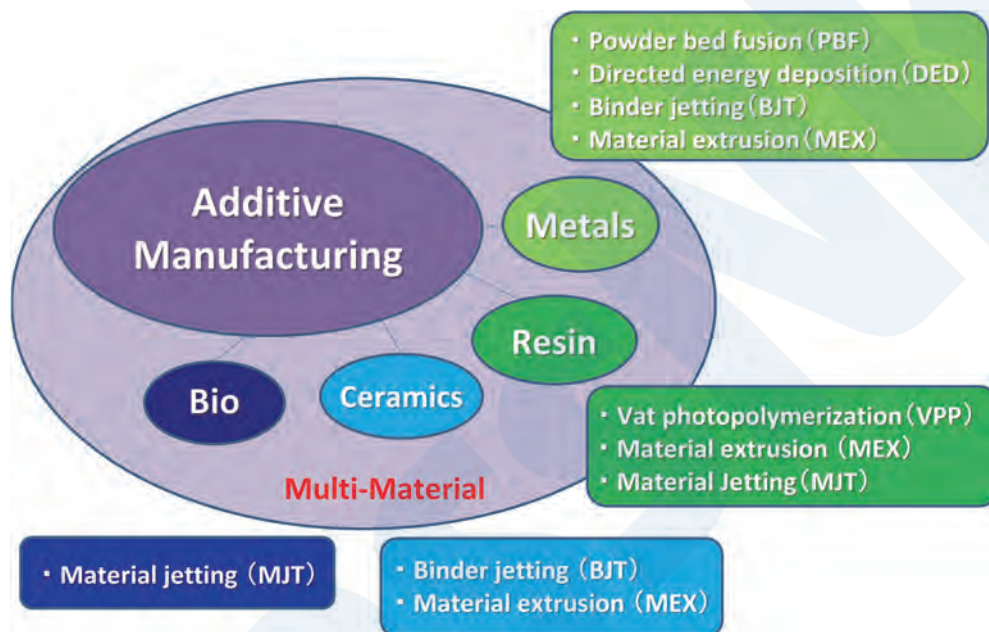
Fig. 1　Categorization of main AM technologies used for feedstocks

2.2　Handling of Metallic Marine Equipment Manufactured with AM (Part 2 of ClassNK Guidelines)

2.2.1　General

(1) Application

ClassNK (hereinafter, also referred to as the Society) regards AM technology as an alternative to casting technology and assumes that there will be cases in which products and parts that have been manufactured using casting technology until now will be manufactured using AM technology in the near future. Accordingly, products which are cast products used in ships and require the approval of the Society are considered to be the objects of application of these Guidelines. The specific targets of application are assumed to be the metallic products mentioned in Chapter 3, Part 1 of Guidance for the Approval and Type Approval of Materials and Equipment for Marine Use (in case NK approval materials are used), as shown in the following Table 2. A separate approval scheme has been prepared to respond to requests for approval of metallic products other than those in Table 2 (called "not NK approval material" in the table), and its content is introduced in section 2.2.5 below.

Table 2　Examples of products subject to application of the Guidelines

Material classification		Product classification
Castings	Carbon steel castings*	(1) Component parts for hull
	Low-alloy steel castings	(Examples : stern frames, rudder frames, rudder stocks, etc.)
	Stainless steel castings	(2) Component parts for Diesel engines
	Steel castings for low temperature services	(Examples : connecting rods, piston rods, piston crowns, cylinder covers, etc.)
	Spheroidal graphite iron castings	(3) Crankshafts
		(4) Component parts for shafting
	Grey iron castings	(Examples : thrust shafts, intermediate shafts, propeller shafts, etc.)
		(5) Component parts for power transmission gears
Forgings	Carbon steel forgings*	(Examples : reduction gears, reduction gear shafts, etc.)
	Low-alloy steel forgings	(6) Component parts for steam turbines
	Stainless steel forgings	(Examples : turbine rotors, turbine discs, turbine blades, etc.)
		(7) Component parts for piping (Examples : valves, pipe fittings, etc.)
	Steel forgings for low temperature services	(8) Component parts for cargo gears
		(Examples : gooseneck pins, gooseneck brackets, etc.)
		(9) Component parts for boilers and pressure vessels
		(except those for low temperature service.)
		(10) Component parts for ships carrying liquefied gases in bulk

(2) Approval flow

　　The approval flow in these Guidelines is shown in Fig. 2. As mentioned in the above (1), when products that fall under Table 2 are to be manufactured using AM technology, the flow denoted by "NK approval material" in Fig. 2 is applied. In case an applicant wishes to obtain approval on a voluntary basis for a metallic product which is not included in Table 2 (i.e., use a not NK approved material), the flow denoted by "Not NK approval material" is applicable. The detailed contents of the items in the flow shown in Fig. 2 are described in 2.2.2 "Type Approval of Feedstocks," 2.2.3 "Approval of Manufacturing Process," 2.2.4 "Test and Inspection of Products" and 2.2.5 "Preliminary Examination of Products to be Manufactured."
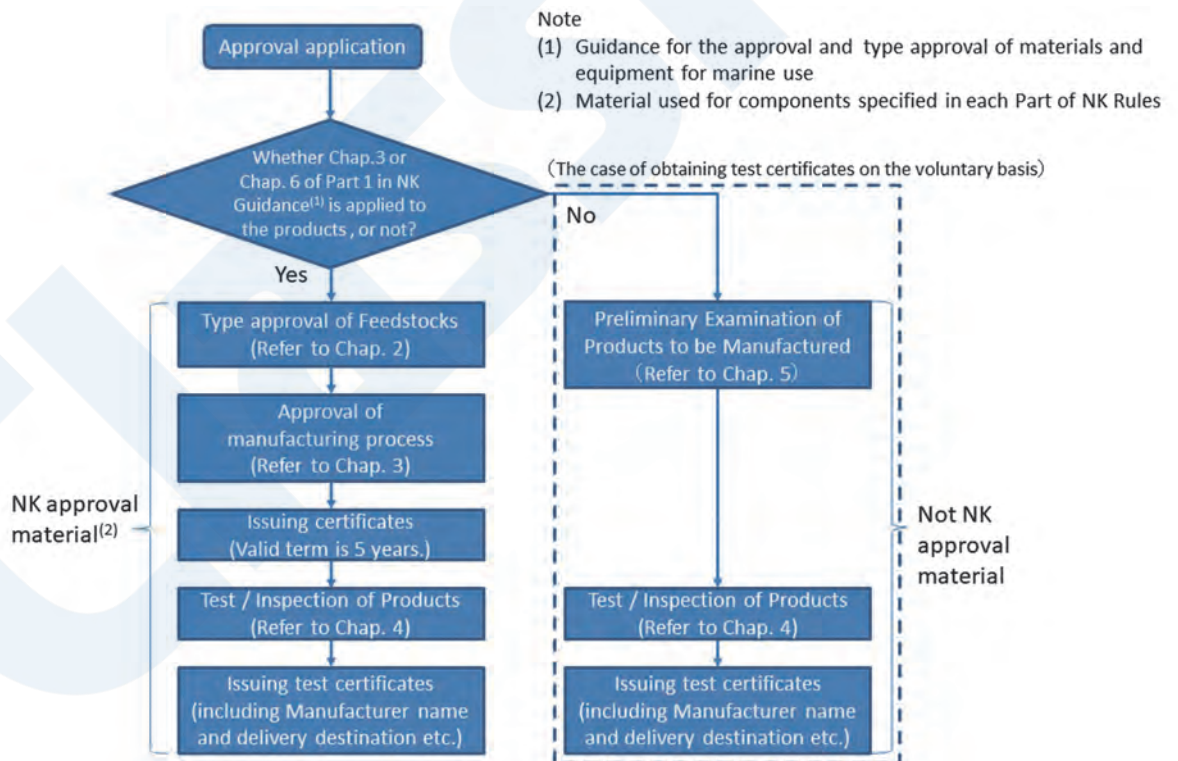
Fig. 2　Approval flow

(3) Feedstocks and product material symbols

　　For the symbols of AM feedstocks and products, the symbols defined in public standards such as Part K of the Society's Rules for the Survey and Construction of Steel Ships or international or national standards (e.g., JIS, ISO, etc.) recognized as appropriate by the Society are to the used.

　　For feedstocks for AM, the designation -F-AM is to be added after the material symbol of the feedstock, and is to be followed

by the symbols indicating the type of heat treatment, as described below (Table 3) and the material symbol for the type of AM (Table 4). When necessary, the symbols for the hydrogen content (-H5, -H10, -H15) defined in Chapter 6, Part M of Rules for the Survey and Construction of Steel Ships may also be used.

For products manufactured by AM, the designation -AM, the symbols indicating the type of heat treatment in Table 3 and the material symbols indicating the type of AM technology used in Table 4 are to be added after the material symbol of the material.

Table 3　Symbols indicating type of heat treatment

-A	As printed
-SR	Stress relieve heat treated
-SA	Solution annealed / e.g., for homogenization
-HIP	Hot isostatic pressed
-HPHT	High pressure heat treatment
-X	Other heat treatment

Table 4　Symbols indicating type of AM technology

MJT	Material jetting
PBF-LB	Powder bed fusion for laser beam melting
PBF-EB	Powder bed fusion for electron beam melting
PBF-SL	Powder bed fusion for selective laser melting
LMD	Laser metal deposition
WAAM	Wire arc additive manufacturing
Other AM	Must be recognized as appropriate by the Society

Examples of the description of material symbols are shown below.

KSCA45-F-AM-A-WAAM:

Feedstock for low-alloy steel castings KSCA45 as-printed by wire arc additive manufacturing

KFCD45-AM-A-PBF-LB:

AM product of spherical cast graphite cast iron KFCD45 as-printed by powder bed fusion for selective laser melting

2.2.2　Type Approval of Feedstocks

(1) Flow of type approval

The flow of type approval of feedstocks is shown in Fig. 3. Here, as the "Application," it is assumed that the application for type approval is submitted by the material supplier. The details of the respective items are shown below in (2) and the following sections. Materials approved by the Society are required to be used in main structures such as the hull structure, engine, etc. in ships which are registered as ClassNK ships. The same concept is also applied to materials for metallic marine equipment, etc. which is manufactured by AM.
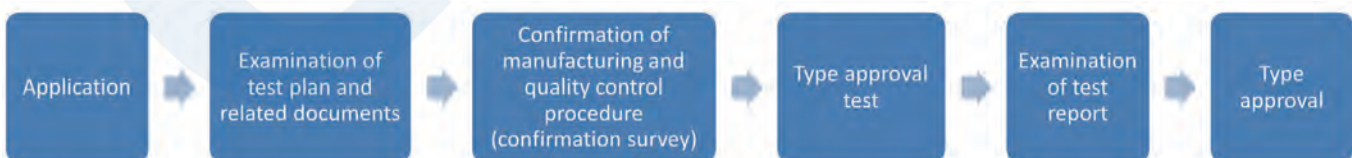

Fig. 3　Flow of type approval of feedstocks

(2) Submitted documents

Table 5 shows the minimum level of the documentation which is to be submitted when applying for type approval. Some of the submitted documents may be omitted in case the feedstock has already received type approval by the Society and these documents would duplicate those submitted in the previous application.

Table 5　Documents to be submitted for type approval of feedstocks

		Submitted documents
	①	Application for type approval of feedstocks
	②	Type approval test plan (including acceptance criteria)
	③	Outline of manufacturing plant (a) Name and location of plant (b) History (c) Organization and number of employees
	④	Documents for manufacturing processes (a) Manufacturing processes (including the flowchart of each of the main processes) (b) Outline of the main manufacturing facilities
	⑤	Documents for feedstocks (including information such as the names and locations of material suppliers) (a) Manufacturing process and type of feedstocks (b) Feedstock characteristics (e.g., in the case of powders, flowability and fillability) 　● Wire type: Documents concerning the type of core wire, chemical composition, acceptance procedure, wire drawing, rust prevention and wire diameter 　● Powder type: Documents concerning the main composition, density, surface area, particle size distribution, flow property, uniformity/equivalence, morphological characteristics, inter-particle friction, particle agglomeration, etc. (c) Characteristics of products manufactured by AM (tensile strength range, etc. for each AM technology) (d) Management method in AM site (e) Reuse criteria and methods (if applicable)
	⑥	Documents for quality management of feedstocks (a) Quality management system and criteria (b) In-house inspection standards and inspection facilities (c) In-house inspection department and complaint handling department (d) Example of shipping certificate
	⑦	Documents for past manufacturing record for main feedstocks
	⑧	Documents for chemical composition of feedstocks
	⑨	Documents for heat treatment (if performed)
	⑩	Documents for storage methods and storage periods before and after unsealing (if performed)
	⑪	Documents for packaging, shipping marking and traceability
	⑫	Documents for the use method and additive manufacturing technology to be applied (including recommended conditions)
	⑬	Other documents as deemed necessary by the Society

(3) Confirmation of manufacturing and quality control procedure (confirmation survey)

　The purpose of this survey is to confirm that the applicant has the capability (facilities, technology, quality management and in-house inspection department) to consistently manufacture the feedstock which is the object of certification at the same level or exceeding the level of the feedstock used in the type approval test with uniform and continuous quality. In conducting the survey, mainly the following items are confirmed.

● Manufacturing processes
● In-house inspection and complaint handling department
● Manufacturing facilities and inspection facilities
● Company standards, work standards, the quality management system and their implementation status

(4) Type approval test

　Tests in connection with the following items (Table 6) are to be conducted in accordance with the test plan approved by the Society. The purpose of these tests is to confirm the soundness of the material.

Table 6　Type approval test

Test item	Content of test
Analysis of chemical composition	The analysis of the chemical composition is to be conducted by a method, such as JIS G 0321, which is recognized as appropriate by the Society to confirm that the analysis result is the same as the value shown in the document (Submitted documents (8)) submitted previously.
Tensile test	The tensile test is to be conducted using a test piece prepared at the same time as the product (certified maximum dimensions) manufactured using the feedstock to confirm that the test result conforms to the acceptance criteria described in the test method approved in advance. For tensile test pieces, considering the anisotropy of the structure due to rapid melting and solidification, at least 3 test pieces are to be prepared for each of the test angles as shown in Fig. 4 to Fig. 6.
Structure observation	The structure of the test pieces is to be observed in cross sections in each of the directions x, y and z to confirm that the structure is continuous and contains no defects (cavities, lack of fusion, etc.) that could possibly cause failure.
Other tests (if recognized as necessary by the Society)	Additional tests may also be required, such as the hardness test, bending test, impact test, surface roughness test, brittle fracture test, fatigue test, corrosion test, hydrogen test, powder reuse test, particle size distribution test, particle morphology test, metal powder flow test, repose angle test, shearing strength test and compressive strength test.
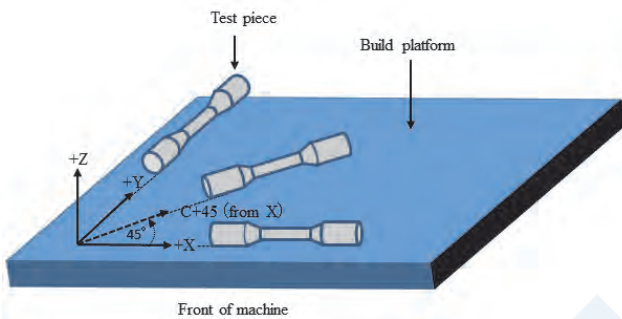
Fig. 4　Tensile test piece [0 degrees]
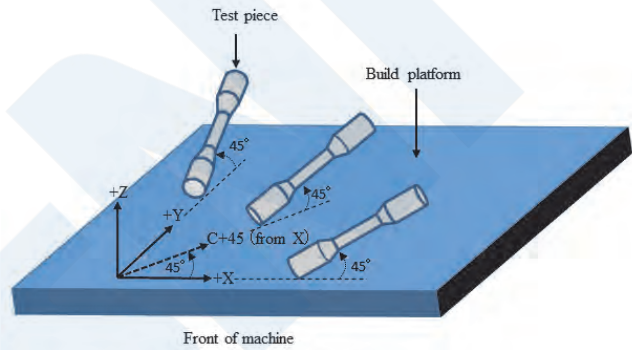
Fig. 5　Tensile test piece [45 degrees]
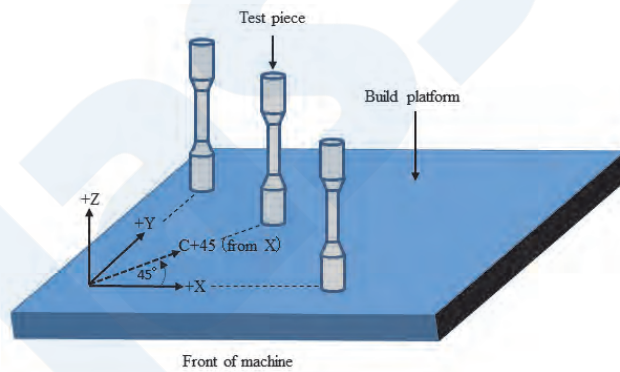
Fig. 6　Tensile test piece [90 degrees]

(5) Acceptance criteria

The acceptance criteria are to be determined by the applicant with reference to public standards such as Part K of Rules for the Survey and Construction of Steel Ships or international standards or national standard (e.g., JIS or ISO) recognized as appropriate by the Society.

(6) Notification of type approval

The Society issues a type approval certificate for each brand for feedstocks recognized as appropriate in accordance with the documentary examination, confirmation of the manufacturing and quality control procedure and test report. The validity period of the type approval certificate is to be one year from the date of issuance.

2.2.3　Approval of Manufacturing Process

(1) Flow of approval

The approval of the manufacturing process means that it is proven that the manufacturing process can be judged appropriate

for the product in question by conducting the examinations, tests and inspections of the product, based on prior confirmation of the manufacturing process and quality management for a representative product, premised on uniformity of product quality. The flow of this approval procedure is shown in Fig. 7. Here, it is assumed that the "Application" is submitted by the owner who controls the entirety of the AM system.

| Application for approval | ➡ | Examination of test plan and related documents (approval of test plan) | ➡ | Confirmation survey (factory inspection) | ➡ | Approval test | ➡ | Examination of test report | ➡ | Approval |

Fig. 7   Flow of approval of manufacturing process

(2) Submitted documents

Table 7 shows the minimum level of documentation which is to be submitted when applying for approval of the manufacturing process. Some of the submitted documents may be omitted in case the product has already received the approval of the Society and these documents would duplicate those submitted in the previous application process.
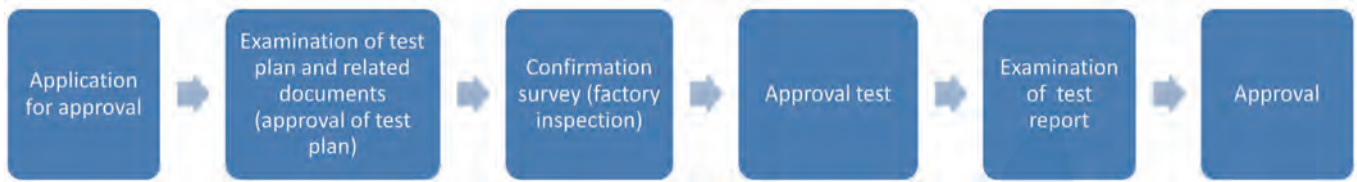
Table 7   Documents to be submitted for approval of manufacturing process

	Submitted documents
①	Application form for approval of the manufacturing process
②	Approval test plan (including acceptance criteria)
③	Outline of the manufacturing plant (a) Name and location (b) History (c) Organization and number of employees
④	Documents for the additive manufacturing machine to be used (including the maximum dimensions and maximum thickness)
⑤	Documents for manufacturing processes (including documents describing the deposition rate and topology optimization)
⑥	Documents for feedstocks (including information such as the names and locations of material suppliers) (a) Manufacturing process (b) Feedstock characteristics (e.g., flowability and fillability in the case of powders) (c) Management method (d) Criteria and method of reuse (if applicable) (e) Quality management
⑦	Documents for quality management of products (including testing machines, etc.) (a) Quality management system and management criteria (b) In-house inspection standards and inspection equipment (c) In-house inspection department and complaint handling department (d) Example of shipping certificate
⑧	Documents for heat treatment methods (if applicable) (a) Heat treatment furnaces (types, dimensions, locations of heat source and thermocouples, etc.) (b) Heat treatment conditions (temperature, holding time, cooling medium, etc.) (c) Heat treatment record-keeping method
⑨	Documents for nondestructive testing (including employee list)
⑩	Documents for production records of main products
⑪	Documents for the chemical composition and mechanical properties of products
⑫	Documents for the weldability of products (if applicable)
⑬	Documents for the surface state (roughness, finishing state, etc.)
⑭	Documents for repair procedures (including the allowable condition of flaws)
⑮	Other documents as deemed necessary by the Society

(3) Confirmation survey (factory inspection)

The factory inspection is conducted to confirm that the applicant possesses the facilities, processes, quality management and other capabilities necessary to manufacture the product with uniform quality. This inspection is conducted at an appropriate time

so that the actual AM system, manufacturing process, etc. can be surveyed.

(4) Approval test

The applicant is to conduct tests of the following items (Table 8) in accordance with the approved test plan. The purpose of this test is to confirm the appropriateness of the said manufacturing process using products manufactured based on the predetermined manufacturing process.

Table 8　Approval test of manufacturing process

Test item	Content of test
Tensile test	The tensile test is to be conducted using test pieces prepared at the same time as the product to confirm that the test result conforms to the acceptance criteria described in the test method approved in advance. For tensile test pieces, as in the type approval test of the feedstock, at least 3 test pieces are to be prepared for each test angle, as shown in Fig. 4 to Fig. 6.
Structure observation	The structure of the test pieces is to be observed in cross sections in each of the directions x, y and z to confirm that the structure is continuous and contains no defects (cavities, lack of fusion, etc.) that could possibly cause failure.
Nondestructive test	The nondestructive test of the product is to be conducted by a method which is capable of detecting internal defects and surface defects considered detrimental in use to determine whether the said product contains internal or surface defects that would be detrimental in use.
Visual inspection	A visual inspection of the external appearance of the product is to be conducted to determine whether defects considered detrimental in use are present on the product surface.
Analysis of chemical composition	The analysis of the chemical composition is to be conducted by a method, such as JIS G 0321, which is recognized as appropriate by the Society to confirm that the analysis result is the same as the value shown in the document (Submitted documents ⑪) submitted previously.
Other tests (if recognized as necessary by the Society)	Additional tests may also be required, such as the hardness test, bending test, impact test, surface roughness test, brittle fracture test, fatigue test, corrosion test, shearing strength test, compressive strength test, weldability test, etc.

(5) Acceptance criteria

The acceptance criteria are to be determined by the applicant with reference to public standards such as Part K of Rules for the Survey and Construction of Steel Ships or international standards or national standard (e.g., JIS or ISO) recognized as appropriate by the Society.

(6) Approval certificate

The Society approves the manufacturing process for the product using an AM system which the Society recognizes as appropriate in accordance with the documentary examination, factory inspection and test report and issues a Certificate of Approval. The validity period of the Certificate of Approval is to be 5 years from the date of approval.

2.2.4　Test and Inspection of Products

(1) Flow of test and inspection of products

The flow of the test and inspection procedure conducted prior to shipment of the product is shown in Fig. 8. Here, it is assumed that the "Application" is submitted by the owner of the AM system or the owner of the AM system who contracted to perform this test and inspection work.

Fig. 8　Flow of test and inspection of product

(2) Submitted documents

Prior to conducting the test and inspection of a product, the applicant is required to submit the test and inspection plan to the Society. The acceptance criteria for the tests and inspections are also to be included in this plan.

(3) Test and inspection

The applicant is to conduct the tests and inspections for the following items (Table 9) in accordance with the approved test and inspection plan. The purpose of these tests is to confirm the soundness of the product by using a representative product.

Table 9   Approval tests of product

Test item	Content of test
Mechanical test	The following tests are to be conducted to confirm that the product conforms to the acceptance criteria described in the approved test and inspection method. (1) Tensile test (see Table 6) (2) Hardness test (3) Impact test * (*The Society may allow omission of this test in some cases, depending on the feedstock used.)
Structure observation	The structure of the test pieces is to be observed in cross sections in each of the directions x, y and z to confirm that the structure is continuous and contains no defects (cavities, lack of fusion, etc.) that could possibly cause failure.
Nondestructive test	The nondestructive test of the product is to be conducted by a method which is capable of detecting internal defects and surface defects considered detrimental in use to determine whether the said product contains internal or surface defects that would be detrimental in use.
Visual inspection	A visual inspection of the external appearance of the product is to be conducted to determine whether defects considered detrimental in use are present on the product surface.
Dimension measurement	Dimensional measurement of the product is to be conducted to determine whether the dimensions are as designed.
Analysis of chemical composition	The analysis of the chemical composition is to be conducted by a method, such as JIS G 0321, which is recognized as appropriate by the Society to confirm that the analysis result is the same as the value shown in the document (Submitted documents (11)) submitted previously.
Other tests (if recognized as necessary by the Society)	Additional tests may also be required, such as the bending test, surface roughness test, brittle fracture test, fatigue test, corrosion test, shearing strength test, compressive strength test, etc.

(4) Acceptance criteria

The acceptance criteria are to be determined by the applicant with reference to public standards such as Part K of Rules for the Survey and Construction of Steel Ships or international standards or national standards (e.g., JIS or ISO) recognized as appropriate by the Society.

(5) Marking of the product

Products which pass the test and inspection procedure are to be stamped with the stamp of the Society. In cases where stamping would not be appropriate, the indication may be provided by another appropriate method, such as imprinting a seal, etc.

(6) Test and inspection certificate

In addition to the above (5), the Society issues a "Test and Inspection Certificate" for products which pass the test and inspection procedure. This certificate is not indicated a validity period and only certifies the fact of the inspection.

2.2.5   Preliminary Examination of Products to Be Manufactured

(1) Flow of examination

This examination is a requirement in case the applicant wishes to obtain approval on a voluntary basis for a metallic product other than those in Table 2 (i.e., use a not NK approval material). The flow of the approval is shown in Fig. 9. Here, it is assumed that the "Application" is submitted by the owner of the AM system.

Fig. 9   Flow of preliminary examination of products to be manufactured

(2) Submitted documents

In order to confirm the appropriateness of the application of these Guidelines to the product which is scheduled to be

manufactured using the AM system, it is necessary to submit the documents listed in Table 10 when requesting the examination. If no particular problems in the application of these Guidelines are confirmed as a result of the examination, the Society notifies the applicant to submit a test and inspection application as defined above in 2.2.4.

Table 10　Documents to be submitted for preliminary examination of products to be manufactured

	Submitted document
①	Detailed documents for the product to be manufactured (e.g., structural drawing, material supplier, brand of feedstock, laminated structure, internal structure, etc.)
②	Specification of AMmachine to be used
③	Documents for AM processes for the product to be manufactured (including documentation showing that it is possible to perform AM with uniform quality at any position in the build chamber or on the build platform)
④	Documents for quality management (including the acceptance criteria for feedstocks)
⑤	Documents for the chemical composition and mechanical properties of the product
⑥	Other documents recognized as necessary by the Society

(3) Test and inspection

The soundness of the product is to be confirmed by conducting the tests and inspections defined in the requirements of the above 2.2.4. Prior to conducting the said tests and inspections, a test and inspection plan, including the acceptance criteria, is to be prepared and submitted to the Society. In preparing the acceptance criteria, the acceptance criteria are to be determined in accordance with public standards such as Part K of Rules for the Survey and Construction of Steel Ships or international standards or national standards (e.g., JIS or ISO) recognized as appropriate by the Society.

(4) Marking of the product

As in the above 2.2.4, products which pass the test and inspection procedure are to be stamped with the stamp of the Society. In cases where stamping would not be appropriate, the indication may be provided by another appropriate method, such as imprinting a seal, etc.

(5) Test and inspection certificate

As in the above 2.2.4, the Society issues a "Test and Inspection Certificate" for products which pass the test and inspection procedure.

2.3　Characteristics of Metal Powder (Appendix 1 of the Society's Guidelines)

Focusing on metal powders, which are important in the manufacture of metallic products with AM technology, Appendix 1 summarizes the basic items in connection with the characteristics, storage and management methods for metal powders and measures and response in case of unforeseen accidents. The overview of each item is as shown below (Table 11).

Table 11　Content described in Appendix 1 (overview)

Characteristics of metal powders :	✓ Flowability, spreadability and fillability are important characteristics of the metal powders required in AM. ✓ The typical particle diameters of powders used in AM technologies are as follows: ・Laser beam powder bed method: 20 to 45 μm ・Electron beam powder bed method: 45 to 105 μm ・Deposition method: 45 to 105 μm
Storage and management methods :	✓ Powders are not to be stored in excessively humid areas, and must be stored in a cool, dark place. ✓ The powder management method should be described in a manual. ✓ Before using powder, the moisture content (hygroscopicity) in the powder must be measured using a hygrometer and is to be controlled to less than the threshold value determined by the user company. ✓ For recycled powder, the powder shape and oxygen content are to be measured periodically and controlled.
Measures and response to unforeseen accidents :	✓ In combustion of metal powders, ignition is caused by the combination of (1) a combustible material, (2) oxygen and (3) an ignition source. Therefore, any one of these three elements must be removed. ✓ If ignition occurs during work, the supply of oxygen is to be blocked by using a fire extinguisher for metal powder fires and drying sand. Foam-type fire extinguishers are not to be used, and fire-fighting using water is also strictly prohibited because hydrogen may be generated.

REFERENCES

1)   ClassNK, Guidelines for Additive Manufacturing (3D Printing), (2021)

Estimation and Use of Wave Information for Ship Monitoring

Wataru FUJIMOTO[*], Rei MIRATSU[*], Kinya ISHIBASHI[*], Tingyao ZHU[*]

1.　INTRODUCTION

In recent years, active development of ship monitoring and digital twin technologies has been underway in the ship field. For example, in the field of propulsion performance, the Japan Maritime Cluster Collaborative Research on Evaluation of Ship Performance in Actual Seas (OCTARVIA) Project has been carried out as joint research by 25 organizations in the Japanese maritime industry [1], and as part of this, an understanding of the meteorological and oceanographic conditions that ships encounter is necessary and indispensable [2]. In the structural field, research on digital twin for ship structures has been carried out, and estimation of the encountered sea states by ships has also attracted strong interest in this field [3]. In the joint symposium "Frontline of Ship Monitoring" of the Kansai Branch of the Japan Society of Naval Architects and Ocean Engineers (JASNAOE) and KFR/KSSG held in March 2022, estimation and use of wave information was a common topic in these two fields, and the fact that there are diverse types of wave information was recognized [4]. Furthermore, in order to use information related to ocean waves safely and at an advanced level, use must be based on its respective strengths and limitations of this information.

Nippon Kaiji Kyokai (ClassNK) participates in various types of monitoring and digital twin projects and has also conducted analyses of wave data to promote research and development in the industry. Through these initiatives, the organization has gained certain knowledge of the requirements for wave data in various applications.

This paper examines the use of wave data in ship monitoring, defined as a general term in a sense that also includes digital twins for ship structures (DTSSs). First, a brief explanation of the observation devices and analysis techniques that are generally in wide use is presented, followed by a discussion of their applicability to ship monitoring, while also presenting a review of the features of the main types of wave information.

2.　SHIPBOARD OBSERVATION DATA: CENTERING ON RADAR

Radar is a powerful device for observing a wide wavefield in the vicinity of a ship and has attracted considerable interest in recent years. However, since there are many areas that cannot be observed directly because they are hidden by the crests of waves, interpolation of those areas by some technique is necessary. The following presents an overview of the principle of radar observation, the types of radar and their features and limitations.

2.1　Principle of Radar

Because the wavelength of microwaves is near that of capillary waves, they are strongly scattered in the direction opposite the microwave irradiation direction by the mechanism called Bragg resonance scattering (Fig. 1). For this reason, observation of waves by radar is limited to conditions where the wind velocity is sufficient to generate capillary waves (Fig. 1). Here, capillary waves are sometimes called "surface tension wave" and refers to ripples that are formed by surface tension as the restoring force.
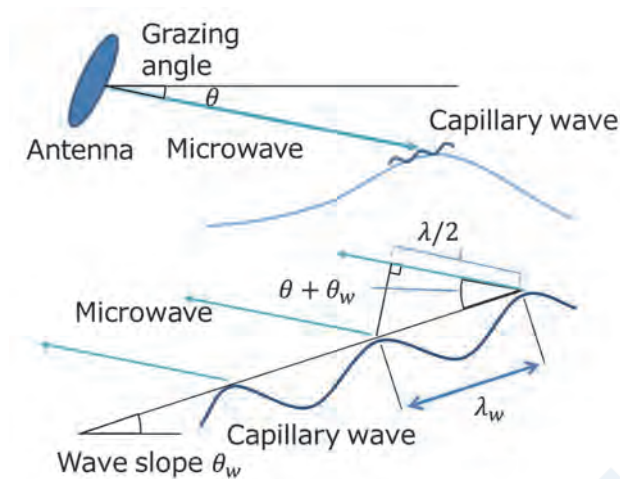
---

[*] Research Institute, ClassNK

Fig. 1　Schematic diagram of wave observation by microwave radar

(Top) Arrangement of antenna and ocean wave, (bottom) enlarged diagram at scale of capillary wave

When $\lambda/2 = \lambda_w \cos(\theta + \theta_w)$, microwaves are strongly reflected to the antenna by Bragg resonance scattering.

The intensity of the wave scattering, as known as radar cross section (RCS), changes by the following mechanism [5].

① Shadowing modulation

　Effect in which the opposite side of the wave crest as seen from the radar is hidden (shadowed) (Fig. 2). The installation height of ship radar is around several 10 m, while the observation radius of X-band radar is roughly several km, and shadowing becomes dominant as the area becomes more distant from the radar. Since it is necessary to use observation values from as far away as possible in wave forecasting, shadowing modulation is very important.

② Tilt modulation

　Effect in which radar reflection changes depending on the angle of the wave surface (Fig. 2). As the distance from the radar increases, only the crest of the wave is observed. Therefore, the slope of the wave surface decreases and tilt modulation becomes weak. Although tilt modulation is strong in the range near the radar, this area is excluded from the observation range in many cases because the reflection is too strong.
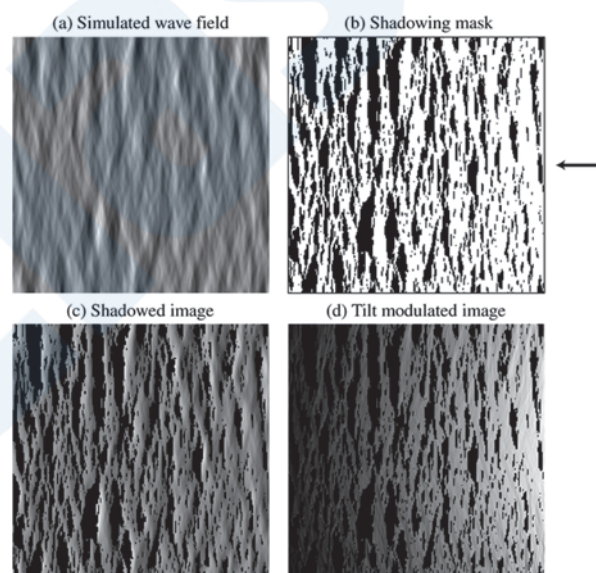
Fig. 2　Images of shadowing modulation and tilt modulation [5]

©American Meteorological Society. Used with Permission.

It is necessary to note that radar does not measure the wave profile directly, but only measures the RCS. The standard techniques for estimating the wave spectrum from the radar reflection [5] are as follows.

①　The spatiotemporal data $\rho(\boldsymbol{x}, t)$ of the radar reflection are acquired, and their rectangular region is extracted (Fig. 3 (a),

(b)). 3D FFT (**F**ast **F**ourier **T**ransformation) is performed, and the image spectrum of $(\boldsymbol{k}, \omega)$ is obtained (Fig. 3 (c)). Here, $\boldsymbol{x} = (x, y)$ is the horizontal spatial coordinate, t is time, $\boldsymbol{k} = (k_x, k_y)$ is the wavenumber in the horizontal direction and ω is the angular frequency.

② From the image spectrum of $(\boldsymbol{k}, \omega)$, bandpass filtering is applied only to components which follow the linear dispersion relation (Fig. 3 (d)). Here, the linear dispersion relation adjusted for the Doppler effects of the current velocity and ship's velocity is used. The filtered-out components are regarded as noise.

③ In order to consider shadowing modulation, a **M**odulation **T**ransfer **F**unction (MTF) $M(k)$ is introduced. Since it is known empirically that $M(k)$ follows the power law, tuning is performed by comparing the exponent q, assuming $M(k) = k^{-q}$, with other observational values (e.g., data from buoys, etc.) (Fig. 3 (e); the black line and red dotted line were acquired by radar and buoy observation, respectively). Here, $k = |\boldsymbol{k}| = \sqrt{k_x^2 + k_y^2}$.

④ The effect of shadowing is corrected from the image spectrum by using the MFT, and the wave surface is estimated by inverse 3D FFT (Fig. 3 (f)).

⑤ The significant wave height is estimated by comparison with buoy observation results. That is, a regression formula is created by comparing the **S**ignal **N**oise **R**atio (SNR) of the bandpass-filtered signal in ②, in which other components were treated as noise, with the wave height measured by the buoy, and thereafter, the wave height is estimated based on this regression formula.

For highly accurate observation of ocean wind waves, calibration of the radar by using a buoy or other observation device is extremely important [7]. If a wave radar system fixed on the coast is available, calibration is comparatively easy, since the weather conditions are limited and buoys and other observation devices are also easy to install. However, on ships which navigate in the open sea, the weather conditions change greatly, and in some cases it is difficult to prepare a separate observation device for use as a reference.
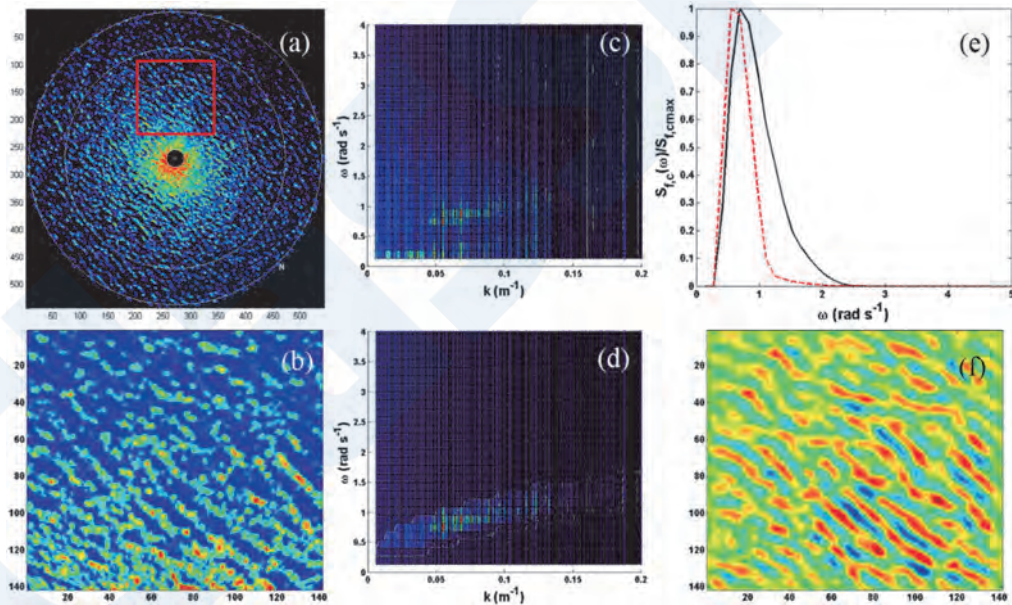
Fig. 3　Images of analysis of radar reflection images [6]

2.2　Types of Radar

Radar is classified according to its microwave wavelength. Mainly the X band (8 to 12 GHz) and the S band (2 to 4 GHz) are used in ship radar.

Because the X band is close to the wavelength of capillary waves, and intensity of scattering, that is, the radar cross section (RCS) is large, its spatial resolution is finer than that of the S band. However, as a weak point, during rainy weather, the microwaves are scattered by raindrops and accuracy easily decreases. Although the S band is also used, its resolution is coarse in comparison with the X band due to its longer wavelength. On the other hand, S-band radar has the advantage that observational accuracy is relatively robust to precipitation because of its long wavelength.

Cheng and Chien (2017) [8] compared X-band radar and S-band radar installed in a coastal area in Taiwan and illustrated the differences in spatial resolution and the effects of precipitation visually.

Section 2.1 described a type of radar in which the phases of the transmitted waves irradiated from the radar device are not controlled, that is, noncoherent radar. The type called coherent radar, in which the phases are controlled, measures the particle velocity on the water surface by the Doppler effect [7]. In some cases, this is also called Doppler radar [9]. A commentary on Doppler radar can be found in Kanrin – Bulletin of the Japan Society of Naval Architects and Ocean Engineers [10].

2.3 Other Shipboard Observation Data: Ship Wavemeters

Among the various types of shipboard wave measurement devices, ship wavemeters are also widely used. Ship wavemeters are mainly installed on bow and directly measure the change in distance (relative water level) between the sensor and the sea surface directly under it by a microwave technique, etc. [11]. In obtaining the water level from the still water surface (absolute water level), the vertical movement of the ship measured by an accelerometer or the like installed on the bow is subtracted from the relative water level. While the reliability of the wave height is comparatively high, only the point time-series wave height can be obtained, and it is not possible to measure the wave direction.

3. WAVE MODELS

Wave models make it possible to estimate waves comprehensively worldwide, and public meteorological agencies and private weather companies provide wave model data. Applications include use in weather routing for ships and activities for wave prediction (wave estimation) in designated waters for fixed offshore structures. The following describes what a wave model solves, and the points to note from the viewpoint of their use in ship monitoring.

3.1 Basic Equations

In a wave model which is widely used at present, the wave power spectrum $S(k, \theta)$ is obtained by solving a time-development equation for the amount of conservation (wave action conservation law) called wave action $N \equiv S(k, \theta)/\sigma$ [12][13].

$$\frac{\partial N}{\partial t} + \frac{\partial}{\partial x}\dot{x}N + \frac{\partial}{\partial y}\dot{y}N$$
$$+ \frac{\partial}{\partial k}\dot{k}N + \frac{\partial}{\partial \theta}\dot{\theta}N = \frac{S_{force}}{\sigma} \qquad (1)$$

$$\dot{x} = c_g \cos\theta + U_x$$
$$\dot{y} = c_g \sin\theta + U_y \qquad (2)$$
$$\dot{k} = -\frac{\partial\sigma}{\partial d}\frac{\partial d}{\partial s} - \mathbf{k}\cdot\frac{\partial\mathbf{U}}{\partial s}$$

$$\dot{\theta} = -\frac{1}{k}\left[\frac{\partial\sigma}{\partial d}\frac{\partial d}{\partial m} - \mathbf{k}\cdot\frac{\partial\mathbf{U}}{\partial m}\right] \qquad (3)$$

Where $\sigma^2 = gk\tanh kd$ is the angular frequency of a component wave, g is gravitational acceleration, $\mathbf{k} = (k_x, k_y)$ is the wavenumber of a component wave and d is water depth. Here, $k = |\mathbf{k}| = \sqrt{k_x^2 + k_y^2}$. $c_g \equiv \partial\sigma/\partial k$ expresses the wave group velocity, and $\mathbf{U} = (U_x, U_y)$ is the current velocity due to ocean currents, etc. It should be noted that σ is the angular frequency in a coordinate system which is moved along a current velocity $\mathbf{U}$ by ocean currents, tidal currents or the like. Furthermore, θ expresses the wave direction of a component wave, and s and m represent a coordinate system parallel and perpendicular to direction θ, respectively, and S_{force} is an external force term called the source term (described in the following). The coordinate system described above is shown in Fig. 4.
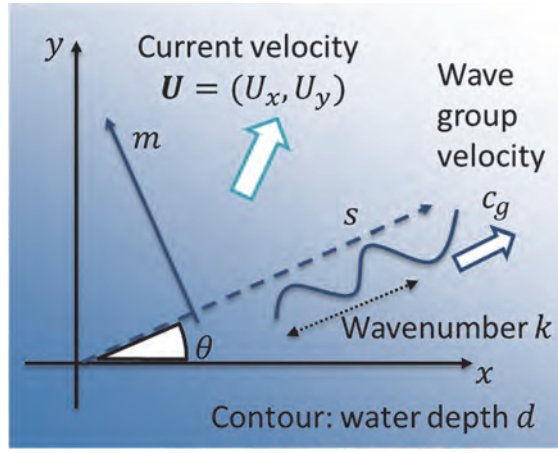
Fig. 4 Coordinate system considered by wave model

First, the meaning of Eq. (1) will be considered. $\frac{\partial}{\partial x}\dot{x}N + \frac{\partial}{\partial y}\dot{y}N$ is an advective term for spatial direction and is similar to the advective term in the Navier-Stokes equation. As can be understood from Eq. (2), the velocity at which a wave action N is conveyed by advection depends on the wave group velocity c_g at which the energy of the waves propagates and the velocity $\boldsymbol{U}$ due to ocean and tidal currents.

In a wave action equation, a derivative term $\frac{\partial}{\partial k}\dot{k}N + \frac{\partial}{\partial \theta}\dot{\theta}N$ with respect to the spectrum space (k, θ), also appears. This includes the differentiation of the coordinate system (s, m) parallel and perpendicular to the wave direction θ for the water depth d, i.e., $\frac{\partial \sigma}{\partial d}\frac{\partial d}{\partial s}$ and $\frac{\partial \sigma}{\partial d}\frac{\partial d}{\partial m}$. This represents diffraction and refraction of the wave by the sea bottom topography. Because the effect of diffraction and refraction by the bottom topography is large in coastal waters, it is necessary to increase the accuracy of the differentiation term for the water depth d. Thus, it is necessary to improve spatial resolution.

Although the terms $\frac{\partial \boldsymbol{U}}{\partial s}$ and $\frac{\partial \boldsymbol{U}}{\partial m}$ appear, these expresses the velocity gradient of the current velocity $\boldsymbol{U}$ as seen from the wave direction θ. The refraction of the wave by the current velocity $\boldsymbol{U}$ is expressed by this term.

Wave parameters such as the significant wave height, the mean wave period and the mean wave direction are obtained by integrating the wave spectrum $S(k, \theta)$. Some meteorological agencies and weather companies also provide wave parameters, such as parameters in which multiple spectral peaks corresponding to wind waves and swells are decomposed. Since the wave spectrum itself involves an extremely large volume of data in comparison with integrated wave parameters, some organizations do not provide wave spectra.

3.2　Source Term

The external force term S_{force}, which is called the "source term," mainly includes the following terms:

$$S_{force} = S_{in} + S_{ds} + S_{nl} + \cdots$$

S_{in} shows the development of an ocean wave by wind. To drive an ocean wave model, wind velocity data published by various meteorological agencies, or estimated values of the wind velocity calculated independently by a downscaled weather model, are used. For example, the Japan Meteorological Agency (JMA), the **N**ational **O**ceanic and **A**tmospheric **A**dministration (NOAA) in the United States and the **E**uropean **C**entre for **M**edium-**R**ange **W**eather **F**orecasts (ECMWF) publish estimated wind velocity values. Since the accuracy of the wind velocity directly affects the accuracy of the ocean wave model, it is necessary to verify the accuracy of the wind velocity before running the ocean wave model.

S_{ds} expresses the dissipation of wave energy by breaking waves (whitecaps, etc.). S_{in} and S_{ds}, which show the input and dissipation of energy in the ocean wave field, are important in estimation of the significant wave height.

S_{nl} shows the nonlinear interaction between component waves [14]. In the case of a linear wave, the energy of the component waves is always constant and the wave spectrum is invariable, but due to nonlinearity, the wave spectrum changes by exchanges of energy between component waves and wave spectrum changes. This term is closely related to the shape of the wave spectrum.

In addition to the above, friction between ocean waves and the sea bottom and the interaction between ocean waves and sea

ice are incorporated in S_{force}, etc., making it possible to consider various physical processes in the ocean wave model.

3.3　Ocean Wave Model Programs

The ocean wave models which are mainly used in ocean wave forecasting at present are called third-generation ocean wave models, and provide explicit solutions for detailed physical processes in the spectrum space, as described in Sections 3.1 and 3.2. The main third-generation ocean wave model programs are introduced here.

WAM (**WA**ve **M**odeling) was developed by the **Wa**ve **M**odel **D**evelopment and **I**mplementation Group (WAMDI Group) and was the first of the third-generation ocean wave models [15) 16)]. The ECMWF meteorological agency has developed an internal model derived from WAM called ECWAM [17)].

WAAVEWATCH III [18)] was developed centering on the NOAA. Since it is an open source program, active improvement by universities and research institutes is continuing.

SWAN (**S**imulating **WA**ves **N**earshore) [19)], which was developed by Delft University of Technology, prioritized analysis of waves in coastal regions from the outset, and at present, use of this program still centers on coastal areas and storm surge. It is also an open source program.

Depending on the meteorological agency or weather company, some have developed independent models. The wave model used by the Japan Meteorological Agency is MRI-III, which was developed by the Meteorological Research Institute [20)].

3.4　Temporal Evolution of Ocean Wave Model

Because atmospheric circulation has the nature of chaos, if there is an error in the initial values, the error in the predicted values will also increase exponentially due to the phenomenon called "butterfly effect." For example, an error in an atmospheric disturbance such as a mid-latitude low pressure system will double in about 2 to 3 days and will reach its maximum in around 10 days [21)]. This means that the limit for weather forecasting in the middle latitudes is approximately 10 days.

The limit for weather forecasting in the middle latitudes is also important for wave forecasting because there are cases where the wave height increases due to strong extratropical cyclone. The courses of typhoons and other tropical cyclones also depend on the atmospheric pressure pattern in the mid-latitudes and the position of the prevailing westerlies. Thus, the forecasting limit for ocean waves, which are driven by wind, is limited by the forecasting limit for weather, and as a guideline, that limit is considered to be no more than about 10 days.

When using wave forecasting values in ship monitoring, it is necessary to hold the forecasting period to approximately 10 days. Within the forecasting limit, ensemble forecasts are used as data for considering the uncertainty of forecast values for weather and ocean waves. An ensemble forecast is a set (ensemble) of forecasts which is obtained by generating several dozen initial values with perturbations, and then calculating an atmospheric/wave model based on those values. Ensemble forecasting is already used in forecasting of typhoons and seasonal forecasting for flood control and agriculture [22)], and is also thought that ensemble forecasting might also be used in ship monitoring in the future. The JMA, NOAA, ECMWF and other meteorological agencies provide ensemble forecasts for ocean wind waves. Fig. 5 shows the visualization of the data of the ECMWF's wave ensemble forecast ENS-WAM [23)] for a certain coastal navigation route in Europe. The initial value is for November 22, 2021, and the forecast covers a four-day period. Each forecast in the ensemble (N = 50) is color coded. As can be seen from the figure, when the forecast period becomes longer, the variation of the significant wave height and other wave parameters becomes larger. As a point to note in ensemble forecasting, ensemble calculations frequently have coarser spatial resolution than deterministic forecasts that present only one initial value, corresponding to the large number of forecasts in the ensemble.

To maintain the forecasting accuracy of a weather model, it is necessary to continue to reflect the state of the atmosphere, which is chaotic, in the weather model. Therefore, measured values are reflected periodically in the model by data assimilation [21)]. Three types of estimated values are used in weather and wave models, depending on the data assimilation and time axis [24)]. The first is the estimated value of the actual situation (nowcast), in which a value is obtained by data assimilation using measured values, which is performed for the initial time of the estimated value given by a numerical model. The second value (forecast) is a value in which the future with respect to that time is estimated based on the nowcast, and the third (hindcast) is an additional value, in which the meteorological and oceanographic conditions in the past are estimated by using fixed observation values covering the entire analysis period. Because the volume of data that can be applied in data assimilation increases in the order of hindcast > nowcast > forecast, the accuracy generally tends to higher in the same order.

Use of hindcast is recommended when a real-time analysis is not needed, for example, when the aim is to determine the condition of a ship in the past. For cases that exceed the limit of the above-mentioned forecast period, for example, when

evaluating the ship safety, it is desirable to acquire wave hindcast for a long period (on the order of several decades) and carry out a statistical analysis of that data.

Wave hindcast mainly consist of two types: ① Type using only hindcast for the wind field without data assimilation for waves, and ② Type in which data assimilation is also performed for waves using data from marine satellite altimeters, buoys, etc. The wave hindcast dataset called IOWAGA [25] and ERA5 [26] are used in the 2022 Comprehensive Revision of Part C of the ClassNK Rules for the Survey and Construction of Steel Ships [27]. IOWAGA corresponds to Pattern ①. WAVEWATCH III is driven by the NOAA wind product CFSR and the calibration using marine altimeter data and buoy data is performed by the Institut Français de Recherche pour l'Exploitation de la Mer (IFREMER). ERA5 corresponds to Pattern ②, where ECWAM is driven by ECMWF and the analysis values are obtained by data assimilation with satellite altimeter data [28].
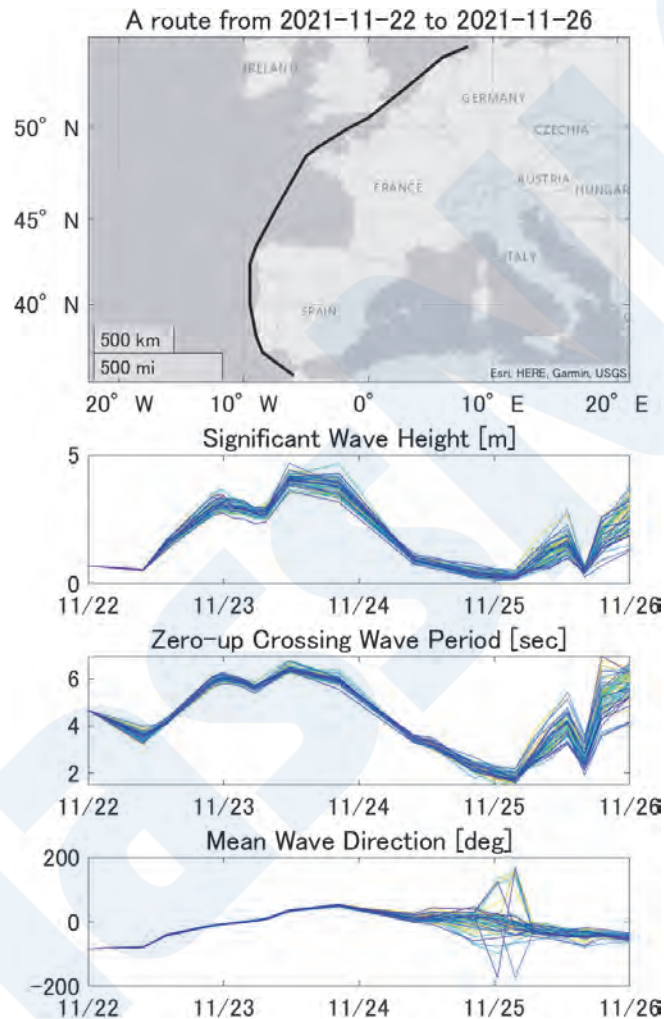

Fig. 5　Example of visualization of data for ECMWF wave ensemble forecast ENS-WAM [23]
for the example of a certain European coastal route

3.5　Issues of Wave Models

There are still issues in accurately considering the dispersion relationship, dissipation, etc. of swells that arrive from distances of several 1,000 km or more [29]. For example, when the results obtained by buoy observation and wave model calculations were compared, cases in which there was a difference of several tens of hours in the swell arrival time have been reported [30]. While data assimilation of swells is possible by using marine satellite altimeter data, it is difficult to capture all swells [29].

As mentioned above in Section 3.1, the effects of the current velocity U include advection and refraction of waves. A number of strong ocean currents exist in various ocean areas of the world, including the Mexican Gulf Stream (Gulf Stream), the *Kuroshio* (Black Current) near Japan and the Agulhas Current in the Indian Ocean as representative examples. It has also been pointed out that wave heights are affected by vortexes in these currents, which reach a scale of 10 km to 100 km [31]. To determine whether the effect of these currents is incorporated in a wave model or not, a comparative study with measured data, etc. is

recommended. (Note: In the above-mentioned IOWAGA and ERA5, good agreement with buoy measurements was confirmed in the North Atlantic Ocean [32)-34)].) The JMA's Meteorological Research Institute devised an equation for correction of the forecast values of ocean currents [35)], and the waters that are affected by ocean currents are shown in JMA wave forecast charts [36)].

There are cases where ships sail along ocean currents to improve ship fuel economy. To grasp the fuel consumption performance of ships in such cases, it is desirable to confirm the position accuracy of ocean currents and the effect of the current on waves.

4. OBSERVATION DATA FOR VERIFICATION

In many cases, wave models and radar are verified or calibrated by using observational data acquired by buoys, marine satellite altimeters, etc. which are not located on shipboard. Therefore, although the topic of this paper is application of wave data to ships, non-shipboard observation data for use in verifications will also be introduced here as background knowledge.

4.1 Buoys

Buoy data are considered to be the most basic and reliable form of wave observation data. With a buoy, it is possible to estimate the wave height and frequency spectrum by measuring the displacement of the buoy in the z direction. If data such as the displacement in the x, y and z directions and wave slope can be measured, it is also possible to estimate the 2-dimensional frequency and directional wave spectrum by the Maximum Entropy Principle (MEP) [37)].

In Japan, the data from GPS wavemeters is also aggregated in the NOWPHAS wave information observation network [38)], which is operated by the Ports and Harbours Bureau of the Ministry of Land, Infrastructure, Transport, and Tourism (MLIT). These GPS wavemeters measure the position of buoys with accuracy of several cm by GPS, and are installed with single point mooring in waters with a depth of 100 to 400 m about 10 to 20 km from the coastline [39)]. These are large-scale buoys with a diameter of 5 to 7 m and a total height of 10 to 19 m. A total of 18 buoys have been installed along the Tohoku coast in northeastern Japan and from the Tokai area south of Tokyo to the western island of Kyushu.

In addition to the above, NOAA has deployed buoys in the Atlantic and Pacific Oceans and publishes the information obtained [40)], while in Europe, the **C**opernicus **M**arine **E**nvironment **M**onitoring **S**ervice (CMEMS) makes data available to the public on the internet [41)].

Smaller buoys have also appeared in recent years. For example, the company Sofar Ocean developed a compact, lightweight buoy called Spotter, which has a diameter of 42 cm and weight of approximately 7.5 kg [42)], and has deployed this buoy since 2019, creating an observation network that now provides global coverage (Fig. 6). Using these buoys, the company performs data assimilation not only for wave height, but also for wave period and wave direction, thereby improving forecasting accuracy for swells [43)]. In addition, there are also many other types of compact buoys, and an article providing a detailed commentary is available [44)].
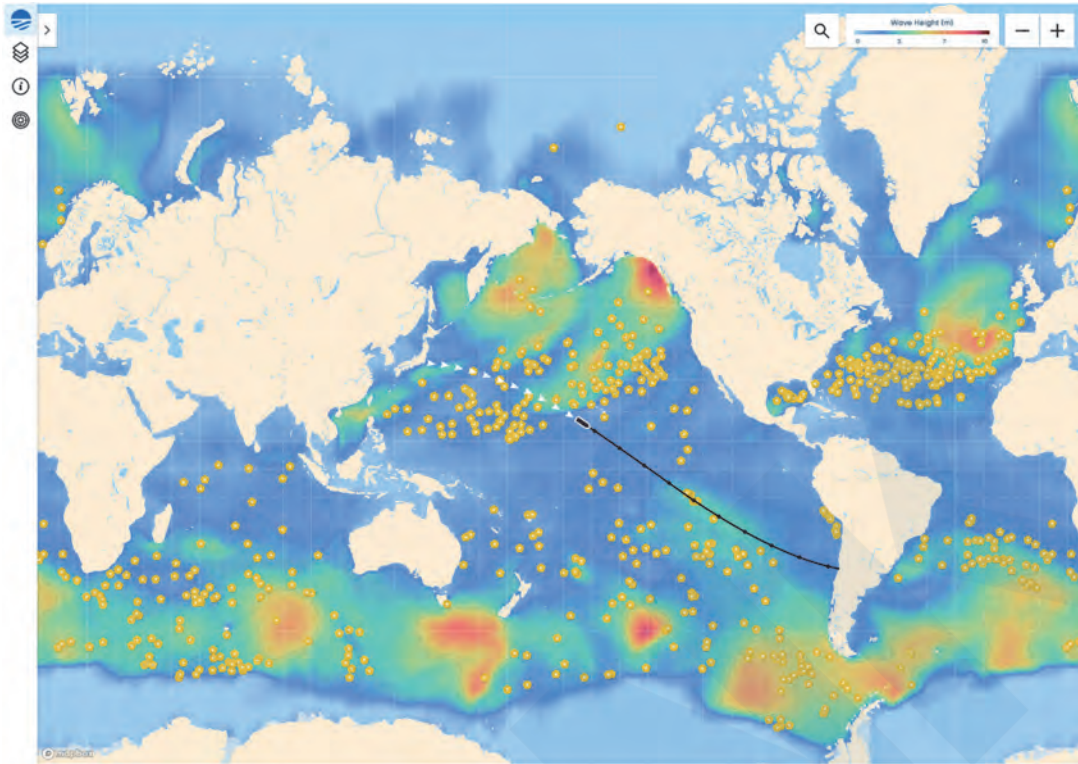
Fig. 6   Map of buoys deployed by Sofar Ocean as a July 2022 [45)]
(yellow dots: buoys, contour lines: wave height)

4.2   Marine Satellite Altimeters

Marine satellite altimeters are capable of measuring the significant wave height by irradiating microwaves on the sea surface, receiving the reflected signals and measuring the transmission time (reference paper [46)], Section 3.3.1). They are used in accuracy verification, calibration and data assimilation of wave models.

Marine satellite altimeters orbit the entire planet with a trajectory similar to a ball of wool (e.g., Fig. 7) and return to their original position in about 10 to 35 days. Multiple satellite altimeters are currently in operation, enabling simultaneous coverage of a wide range. However, since the data are only obtained in the form of moving points, this does not mean that data can be obtained densely and comprehensively for the entire planet. A wave model is necessary in order to obtain a comprehensive grasp of wave worldwide.

The data acquired by marine satellite altimeters are calibrated with buoy data, and datasets combining observational data from multiple satellites for a period of more than 30 years are now available [47) 48)].

Recently, a few satellites estimate wave spectra by using **S**ynthetic **A**perture **R**adar (SAR). Detailed descriptions of this type of satellite are available in the literature [46) 49)].
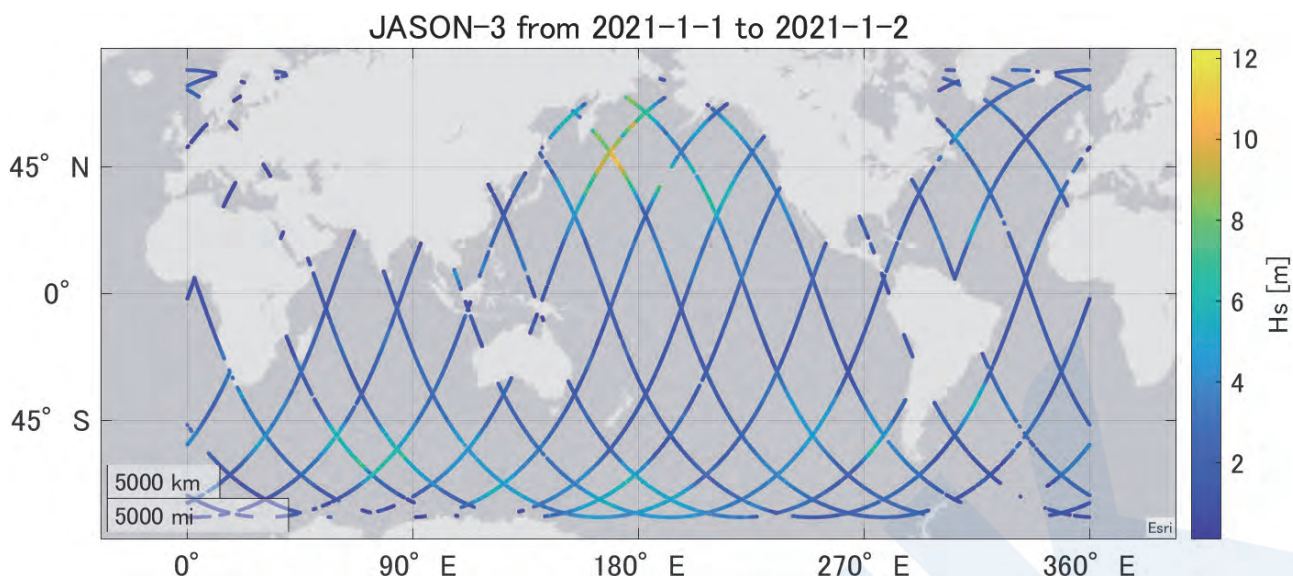
Fig. 7   Example of observed significant wave height and trajectory of satellite JASON-3 on a certain day
Calibrated data of Ribal & Young (2019) [47)] were used.

5.   DISCUSSIONS: APPLICATION TO VARIOUS TYPES OF SHIP MONITORING

Various types of vessel responses, such as ship motion, stress and added resistance in waves, are required in digital twins for ship structures, monitoring of ship performance in actual seas and related applications. The basic technique for this purpose is a forward analysis method in which the wave spectrum is multiplied by the square of RAO (**R**esponse **A**mplitude **O**perator) obtained in frequency domain. This is so-called short-term prediction of ship response. Techniques utilizing data assimilation and calibration reflecting the measured values of stress and other responses are also available. However, in the sense that the forward analysis does not require measured response values, this technique has the advantages of simplicity and low analysis cost. The following considers the required conditions for wave data to realize various types of ship monitoring, assuming the use of a forward analysis technique.

First, the wave parameters to be obtained are important. In particular, the wave height, wave period and wave direction are essential data for every possible ship response (motion, stress, added resistance in waves, etc.). The usefulness of the wave spectra obtained from wave models and radar will be considered. If the RAO has a gently-varying shape, the dependence of the response on the wave spectral shape will be small. Conversely, if the RAO peak has a sharp shape, the dependence of response on the wave spectral shape is considered to be large. For example, in many cases the RAO peak for roll is sharp, and the peak varies sensitively with GM and ship speed. Although this suggests the possibility that use of wave spectral data may be effective for the short-term prediction of responses with sharp RAO peak, future study is necessary.

The next point is the time range. In fatigue assessment of ship structures, fuel consumption performance and the like, a real-time analysis is not required, and an *ex-post facto* analysis is sufficient. In such cases, hindcast , which are generally considered to be more accurate than nowcast, might be suitable for those applications. Naturally, shipboard observational data such as wave radar data can only be acquired from the past up to the present. When predictions of future responses are desired, forecast obtained by a wave model are necessary. If the uncertainty of predictions within the forecast limit (approximately 10 days) is evaluated by ensemble forecasting, it is also considered possible to assess the uncertainty of responses originating from the uncertainty of forecast values.

Finally, the spatial range must be considered. Wave models can cover almost all ocean areas, and it is possible to extract wave data at a ship's position. However, assuming data are not shared between ships, shipboard observational data are the results of observation of only waves at the ship's position.

Based on these requirements, the types of wave data that are suitable for various types of ship monitoring were roughly arranged, as shown in Table 1.

Table 1　Applicability of wave data for various types of ship monitoring
(○: Applicable, △ : Applicable depending on the case, × : Not applicable)

| Category | Type of data | Property of data | | | | |
| | | Estimable parameters | | | Range covered | |
		Wave height	Wave period / wave direction	Wave spectrum	Time	Space
Wave model	Hindcast	○ Data assimilated with observational data.	○	○	Past	○ Can be acquired for almost all ocean areas and ship positions. However, a high resolution wave model is necessary in near-coastal waters.
	Nowcast	○	○	○	Present	
	Deterministic prediction	○	○	○	Future	
	Ensemble forecast	○ In many cases spatial resolution is coarser than that of deterministic prediction.			Future (considers uncertainty of forecast)	
Shipboard observation data	Wave radar	○ Care is required regarding precipitation and calibration.	○	○	Present	○ Shipboard observation
	Ship wavemeter	○	× Cannot measure wave direction.	×		
Observational data for verification	Satellite altimeter	○	△ Recently, a few satellites also estimate wave spectra [46]		Past / present	Full global coverage. Low spatial density of data.
	Buoy	○	○ Requires measured data with at least 3 degrees of freedom.			

| Category | Type of data | Application | | | |
| | | Past | | Present | Future |
		Fatigue assessment (stress)	Fuel consumption performance evaluation (added resistance in waves)	Ship motion, stress and added resistance in waves	
Wave model	Hindcast	○ If real time is not required, hindcast data are suitable, as accuracy is generally high.		/	/
	Nowcast	○	○	○	
	Deterministic prediction	/	/		○
	Ensemble forecast	/	/		○
Shipboard observational data	Wave radar	○	○	○	/
	Ship wavemeter	△ Because only wave height is measured, it is necessary to use shipboard wavemeter data in combination with other data.			/

6.　CONCLUSIONS

　This paper introduced and compared the outline and other features of various types of wave data for application to ship monitoring, which is currently a subject of active research and development. Technologies for wave estimation are diverse and are advancing rapidly. Due to space limitations, the commentary in this paper was limited to observational devices and analytical techniques that are generally in wide use. Although the outlines of the various technologies were introduced in simple terms here, the reader may refer to the reference literature for details.

　For readers who wish to make a deeper investigation of the field of ocean wave, several textbooks are also introduced below.

① 　"Physics of Ocean Waves" by Hisashi Mitsuyasu [50]

　　This book is suitable for beginners, and provides a simple explanation of essential topics such as wave statistics and signal processing, the wave generation and development process, observation by buoys, etc. However, it is difficult to obtain, as it is out of print.

② 　"Analysis and Forecast of Ocean Waves" by Ichiro Isozaki and Yasushi Suzuki [51]

　　A comprehensive treatment covering topics from the fundamentals of ocean waves to observation, ocean surface waves

and wave models. In particular, this text provides a detailed description of the operation of wave models in the seas near Japan.

③ "The Interaction of Ocean Waves and Wind" by Peter Janssen [52]

A textbook that gives a detailed explanation of wave models, written by an expert of the ECMWF.

④ "Ocean Wave Dynamics" by Ian Young and Alexander Babanin [53]

A text for graduate school students and researchers, which was published in 2019 and covers recent research results. It is an omnibus-type work written by experts in various fields including wave models, satellite observation, nonlinear waves, etc.

In addition, the KANRIN published by the Japan Society of Naval Architects and Ocean Engineers included Special Issues entitled "Frontier of Ocean Wave Research" in Vol. 98 [54] and "Use of Weather Information in the Ship and Offshore Fields" in Vol. 77 [55]. Also, the Working Group of the Forum for Operational Oceanography Surface Waves in Australia has arranged the issues for future wave research under the title "15 Priorities for Wind-Waves Research"[29]. Here, a questionnaire survey of stakeholders in wave-related fields, including persons at research institutes and government-affiliated organizations, private companies was conducted, the issues were arranged by the Steering Committee and the results of a revote by the stakeholders are summarized. Interested readers may also refer to the articles included in "15 Priorities" for the current limits of wave data and wave models and the issues for future wave research. It may be noted that "15 Priorities" mentioned *Better Engagement of maritime industries with research* as one issue.

As noted in the Introduction to the present paper, it is necessary to utilize the wave data which is currently provided in ship monitoring based on an understanding of its usefulness and limitations. The authors will be happy if this paper contributes to the use of wave data in ship monitoring. We also hope that *Better Engagement of maritime industries with research* will be realized through the development of ship monitoring to maritime industries.

REFERENCES

1) National Maritime Research Institute (NMRI), "Joint Research of Maritime Cluster – Start of Evaluation of Ship Performance in Actual Seas Project (OCTARVIA) Phase 2," 2022. https://www.nmri.go.jp/news/press/press20220315.html

2) N. Sogihara and T. Yonezawa, "Establishment of Ship Performance Monitoring Method in Actual Seas," *Karin Bull. Japan Soc. Nav. Archit. Ocean Eng.* Vol. 82, pp. 6-11, 2019.

3) M. Fujikubo, "R&D of Digital Twin for Ship Structures," J. Jap. Weld. Soc., Vol. 90, No. 1, pp. 36-43, 2021, doi: 10.2207/jjwa.90.36.

4) A. Maki, "Kansai Branch News," *Karin Bull. Japan Soc. Nav. Archit. Ocean Eng.*, Vol. 102, p. 48, 2022.

5) J. Nieto Borge, G. R. Rodríguez, K. Hessner, and P. I. González, "Inversion of Marine Radar Images for Surface Wave Analysis," *J. Atmos. Ocean. Technol.*, vol. 21, no. 8, pp. 1291-1300, Aug. 2004, doi: 10.1175/1520-0426(2004)021<1291:IOMRIF>2.0.CO;2.

6) Y. Qi, W. Xiao, and D. K. P. Yue, "Phase-resolved wave field simulation calibration of sea surface reconstruction using noncoherent marine radar," *J. Atmos. Ocean. Technol.*, vol. 33, no. 6, pp. 1135-1149, 2016, doi: 10.1175/JTECH-D-15-0130.1.

7) W. Huang, X. Liu, and E. W. Gill, *Ocean wind and wave measurements using X-band marine radar: A comprehensive review*, vol. 9, no. 12. 2017. doi: 10.3390/rs9121261.

8) H.-Y. Y. Cheng and H. Chien, "Implementation of S-band marine radar for surface wave measurement under precipitation," *Remote Sens. Environ.*, vol. 188, pp. 85-94, 2017, doi: 10.1016/j.rse.2016.10.042.

9) N. Braun, F. Ziemer, A. Bezuglov, M. Cysewski, and G. Schymura, "Sea-Surface Current Features Observed by Doppler Radar," *IEEE Trans. Geosci. Remote Sens.*, vol. 46, no. 4, pp. 1125-1133, 2008, doi: 10.1109/TGRS.2007.910221.

10) C.-K. Rheem, "Stationary Observation of Coastal Ocean Waves by Doppler Radar," *Kanrin Bull. Japan Soc. Nav. Archit. Ocean Eng.*, No. 98, pp. 8-11, 2021.

11) S. Takeda, "Wave Measurement by Actual Ship," Techno Marine (Bull. of Soc. Nav. Archit. Jpn.), Vol. 831, pp. 36-41, 2002.

12) K. Hasselmann *et al.*, "Measurements of wind-wave growth and swell decay during the Joint North Sea Wave Project (JONSWAP)," Deutches Hydrographisches Institut, 1973.

13) H. L. Tolman and N. Booij, "Modeling wind waves using wavenumber-direction spectra and a variable wavenumber grid," *Glob. Atmos. Ocean Syst.*, vol. 6, pp. 295-309, 1998.

14) K. Hasselmann, "On the non-linear energy transfer in a gravity-wave spectrum Part 1. General theory," *J. Fluid Mech.*, vol. 12, no. 04, p. 481, 1962, doi: 10.1017/S0022112062000373.

15) T. WAMDI Group, "The WAM model - A third generation ocean wave prediction model," *Journal of Physical Oceanography*, vol. 18, no. 12. pp. 1775-1810, 1988. doi: 10.1175/1520-0485(1988)018<1775:TWMTGO>2.0.CO;2.

16) G. J. Komen, L. Cavaleri, M. Donelan, K. Hasselmann, S. Hasselmann, and P. A. E. M. Janssen, *Dynamics and Modelling of Ocean Waves.* Cambridge: Cambridge University Press, 1994. doi: DOI: 10.1017/CBO9780511628955.

17) S. Park, "Part VII : ECMWF Wave Model IFS DOCUMENTATION - Cy38r1 Operational implementation 19 June 2012 PART VII : ECMWF WAVE MODEL Table of contents Numerical scheme," no. June, pp. 1-79, 2012.

18) H. L. Tolman, "User manual and system documentation of WAVEWATCH III," 2016.

19) R. C. Ris, L. H. Holthuijsen, and N. Booij, "A third-generation wave model for coastal regions: 2. Verification," *J. Geophys. Res. Ocean.*, vol. 104, no. C4, pp. 7667-7681, Apr. 1999, doi: https://doi.org/10.1029/1998JC900123.

20) H. Minematsu, "Wave Model Operated by Government Agency at the Japan Meteorological Agency," TENKI (Journal of the Meteorological Society of Japan (JMSJ)), Vol. 56, pp. 669-674, 2009.

21) T. Miyoshi, "Big Data Assimilation and Weather Prediction," Jpn. J. Appl. Phys., Vol. 90, No. 8, pp. 470-475, 2021.

22) M. Yamaguchi, "Risk Assessment in the Use of Weather Data – Various Forms of Ensemble Forecasting –," 2020.

23) ECMWF, "Ocean Wave Model Ensemble 15-day forecast (Set IV - ENS-WAM)." https://www.ecmwf.int/en/forecasts/datasets/set-iv

24) K. Matsuura, M. Maeda, H. Nakano, K. Kuroki, S. Koshida and Y. Sato, "Estimation of Meteorological and Oceanographic Phenomenon and Its Accuracy: For Use Based on the Characteristics of Estimated Values (Special Issue: Use of Weather Information in the Ship and Offshore Fields)," *Kanrin Bull. Japan Soc. Nav. Archit. Ocean Eng.*, No. 77, pp. 6-10, 2018.

25) M. Alday, F. Ardhuin, M. Accensi, and G. Dodet, "A global wave parameter database for geophysical applications. Part 3: improved forcing and spectral resolution," 2021.

26) H. Hersbach *et al.*, "The ERA5 global reanalysis," *Q. J. R. Meteorol. Soc.*, vol. 146, no. 730, pp. 1999-2049, 2020, doi: 10.1002/qj.3803.

27) R. Miratsu, T. Fukui and T. Zhu, "Evaluation of the Ship Operational Effect Based on Actually Encountered Sea States by Ships," ClassNK Technical Journal, Vol. 5, pp. 71-74, 2022.

28) ECMWF, "Forecast User Guide, 2 The ECMWF Integrated Forecasting System, 2.2 Ocean Wave Model - ECWAM," 2022. https://confluence.ecmwf.int/display/FUG/2.2+Ocean+Wave+Model+-+ECWAM

29) D. Greenslade *et al.*, "15 Priorities for Wind-Waves Research: An Australian Perspective," *Bull. Am. Meteorol. Soc.*, vol. 101, no. 4, pp. E446-E461, 2020, doi: 10.1175/BAMS-D-18-0262.1.

30) H. Jiang, A. V Babanin, and G. Chen, "Event-Based Validation of Swell Arrival Time," *J. Phys. Oceanogr.*, vol. 46, no. 12, pp. 3563-3569, 2016, doi: 10.1175/JPO-D-16-0208.1.

31) F. Ardhuin *et al.*, "Small-scale open ocean currents have large effects on wind wave heights," *J. Geophys. Res. Ocean.*, vol. 122, no. 6, pp. 4500-4517, Jun. 2017, doi: https://doi.org/10.1002/2016JC012413.

32) T. Kodaira, K. Sasmal, R. Miratsu, T. Fukui, T. Zhu, and T. Waseda, "Uncertainty in wave hindcasts in the North Atlantic Ocean,", submitted to Marine Structures,, 2022.

33) G. de Hauteclocque, T. Zhu, M. Johnson, H. Austefjord, and E. Bitner-Gregersen, "Assessment of global wave datasets for long term response of ships," *Proc. Int. Conf. Offshore Mech. Arct. Eng. - OMAE*, vol. 2A-2020, no. August, 2020, doi: 10.1115/omae2020-18874.

34) K. Sasmal, T. Kodaira, Y. Kita, R. Miratsu, and T. Zhu, "Modeled and satellite-derived extreme wave height statistics in the North Atlantic Ocean reaching 20 m," *ESSOAr*, 2021.

35) G. Kubo and N. Kohno, "Study of the Effect of Ocean Currents on Waves," Weather Service Bulletin, Vol. 77, pp. S141-S157, 2010.

36) N. Kohno and A. Yamane, "Addition of 'Information on Rough Seas Hazardous to Navigation' to Wave Forecast Charts," Weather Service Bulletin, Vol. 85, pp. 1-12, 2018.

37) N. Hashimoto, "Estimation of Directional Spectra from the Maximum Entropy Principle," Report of the Port and Harbour Research Institute, Vol. 24, No. 3, pp. 123-146, 1985.

38) Ports and Harbours Bureau, Ministry of Land, Infrastructure, Transport, and Tourism (MLIT), "NOWPHAS: Nationwide Ocean Wave information network for Ports and HArbourS."
https://www.mlit.go.jp/kowan/nowphas/index.html

39) Y. Ito, "Basic Knowledge of Port and Harbour Terminology, 'GPS Wavemeter'," Kouwan (Ports and Harbours, magazine published by The Japan Port and Harbour Association), Vol. 3, p. 56, 2017.

40) NOAA, "National Data Buoy Center." https://www.ndbc.noaa.gov/

41) C. M. E. M. Service, "In Situ TAC." http://www.marineinsitu.eu/dashboard/

42) Sofar Ocean, "Spotter Buoy." https://www.sofarocean.com/products/spotter

43) P. B. Smit et al., "Assimilation of significant wave height from distributed ocean wave sensors," Ocean Model., vol. 159, 2021, doi: 10.1016/j.ocemod.2020.101738.

44) Y. Hirakawa, "Measurement of Waves Encountered by Ships and Marine Structures in Oceanic Regions," Karin Bull. Japan Soc. Nav. Archit. Ocean Eng., Vol. 98, pp. 12-16, 2021.

45) Sofar Ocean, "Sofar Ocean." https://weather.sofarocean.com/

46) F. Ardhuin et al., "Observing Sea States," Frontiers in Marine Science, vol. 6. 2019.

47) A. Ribal and I. R. Young, "33 years of globally calibrated wave height and wind speed data based on altimeter observations," Sci. Data, vol. 6, no. 1, p. 77, 2019, doi: 10.1038/s41597-019-0083-9.

48) F. Laboratoire d'Océanographie Physique et Spatiale (LOPS), CNRS, IRD, Ifremer, IUEM, Univ. Brest, Brest, "The Sea State Climate Change Initiative dataset is available," 2019.

49) T. Waseda, "Global Trends and Challenges in Ocean Wave Research," Karin Bull. Japan Soc. Nav. Archit. Ocean Eng., Vol. 98, pp. 1-7, 2021.

50) H. Mitsuyasu, "Physics of Ocean Waves," Iwanami Shoten, Publishers, 1995.

51) I. Isozaki and Y. Suzuki, "Analysis and Forecast of Ocean Waves," Tokai University Press, 1999.

52) P. A. E. M. Janssen, The interaction of ocean waves and wind. Cambridge University Press, 2004.

53) I. R. Young and A. V. Babanin, Ocean Wave Dynamics. WORLD SCIENTIFIC, 2019. doi: doi:10.1142/11509.

54) Japan Society of Naval Architects and Ocean Engineers, Eds., "Frontline of Ocean Wave Research," Karin Bull. Japan Soc. Nav. Archit. Ocean Eng., Vol. 98, 2021.

55) Japan Society of Naval Architects and Ocean Engineers, Eds., "Use of Weather Information in the Ship and Offshore Fields," Karin Bull. Japan Soc. Nav. Archit. Ocean Eng., 2018.

Recent Topics at IMO

— Outline of Discussion at IMO Committees —

Rule Development and ICT Division, External Affairs Department, ClassNK

1. INTRODUCTION

This article introduces recent topics discussed at International Maritime Organization (IMO). At the previous issue, a summary of the topics discussed at 77th Marine Environment Protection Committee (MEPC 77) held in November 2021 and 104th Maritime Safety Committee (MSC 104) held in October 2021 was provided.

This article provides a summary of the decisions taken at 78th Marine Environment Protection Committee (MEPC 78) held from 6 to 10 June 2022 and 105th Maritime Safety Committee (MSC 105) held from 20 to 29 April 2022 as below.

2. OUTCOMES OF MEPC 78

2.1 Greenhouse Gases (GHG) Emission Reduction Measures

Reduction of greenhouse gas (GHG) emissions to address global warming is a universal challenge, and the measures to reduce GHG emissions from international shipping have been deliberated at IMO.

IMO has introduced the Energy Efficiency Design Index (EEDI), the Ship Energy Efficiency Management Plan (SEEMP) and the Data Collection System for fuel oil consumption of ships (DCS) so far. Further, the Initial IMO Strategy on the reduction of GHG emissions from ships, which includes the emission reduction target and the candidate measures to reduce GHG emissions, was adopted at MEPC 72.

2.1.1 Short-term Measures for Reduction of GHG

The initial IMO Strategy on the reduction of GHG emissions from ships specifies the short-term target by 2030 for improved transportation efficiency of at least 40% compared to 2008. To achieve the short-term target, the amendments to MARPOL Annex VI were adopted at MEPC 76 to implement Energy Efficiency Existing Ship Index (EEXI) and Carbon Intensity Indicator (CII) as well as the related Guidelines were also adopted., and these will be commenced in 2023.

(1) Carbon Intensity Indicator (CII)

Operational Carbon Intensity Indicator is rating mechanism for ships, by calculating attained CII based on the operational fuel consumption data. MEPC 76 established Correspondence Group (CG) to revise/update relevant guidelines on DCS and SEEMP, and develop guidelines on correction factors for certain ship types for implementation of CII framework.

At this session, the relevant Guidelines prepared by the said CG and Intersessional Working Group meeting held prior to MEPC 78 were considered and adopted.

Also, further information on CII and SEEMP Part III including these Guidelines are available at the following NK website.

Top page>Products & Services>Statutory Services> SEEMP, IMO DCS and CII

URL:https://www.classnk.or.jp/hp/en/activities/statutory/seemp/index.html

(2) Energy Efficiency Existing Ship Index (EEXI)

EEXI is regulations for existing ships to require the same level of energy efficiency as EEDI for new ships.

At this session, to clarify the applicable limited power of ships fitted with a shaft generator and a method to obtain ship speed Vref from the in-service performance measurement, amendments to Guidelines on the Method of Calculation of the Attained Energy Efficiency Existing Ship Index (EEXI): MEPC.350(78) and Guidelines on Survey and Certification of the Attained EEXI: MEPC.351(78) were adopted and Guidance on methods, procedures and verification of in-service performance measurements: MEPC.1/Circ.901 was newly approved.

2.1.2 Lifecycle GHG and Carbon Intensity Guidelines for Maritime Fuels

For low/zero-carbon fuels, which are expected to become more widely used in the future to decarbonize ships, it is recognized that CO_2 emissions during the manufacturing and distribution processes of these fuels should be taken into account. It is also recognized the significant impact on global warming caused by greenhouse gases other than CO_2, such as methane (CH_4).

Based on this background, MEPC considers developing lifecycle GHG and carbon intensity Guidelines for marine fuel (LCA Guidelines), which assess GHG emissions from marine fuel comprehensively through its manufacture, distribution, and use onboard ships.

At this session, MEPC agreed to establish Correspondence Group for development of the said Guidelines, with a view to finalization at MEPC 80.

2.1.3　Mid/Long-term Measures for Reduction of GHG

The initial IMO Strategy on the reduction of GHG emissions from ships specifies the middle-term target by 2050 to pursue the efforts towards the CO2 reduction of 70% per transport work and to reduce the total annual GHG emissions by at least 50% as well as the long-term target within this century to aims to phase out GHG emissions as soon as possible.

To proceed consideration of Mid/Long-term measures to achieve these targets, MEPC 76, held in 2021, developed work plan as follows:

Phase I (2021-2022):　Collation and initial consideration of proposals for measures
Phase II (2022-2023):　Assessment and selection of measures to further develop
Phase III (2023):　Development of measures for statutory requirements

At MEPC 78, it was agreed to proceed with phase II for further consideration of the candidate measures proposed by each country through intersessional working group meeting held prior to MEPC 78. The leading candidate measures are shown in Table 1 as follows.

Table 1　The candidate measures

GHG Fuel Standard (GFS)	Each ship calculates GFS value, which is expressed in the mass of GHG emissions per unit of energy used on-board a ship (g CO2e/MJ). The reduction factor for the GFS value would be enhanced year by year.
IMO Maritime Research Fund (IMRF)	US$2 per tonne of marine fuel are funded to IMRF, which is used for development of low/zero carbon technologies.
International Maritime Sustainability Funding and Reward (IMSF&R)	Using CII mechanism, ships above upper benchmark level pay funding contributions and ships below lower benchmark level receive rewards.
feebate	Ships using fossil fuels pay for the levy and ships using zero-emission fuels receive rebate.
GHG levy	Ships pay GHG levy for US$100 per tonne of marine fuel. The revenue will be funded to climate change mitigation and adaptation projects under UNFCCC, and subsidized to R&D projects for new technologies under IMO.
Emission Cap-and-Trade System (ECTS)	Based on the annual cap on GHG emissions, each ship is required to acquire and surrender allowances for GHG emissions by auctioning.

2.1.4　Review of Initial IMO Strategy on the Reduction of GHG Emissions from Ships

The initial IMO Strategy on the reduction of GHG emissions from ships adopted in 2018 stipulates that its contents be reviewed every five years. At MEPC 77, recognizing the need to strengthen the ambition of Initial IMO Strategy, it was agreed to conduct a review of the Initial IMO Strategy, with a view to finalization at MEPC 80 to be held in Spring 2023.

At this session, it was agreed to hold intersessional working group meeting prior to MEPC 79 to facilitate discussion for the review of the initial IMO Strategy.

2.2　BWM Convention

2.2.1　Temporary Storage of Treated Sewage and Grey Water

The prohibition on the discharge of treated sewage and gray water in certain ports has led to questions as to whether it is acceptable to temporarily store such water in ballast tanks. However, it is not clear whether the storage of treated sewage and grey water in the ballast tanks are subject to the BWM Convention and/or MARPOL Annex IV.

At this session, it was agreed to continuously consider this issue at future sessions.

2.2.2 Ships Operating at Ports with Challenging Water Quality

Proposals on application of the BWM Convention to ships operating at ports with challenging water quality was made due to concerns on operation of Ballast Water Management System (BWMS) at port area where certain water qualities, such as high level of turbidity, high level of total suspended solids or low salinity, are identified to exceed the operational limitation.

At this session, further fundamental issues, such as the identification of challenging water quality and the feasibility of ballast water exchange plus treatment (BWE+BWT), were recognized, and further proposals on these issues were invited for considerations.

2.3 Air Pollution

2.3.1 Unified Interpretation on Use of Biofuel

Regulation 18 of MARPOL Annex VI prescribes the requirements for the use of fuels derived from petroleum refining and fuels derived by other methods. However, the application of the NOx requirements to biofuel blends, which are expected to be introduced as zero/low-carbon fuels, is not clearly described in the regulation.

At this session, the application of regulation 18 for a biofuel and a biofuel blend were considered and a unified interpretation was approved. According to the unified interpretation, a certified marine diesel engine, which can operate on a biofuel or a biofuel blend without changes to its NOx critical components or settings/operating values outside those as given by that engine′s approved Technical File, is permitted to use such a fuel oil without the additional assessment. Also a fuel oil which is a blend of not more than 30% by volume of biofuel is deemed as blends of hydrocarbons derived from petroleum refining specified in regulation 18.3.1, and additional confirmation of NOx emission is not needed. In other case than above, the onboard simplified measurement method in accordance with 6.3 of the NOx Technical Code 2008 may be used for a verification that the specified engine does not exceed the applicable NOx emissions limit when burning the said fuels.

2.3.2 Designation of SOx Emission Control Area

Regulation 14 of MARPOL Annex VI sets out control measures to reduce emissions of Sulphur Oxides (SOx) and Particulate Matter (PM) from ships and limits the sulphur content in fuel oil used in Emission Control Areas (ECAs) to 0.10% and limits the sulphur content to 0.50% for outside of ECAs. So far, the Baltic Sea, the North Sea, the North American Area and the United States Caribbean Sea Area have been designated as SOx-ECA.

At this session, a proposal to designate the Mediterranean Sea as SOx-ECA was submitted. Following the discussion, draft amendments to MARPOL Annex VI to add the Mediterranean Sea as SOx-ECA were approved. Since no conclusion was reached on the application date for the said draft amendments at this session, these amendments are expected to be adopted at MEPC 79 with further discussion. The earliest possible application of 0.1% sulphur limit in marine fuel oil used on board ships operating in the Mediterranean Sea would be in Spring of 2025.

2.4 Others (Marine Plastic Litter)

2.4.1 Anti-fouling Systems (AFS)

The AFS Convention entered into force in 2008 to prohibit the use of harmful organotin (TBT) in anti-fouling paints used on ships. At MEPC 76, amendments to the AFS Convention to prohibit the use of anti-fouling paints containing cybutryne were adopted.

At this session, to reflect the prohibition of cybutryne, amendments to Guidelines for brief sampling of anti-fouling systems on ships: MEPC.356(78), Guidelines for inspection of anti-fouling systems on ships: MEPC.357(78) and Guidelines for survey and certification of anti-fouling systems on ships: MEPC.358(78) were adopted.

2.4.2 Marine Plastic Litter

With a view to tackling the problem of plastics in the oceans, MARPOL Annex V prohibits discharge of plastics from vessels. However, it was often pointed out that this prohibition regulation was not effective and that some additional actions were needed at IMO level to reduce plastic pollution in the marine environment. To solve this problem, MEPC resolution on Strategy to Address Marine Plastic Litter from Ships was adopted at MEPC 77, which includes vision of aims to strengthen the international framework and compliance with the relevant IMO instruments, endeavoring to achieve zero plastic waste discharges to sea from ships by 2025.

At this session, amendments to MARPOL Annex V were approved to expand the scope of Garbage Record Book, which is required to be provided for vessels of 400 tons or more, to vessels of 100 tons or more. These amendments will be adopted at next session.

2.5　Amendments to Mandatory Instruments

2.5.1　Watertight Doors on Cargo Ships

Amendments to MARPOL Annex I: MEPC.343(78) and IBC Code: MEPC.345(78) to align with the requirements on the condition of watertight doors specified in SOLAS were adopted. Amendments to MARPOL Annex I will enter into force on 1 Jan 2024 and Amendments to IBC Code will enter into force on 1 July 2024.

2.5.2　GESAMP Hazard Evaluation Procedure

Amendments to appendix I of MARPOL Annex II related to the abbreviated legend of the revised GESAMP Hazard Evaluation Procedure, which will enter into force 1 November, were adopted.

3.　OUTCOMES OF MSC 105

3.1　Adopted Mandatory Requirement

Mandatory requirement was adopted at MSC 105 as follows:

(1) Amendments to SOLAS etc. due to modernization of the Global Maritime Distress and Safety System (GMDSS)

Following recent modernization of the GMDSS, the draft amendments to SOLAS II-1, III, IV and V, and the appendix (Certificates), etc., were adopted. In addition, the relevant performance standards, guidelines and guidance were also approved. The main points of the amendments are shown as follows:

1. Definition of "Sea area A3" are modified to "a recognized mobile satellite service supported by the ship earth station carried on board" from "an Inmarsat geostationary satellite".

2. The provisions in SOLAS regulation III/6 related to two-way VHF radiotelephone apparatus and search and rescue locating devices (SART) have been relocated under SOLAS IV.

3. The performance standards for the reception of maritime safety information and search and rescue related information by MF (NAVTEX) and HF, shipborne VHF radio installations, shipborne MF and MF/HF radio installations, Inmarsat-C ship earth stations, etc. were amended.

(2) Amendments to IMSBC Code

The 6th amendments to IMSBC Code including new cargos were adopted.

(3) Amendments to IMDG Code

41st amendments to IMDG Code were adopted, to reflect the biennial amendments to "United Nations Recommendations on the Transport of Dangerous Goods".

3.2　Approved Mandatory Requirements

The following mandatory requirements were approved at this session, and are expected to be considered for adoption at MSC 106 in November 2022.

(1) Amendments to IGC Code

Amendments to add high manganese austenitic steel in Table 6.3 of IGC Code on plates, sections and forgings for cargo tanks, secondary barriers and process pressure vessels for design temperatures below -55°C and down to -165°C, were approved.

(2) Amendments to IGF Code

Amendments to add high manganese austenitic steel in Table 7.3 of IGF Code on plates, sections and forgings for fuel tanks, secondary barriers and process pressure vessels for design temperatures below -55°C and down to -165°C, were approved.

(3) The International Code of Safety for Ships carrying Industrial Personnel (IP Code)

Newly developed IP Code and new SOLAS Chapter XV to make the IP Code mandatory were approved. The IP Code applies to cargo ships and high-speed cargo craft, of 500 gross tonnage and upwards which carry more than 12 industrial personnel, expecting its entry into force on 1 July 2024.

(4) Amendments to 2011 ESP Code

Amendments to 2011 ESP Code which mainly contain the following items were approved.

1. The coating condition criteria of ballast tanks, excluding double-bottom tanks, of bulk carriers were strengthened from "POOR" to "less than GOOD", which are used for the tank examination at annual intervals.

2. For void spaces bounding cargo holds of double-side skin bulk carriers exceeding 20 years of age and of 150m in length and upwards, it is required that the spaces in question should be examined at annual intervals where a hard protective coating is found to be in POOR condition.

3. It was clarified that oil tankers carrying oil in independent tanks which did not form part of the ship's hull were outside the scope of the ESP Code.

4. Timing of tank pressure testing for oil tankers at renewal survey was clarified.

(5) Measures to enhance the safety of ships relating to the use of fuel oil

Triggered by the global 0.5% sulphur limit, which has entered into force on 1 January 2020, further measures to enhance the safety of ships relating to the use of fuel oil have been discussed. In result, draft amendments to SOLAS Chapter II-2 were approved to require that a bunker delivery note for the fuel delivered to the ship shall contain the flashpoint information.

3.3 Approval of Unified Interpretations (UIs), Guidelines and Guidance etc.

The following unified interpretations (UIs), guidelines and guidance etc. were approved during MSC 105.

3.3.1 Unified Interpretations (UIs)

(1) Unified interpretation of the IGC Code

The amendments to the interpretation of paragraphs 5.4.4 and 5.13.2.4 of the IGC Code (MSC.1/Circ.1625) to clarify that the "duct" in gas fuel piping systems should mean to include the equipment enclosure (e.g. gas valve unit enclosure) as well as the structural pipe duct were approved. Meanwhile gas valve unit rooms are exempted from the scope of the requirement, it should be able to withstand the maximum built-up pressure arising in the room in case of a gas pipe rupture, as documented by suitable calculations.

(2) Updated unified interpretation regarding timber deck cargo in the context of damage stability requirements (annex of MSC/Circ.998)

Unified interpretation regarding timber deck cargo in the context of damage stability requirements (annex of MSC/Circ.998) was updated to align with 2011 TDC Code. (IACS UI SC161)

(3) Unified interpretation of Noise Code

Unified interpretation to "workshops other than those forming part of machinery spaces", which is stipulated in paragraph 4.2.1 of the annex to the Code on noise levels on board ships, was approved.

(4) Amendments to unified interpretation of 1988 LL Protocol (MSC.1/Circ.1535/Rev.1)

Amendments to unified interpretation of 1988 LL Protocol (MSC.1/Circ.1535/Rev.1) to add the interpretation of regulation 37 "Deduction for superstructures and trunks" that the deduction for forecastle and other superstructures cannot be applied to ships of type 'B' where the effective length of forecastle is less than 0.07L, were approved.

(5) Amendments to unified interpretation of SOLAS Chapter II-1 (MSC.1/Circ.1362)

Amendments to unified interpretation of SOLAS Chapter II-1 (MSC.1/Circ.1362) to add the interpretation of regulations 5.4 and 5.5 on alterations of lightweight to clarify the condition for implementation of inclining test and update of stability information which may be required in result of the lightweight calculation were approved.

3.3.2 Guidelines, Guidance and Other Circulars

(1) Explanatory notes to the interim guidelines on second generation intact stability criteria (MSC.1/Circ.1627)

Interim Guidelines for the second generation intact stability criteria (MSC.1/Circ.1627) has been published to provide performance-based criteria for assessing five dynamic stability failure modes in waves, namely, dead ship condition, excessive acceleration, pure loss of stability, parametric rolling and surf-riding/ broaching. At this session, the Explanatory Notes to the Interim Guidelines which are intended as a support in the application of the Interim Guidelines by providing further clarifications and explanations to the elements therein, were approved.

(2) Interim guidelines for the safety of ships using fuel cell power installations

As a part of long term consideration on amendments to IGF Code, the Interim guidelines for the safety of ships using fuel cell power installations were approved.

3.4 Consideration of Requirements for Maritime Autonomous Surface Ships (MASS)

Taking into account recent investigation of automation surrounding a ship, it has been discussed at MSC on conventional requirements of safety and environmental protection relating to MASS.

At this session, the road map for developing goal-based MASS Code was endorsed, in which non-mandatory MASS guidelines will be developed in 2024 and mandatory goal-based MASS Code will be developed targeting entry into force in 2028. The details of the Code would be considered by the intersessional correspondence group established at this session.

3.5　New Output on Safety of Newly Built Ships Using Ammonia as Fuel

To achieve GHG reduction target, utilization of alternative fuel is essential and demand for design and/or construction of ammonia-fuelled ships are emerging. Under these circumstances, it was proposed to develop non-mandatory guidelines for ships using ammonia as fuel at MSC 105.

At this session, it was agreed to consider developing guidelines for ships using ammonia as fuel with a target completion year of 2023. Discussion will be started at next CCC Sub-Committee to be held in September 2022.

Relevant to this topic, ClassNK published its "Guidelines for Ships Using Alternative Fuels (Edition 2.0)" in July 2022 to minimize the risks related to ammonia-fuelled ships for the ships, crew, and environment by stipulating requirements for installation, controls, and safety devices.